EXXONMOBIL CANADA LTD.
EASTERN NEWFOUNDLAND OFFSHORE EXPLORATION DRILLING PROJECT (CEAR 80132)

ENVIRONMENTAL IMPACT STATEMENT

APPENDICES

Pursuant to Requirements of the *Canadian Environmental Assessment Act*, *2012*

December 2017

APPENDIX C

Eastern Newfoundland Drilling Noise Assessment: Qualitative Assessment of Radiated Sound Levels and Acoustic Propagation Conditions
(Quijano et al. 2017)

Eastern Newfoundland Drilling Noise Assessment

Qualitative Assessment of Radiated Sound Levels and Acoustic Propagation Conditions

Submitted to:
Colleen Leeder
Stantec Consulting Ltd.
Project number: 121413373

Authors:
Jorge Quijano
Marie-Noël Matthews
Bruce Martin

2 November 2017

P001273-001
Document 01366
Version 2.1

JASCO Applied Sciences (Canada) Ltd
Suite 202, 32 Troop Ave.
Dartmouth, NS B3B 1Z1 Canada
Tel: +1-902-405-3336
Fax: +1-902-405-3337
www.jasco.com

Suggested citation:

Quijano, J., M.-N. Matthews, and B. Martin. 2017. *Eastern Newfoundland Drilling Noise Assessment: Qualitative Assessment of Radiated Sound Levels and Acoustic Propagation Conditions*. Document 01366, Version 2.1. Technical report by JASCO Applied Sciences for Stantec Consulting Ltd.

Disclaimer:

The results presented herein are relevant within the specific context described in this report. They could be misinterpreted if not considered in the light of all the information contained in this report. Accordingly, if information from this report is used in documents released to the public or to regulatory bodies, such documents must clearly cite the original report, which shall be made readily available to the recipients in integral and unedited form.

Contents

Figures

Tables

1. Introduction

JASCO Applied Sciences (Canada) (JASCO) provided qualitative predictions of underwater sound levels for the Flemish Pass Exploration Drilling Program (Statoil Canada Ltd.) and the Eastern Newfoundland Offshore Exploration Drilling Project (ExxonMobil Canada Ltd.). The project areas are shown in Figure 1. The areas include existing Statoil and ExxonMobil exploration licence blocks in the Flemish Pass and Jeanne d'Arc Basin region, and is referred to as the Eastern Newfoundland Exploration Drilling Project Area in this report. The sound sources considered in this desktop study include drill rigs (semisubmersibles and drill ships), dynamic positioning (DP) systems, support vessels, and a vertical seismic profiler (VSP). In this desktop study, we consider three locations: Site A, a 300 m deep location at the edge of the Grand Banks; site B, which is 1500 m deep in the Flemish Pass; and Site C, which is 3000 m deep north of Flemish Cap (Figure 1).

This report:

- Provides data on the ambient noise levels in the Eastern Newfoundland Exploration Drilling Project Area,
- Summarizes the environmental parameters in the Eastern Newfoundland Exploration Drilling Project Area,
- Summarizes the expected project source levels, based on client-provided parameters of drill rig DP systems and VSP arrays likely to be used in this Project,
- Compares environmental properties and source levels between the present Project and the Scotian Basin Exploration Drilling Project (Zykov 2016), and
- Concludes by comparing the radii of possible effects to marine life to those reported in the Scotian Basin Exploration Drilling Project (Zykov 2016).

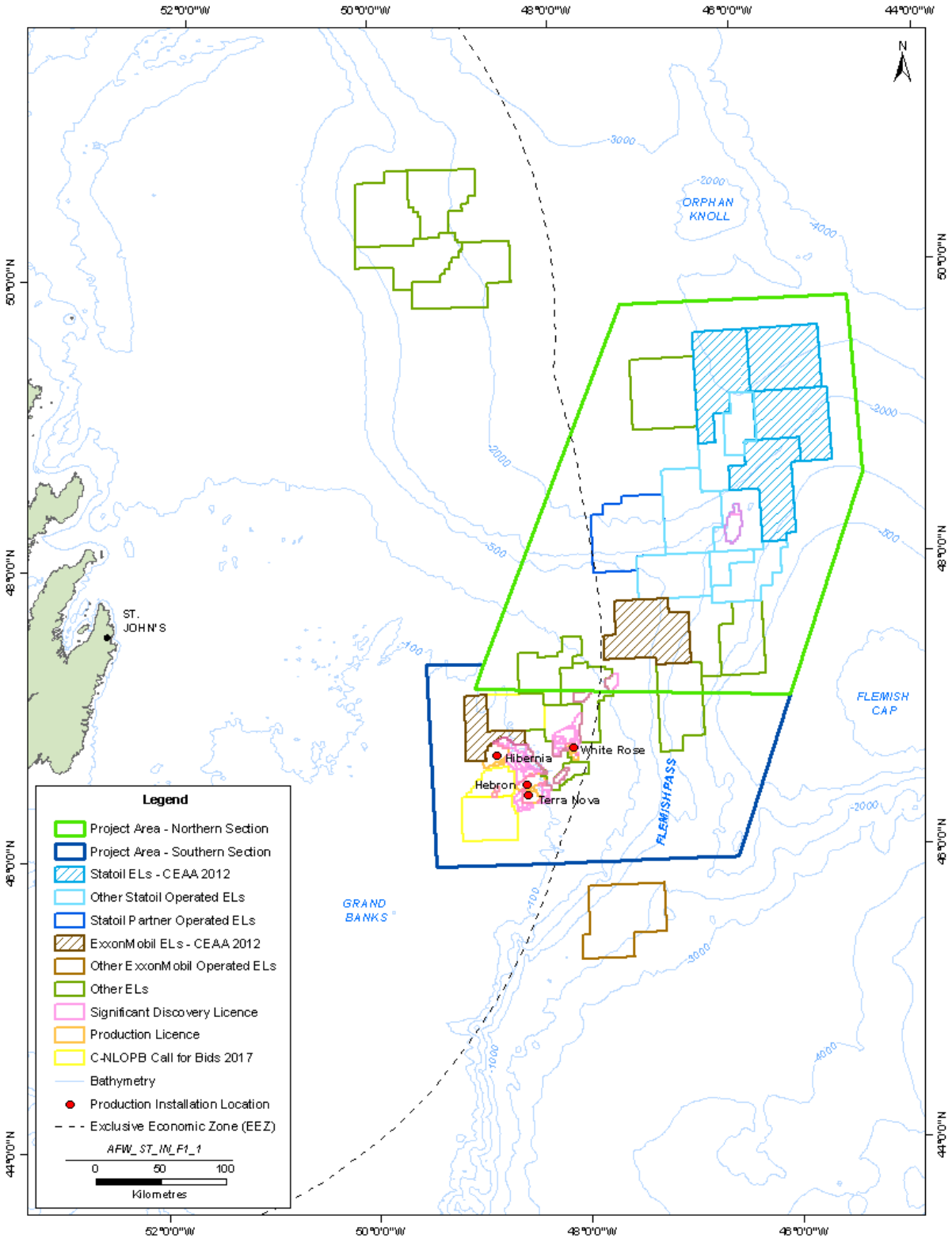

Figure 1. Flemish Pass Exploration Drilling Program and Eastern Newfoundland Exploration Drilling Project Areas (Eastern Newfoundland Exploration Drilling Project Area).

2. Ambient Noise Levels

The impact of sound sources on the ocean soundscape depends on factors such as:

- The source loudness,
- The characteristics of sound propagation, determined by environmental parameters (water depth, sound speed profile, seabed type) and the frequency spectrum of the source,
- The overlap of the frequency content of the new sounds with the existing sounds in the environment.

This section provides an overview of the sound sources in the Project Area. To simplify the discussion of the existing soundscape, we divide the frequency spectrum into five bands. Table 1 provides a classification of known biologic, man-made, natural geologic, and measurement-noise mechanisms as well as the frequency bands associated with their contributions to the soundscape.

Table 1. Typical sound generating mechanisms and their associated frequency bands.

Band name and frequency range	Sound source type			
	Biologic	Man-made	Geologic	Measurement System Noise
Very low frequency: 10–45 Hz (Figure 4)	Fin, blue, Bryde's, Omura's whales	Seismic pulses	Earthquakes	Flow noise, strum
Low frequency: 45–225 Hz (Figure 5)	Fish, baleen whales, pinnipeds	Seismic pulses, large vessels	-	Flow noise, strum
Mid frequency: 225–2250 Hz (Figure 6)	Baleen whales, fish, pinnipeds	Smaller vessels, large vessels at close range, DP	Wind and wave action	-
High frequency: 2250–18000 Hz (Figure 7)	Whistles, sperm whale clicks, baleen song, shrimp	Naval sonar, cavitation bubbles, chains	Sediment movement, rain	-
Very high frequency: >18000 Hz (Figure 8)	Echolocation clicks	Communicating and positioning devices, naval sonar	-	-

"-" symbol means that the corresponding sound source does not have significant energy within the band.

To summarize the soundscapes around the Eastern Newfoundland Exploration Drilling Project Area, we present the distribution of one-minute sound pressure levels from a data collection program conducted by JASCO in 2015-2016. In August 2015, JASCO deployed 20 acoustic recorders along Canada's east coast for the first year of a two-year baseline monitoring program sponsored by the Environmental Sciences Research Fund (ESRF) program. The recorders were retrieved and redeployed in July 2016. Data from six of the recorders are discussed here, as they provide the best available information on the existing sound levels in the Eastern Newfoundland Exploration Drilling Project Area (Figure 2). Stn 18 was in 80 m of water, 35 km from the Hibernia platform in the existing Jeanne D'Arc Basin development area. Data from Stn 7 is presented as an example of a receiver at a location of similar water depth, but far from oil and gas activity. Stns 17 and 19 were in deep water (>1250 m) 200 km south and north of the Flemish Pass respectively. Their data represents the current deep-water soundscape. Stns 4 and 5 are to the southwest of Sable Island. Their data provide examples of the effects of a deep-water drilling rig on the soundscape. Stn 5 was located 13 km from Shell Canada's 2015–2016 Cheshire drilling campaign.

To describe the general characteristics of the soundscape, we present box-and-whisker plots (or boxplots) for each month in each frequency band identified in Table 1. Monthly distributions provide an overview of the range of sound levels and how they change by season. The dominant sound source for each month is indicated by the colour of the boxes. JASCO's experienced analysts identified the dominant sources by inspection of the long-term spectral average figures generated for the ESRF project to identify the sources that would have increased the mean monthly in-band sound pressure level by 3 dB or more from the expected levels in the absence of the source (e.g. Figure 3). A detailed analysis of all detectable sources of sound (e.g. vessels in Figure 3) is beyond the scope of this summary. Section 2.1 discusses the soundscape by frequency band (i.e., the rows of Table 1) and Section 2.2 summarizes the effects of the different sound sources on the soundscape (i.e., the columns of Table 1). In both sections, we will refer to Figure 3 through Figure 8. The boxplots were created from ~2000 one-minute samples collected per month per station. The top and bottom of the boxes show the sound levels exceeded by 25% and 75% of the one minute samples, respectively. The heavy line across the boxes shows the mean monthly sound pressure levels. The lines extending above and below the boxes extend 2 standard deviations from the mean value. The box plots are ordered from north to south.

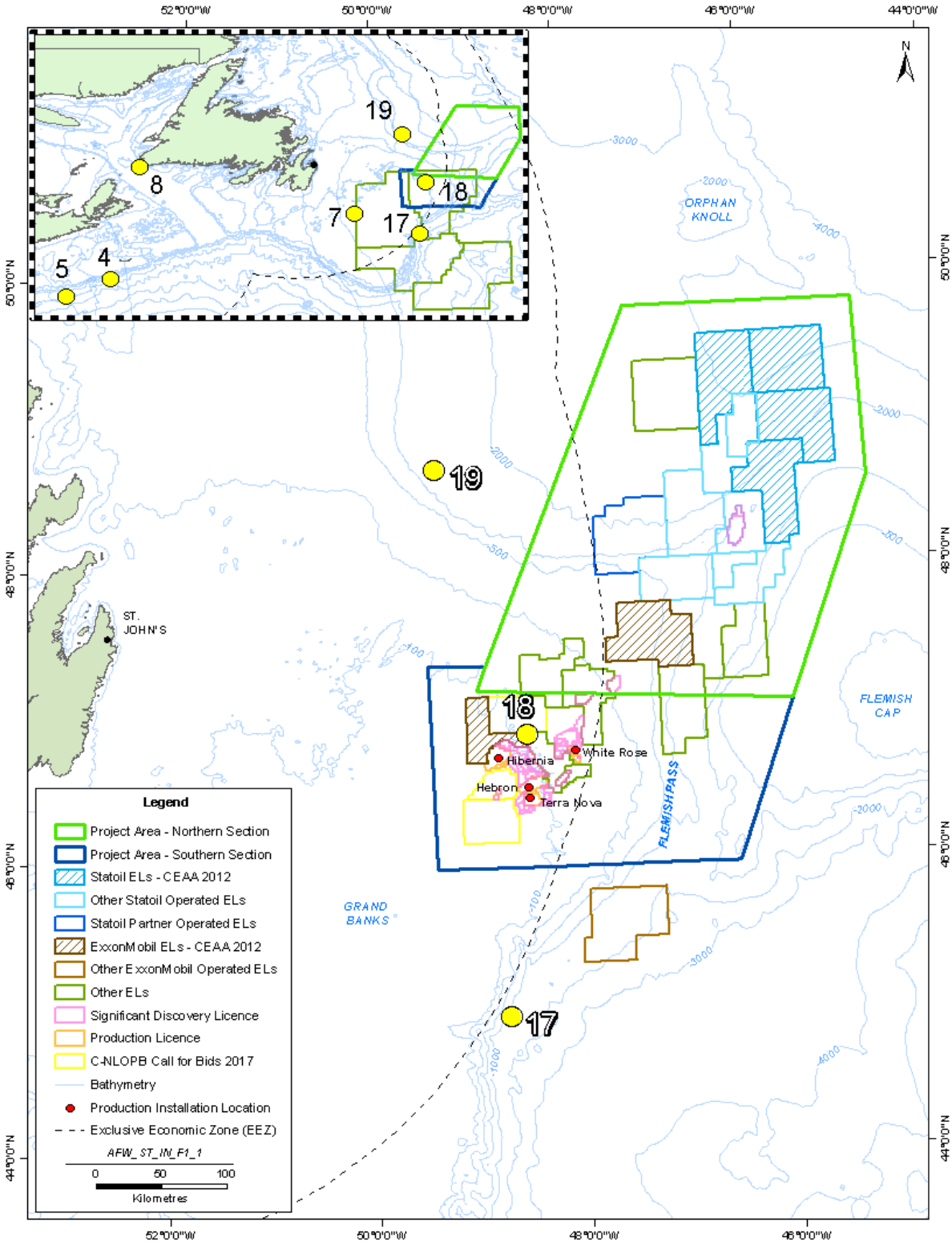

Figure 2. Eastern Newfoundland Exploration Drilling Project Area showing locations of the existing oil production platforms and the JASCO year-long acoustic recorders (yellow dots) deployed as part of an ESRF program. Hebron is expected to produce first oil in December 2017. A zoomed-out view of the Scotian Shelf and Grand Banks is included in the top-left corner for context

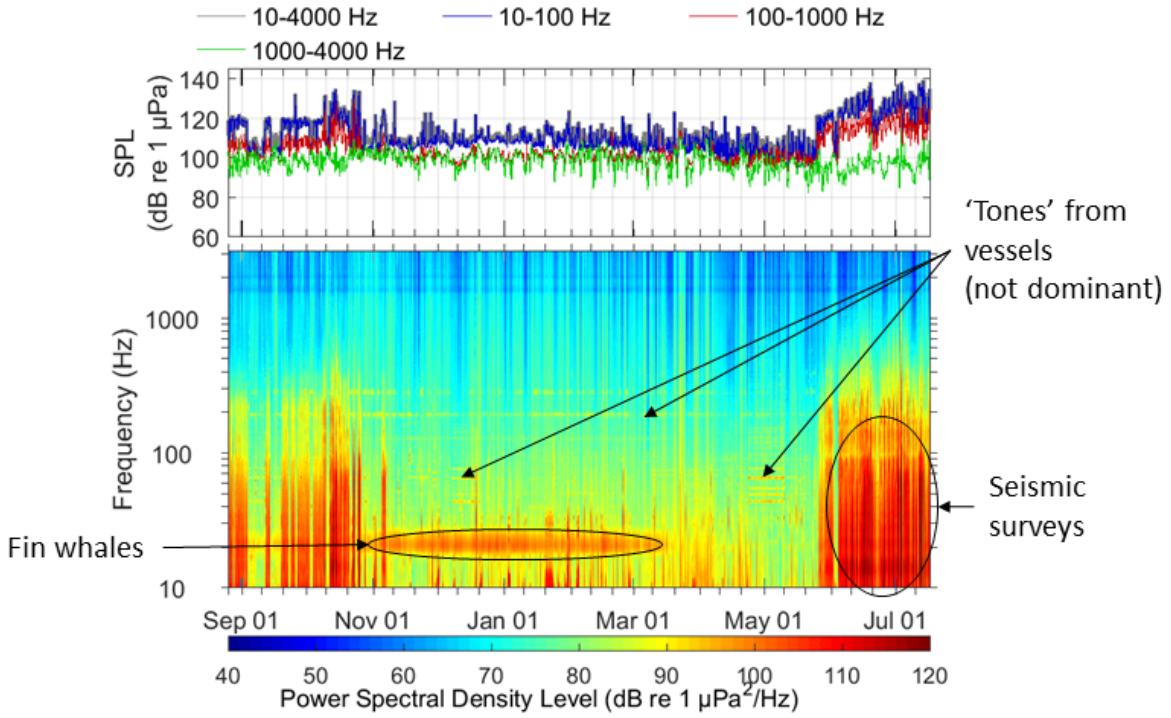

Figure 3. Long-term spectral average from Station 19 showing fin whales and seismic surveys as two dominant sources. Vessels were detectable througout the year, but were not dominant sources in the sense of increasing the per-month sound levels.

2.1. Soundscape by Band

The total sound levels across all bands are referred to as the broadband sound pressure levels (SPL). If a source is identifiable as the dominant source in the monthly broadband sound distributions, then the magnitude of its sounds exceed all other regularly occurring sounds by at least 3–6 dB. In Figure 3, Stn 04 and 17 are good examples of the normal magnitude and distribution of sounds pressure levels in the open ocean. Ambient sound levels are in the range of 100–105 dB re 1 µPa, with levels slightly higher in the winter due to increased wind and wave activity. At Stn 18, the levels are 110–120 dB re 1 µPa continuously, which is due to the platform and support vessel noise from the Hibernia and Hebron oil developments. The effect of the Cheshire well drilling activity at Stn 05 is also obvious by comparison to the nearby Stn 04. The drilling program started in mid October 2015 and continued to mid-March 2016. It was suspended from mid-March until early June after the platform dropped the drill string. The drilling finished at the end of July 2016. Seismic surveys occurred off the Grand Banks in fall 2015, which increased the SPLs at Stn 17 in Sept 2015, and Stn 19 in September and October 2015. Surveys north of the Flemish Pass began again in June of 2016 and resulted in the maximum sound levels presented here of 140 dB re 1 µPa. These values are presented in decibels, which is a logarithmic scale. Thus 140 dB is 10000 times louder than 100 dB.

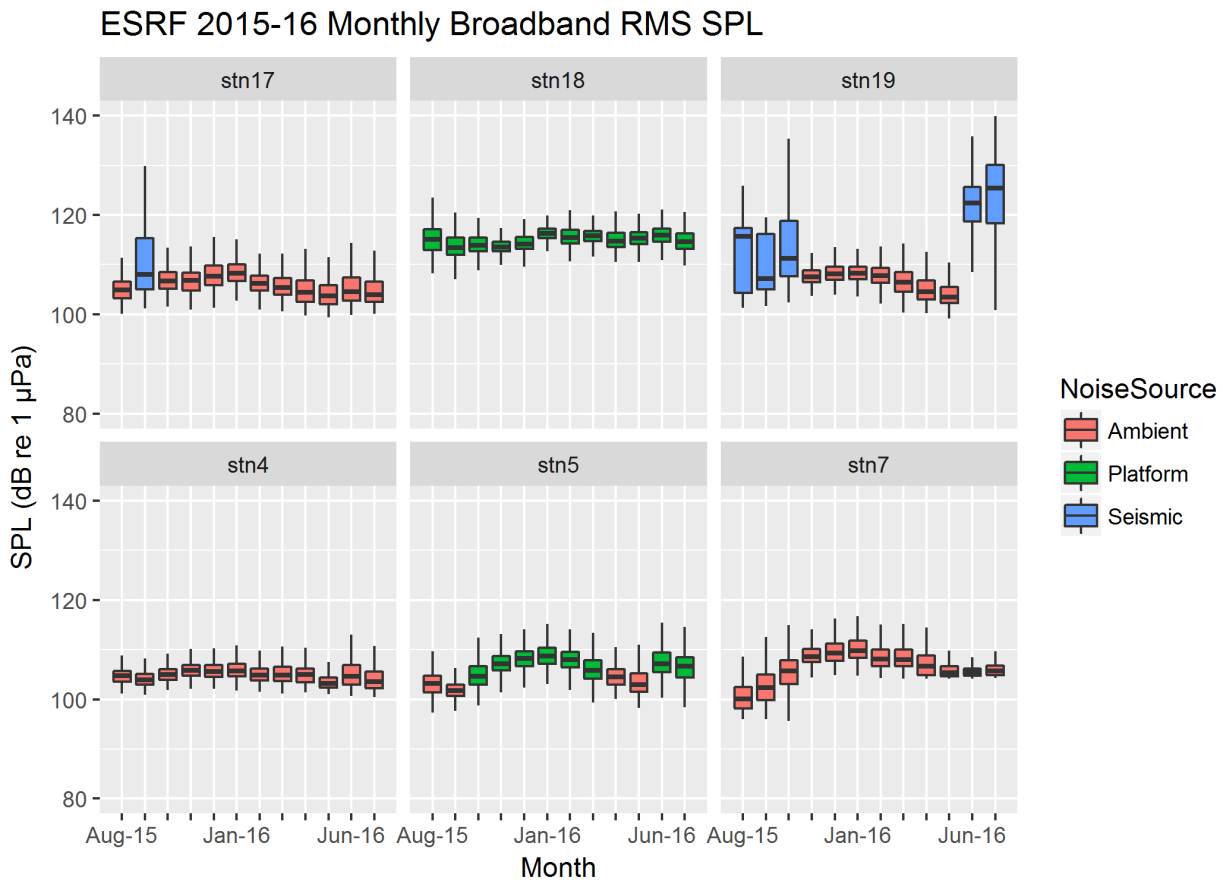

Figure 4. *10–125,000 Hz band*: Distribution of one-minute SPL for selected locations from JASCO's 2015–2016 ESRF data set. Stations 7 and 18 are at <100 m water depth and Stations 4, 5, 17, and 19 are at >1000 m. All measurements were within 10 m of the seabed. Stn 4 and 5 are located off the southwestern Scotian Shelf and represent examples of deep water recordings with and without significant man-made noise sources. Stn 5 is 13 km from Shell's Monteray Jack drilling campaign using the Stena IceMax. Stn 18 is 35 km from the Hibernia platform.

In the very-low frequency band (10–45 Hz, Figure 4), background sound levels in the open ocean are in the range of 90–95 dB re 1 µPa. Fin whales were a dominant noise source for at least four months and up to seven months throughout fall, winter, and spring, which was typical for the ESRF stations that were not ice-covered, especially those over the Scotian Shelf and Grand Banks. North Atlantic fin whales emit a short pulse once every 9–18 seconds from October to March. Seismic survey sounds are a man-made source with high energy levels in this band. They were a major noise source at Stn 19 and 17 in the summer months. The fluctuations in the seismic sound levels were caused by variations of the distance between the seismic survey vessel and the corresponding recorder, as well as by the total number of survey days within each month. Platform and vessel noise were only weakly detectable in this band.

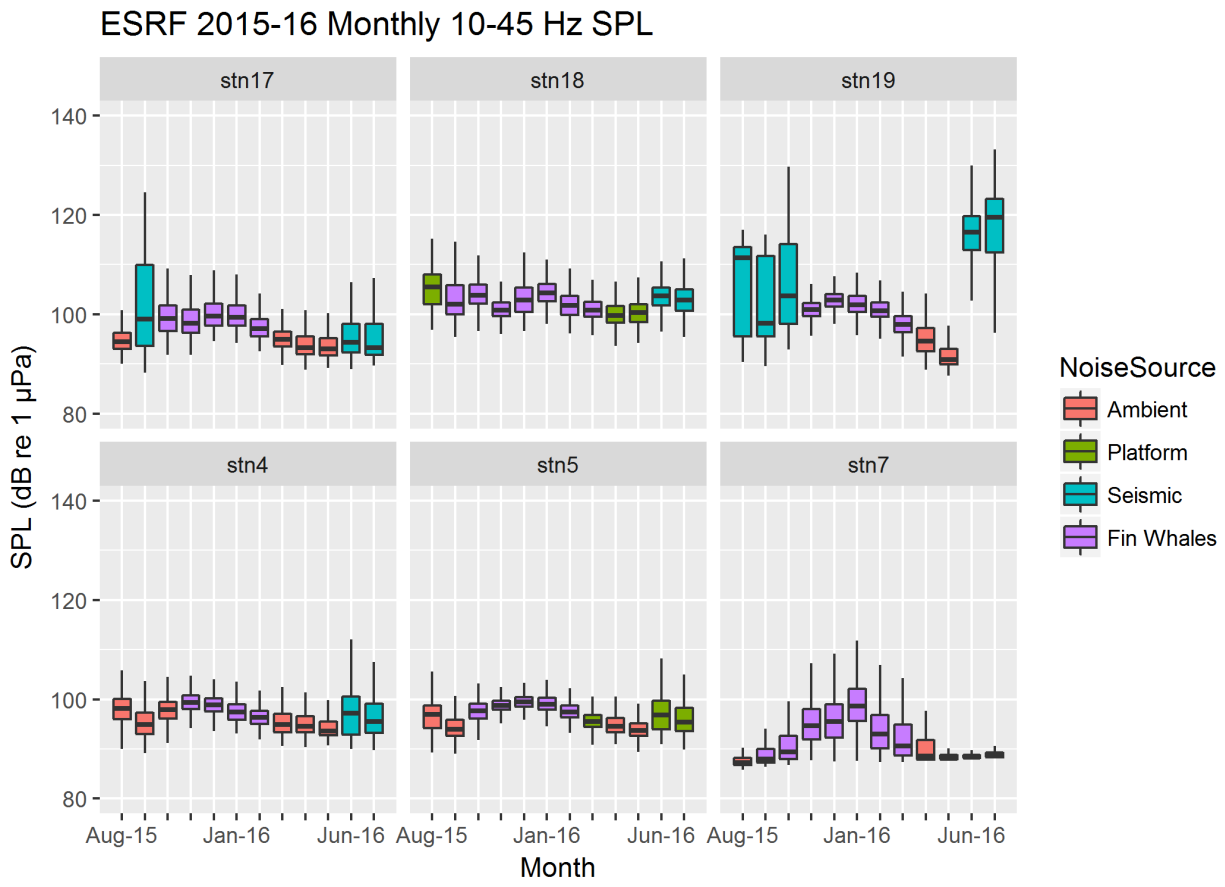

Figure 5. *10–45 Hz band*: Distribution of one-minute SPL for selected locations from JASCO's 2015–2016 ESRF data set. Stations 7 and 18 are at <100 m water depth and Stations 4, 5, 17, and 19 are at >1000 m. All measurements were within 10 m of the seabed. Stn 4 and 5 are located off the southwestern Scotian Shelf and represent examples of deep water recordings with and without significant man-made noise sources. Stn 5 is 13 km from Shell's Monteray Jack drilling campaign using the Stena IceMax. Stn 18 is 35 km from the Hibernia platform.

The low frequency band (45–225 Hz, Figure 5) contained the highest levels of platform noise. At Stn 18, the levels were ~105–115 dB re 1 µPa, nearly the range of the broadband SPL measured at Stn 18. The levels, which varied by small amounts from month-to-month. Stn 05 provides an example of typical platform noise levels for deep-water operations, with the highest levels around 103 dB re 1 µPa during November to February and during June to July. The program occurred from October 2015–July 2016 and was suspended from mid-March to early-June 2016. With respect to platform noise levels representative of operations in shallow water, the sound levels at Stn 18 were ~15 dB and 20 dB higher than those at Stn 7 during winter and summer, respectively. The levels at Stn 18 (35 km from Hibernia) were also considerably higher than those at Stn 05 (13 km from the Cheshire well drilling). This difference is likely due to the presence of three producing platforms near Stn 18 (Figure 2) and the support vessel traffic associated with their activities. Also, the deep waters near Stn 05 result in higher geometric spreading attenuation of the sound compared to the shallow water near Stn 18.

The seismic surveys were again a major source of noise at Stn 17 and Stn 19, although the levels were lower than in the very low frequency band.

Stn 07 shows a wider range of sound levels in the low frequency band in each month compared to the levels from any of the deep stations (17, 19, 04, 05). This is because in the absence of nearby sources of anthropogenic noise, the levels at Stn 07 are mostly driven by underwater noise from wind-driven wave activity, which is significantly higher during winter (November through March).

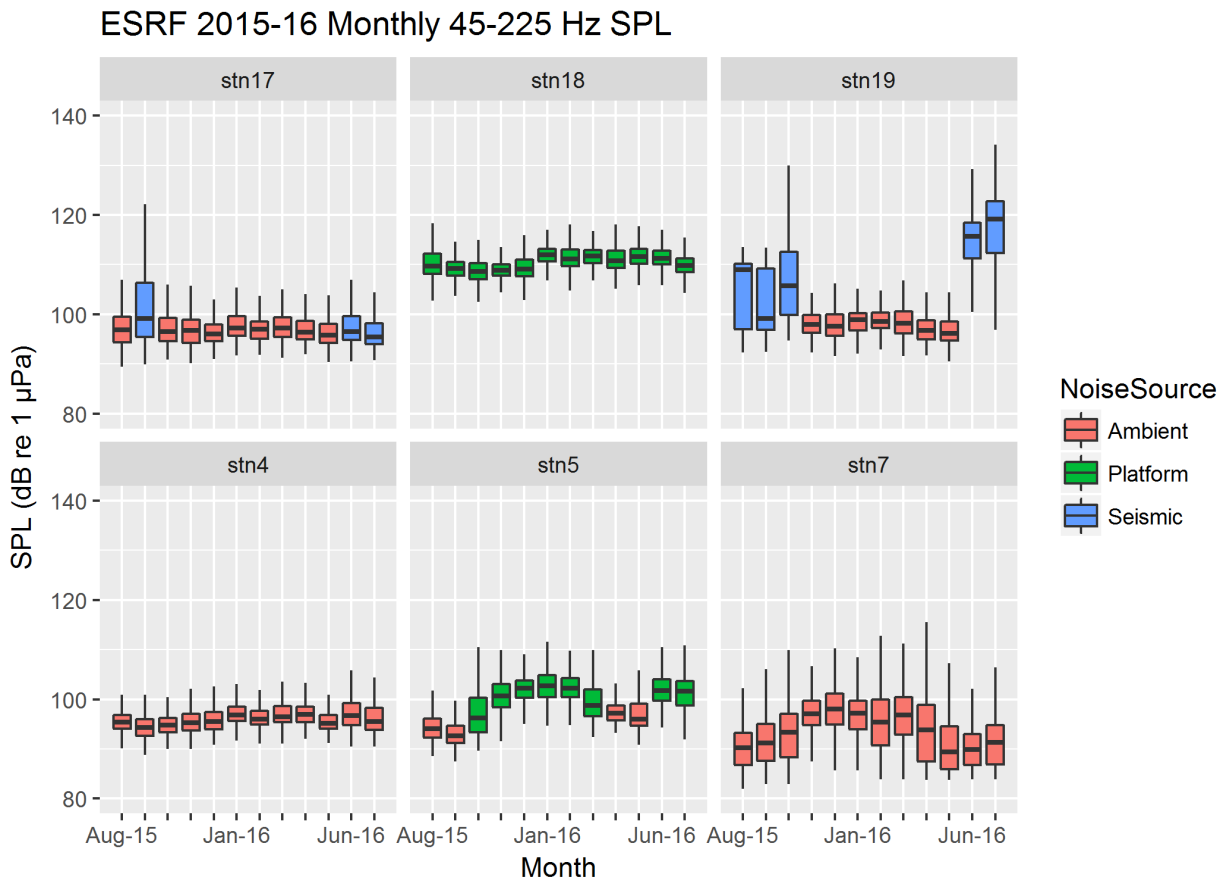

Figure 6. *45–225 Hz band*: Distribution of one-minute SPL for selected locations from JASCO's 2015–2016 ESRF data set. Stations 7 and 18 are at <100 m water depth and Stations 4, 5, 17, and 19 are at >1000 m. All measurements were within 10 m of the seabed. Stn 4 and 5 are located off the southwestern Scotian Shelf and represent examples of deep water recordings with and without significant man-made noise sources. Stn 5 is 13 km from Shell's Monteray Jack drilling campaign using the Stena IceMax. Stn 18 is 35 km from the Hibernia platform.

The mid-frequency band (225–2250 Hz, Figure 6) is the highest band affected by human-related sound sources at the resolution of this analysis. A seismic survey to Stn 19 affected sound levels in June and July. All stations showed a decrease in average sound levels in the summer months due to lower average wind speeds. In the case of Stn 18, the reduced sound levels in this band from the platforms is likely associated with a change in propagation conditions that kept more of the high frequency sounds close to the surface and away from our bottom recorders (see Sections 3.3 and 3.4).

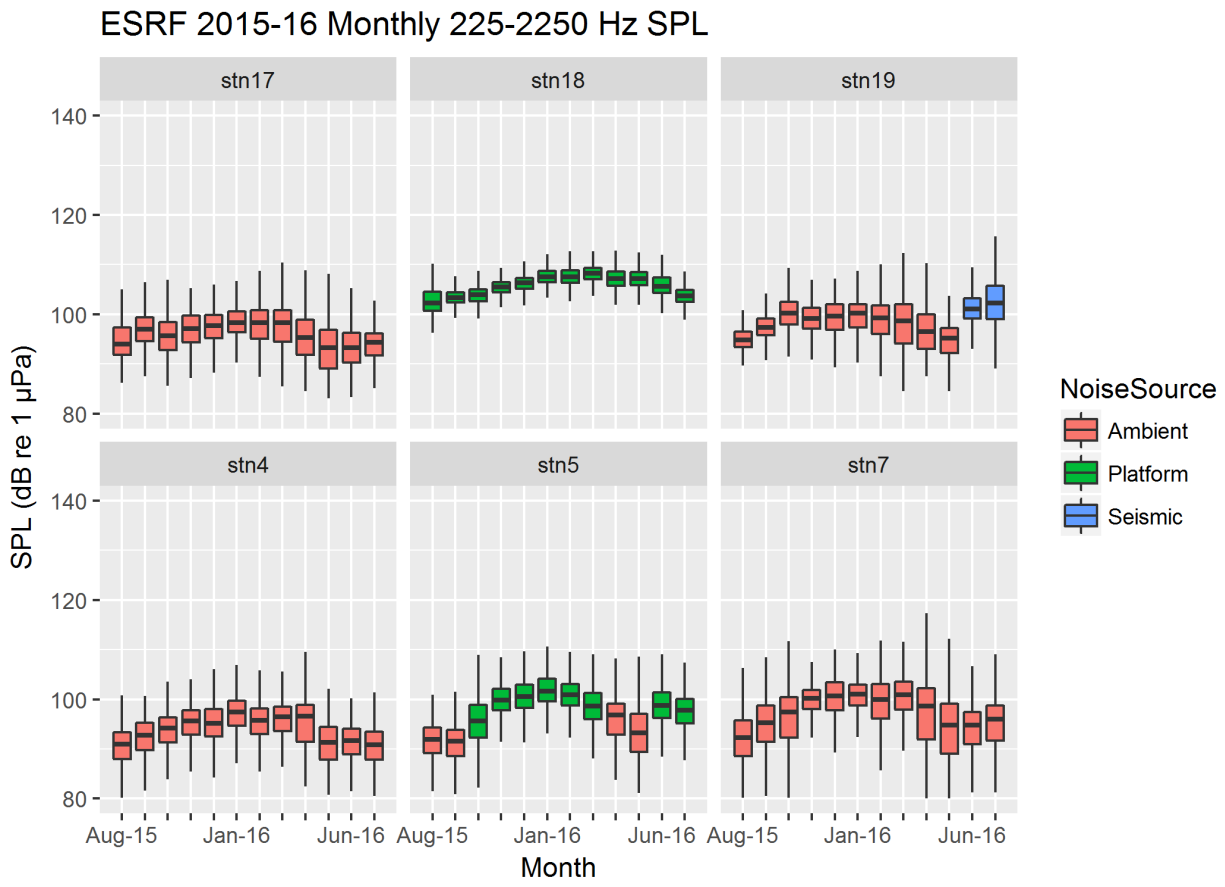

Figure 7. *225–2250 Hz band*: Distribution of one-minute SPL for selected locations from JASCO's 2015–2016 ESRF data set. Stations 7 and 18 are at <100 m water depth and Stations 4, 5, 17, and 19 are at >1000 m. All measurements were within 10 m of the seabed. Stn 4 and 5 are located off the southwestern Scotian Shelf and represent examples of deep water recordings with and without significant man-made noise sources. Stn 5 is 13 km from Shell's Monteray Jack drilling campaign using the Stena IceMax. Stn 18 is 35 km from the Hibernia platform.

In the high frequency band (2250–18000 Hz, Figure 7), all six measurement locations show a cycle of lower sound levels in summer and higher sound levels in winter. The absolute levels and spread of sound levels are similar at all stations.

In the very high frequency band (18000–90000 Hz, Figure 8), the levels shown are known to contain artifacts, caused by hydrophone-self noise frequently exceeding the environmental noise. Higher quality hydrophones were deployed in 2016–2017 to remediate this problem. In our experience, data collected at locations within several kilometres of either a vessel or platform would include energy in both the high-frequency and very high frequency bands.

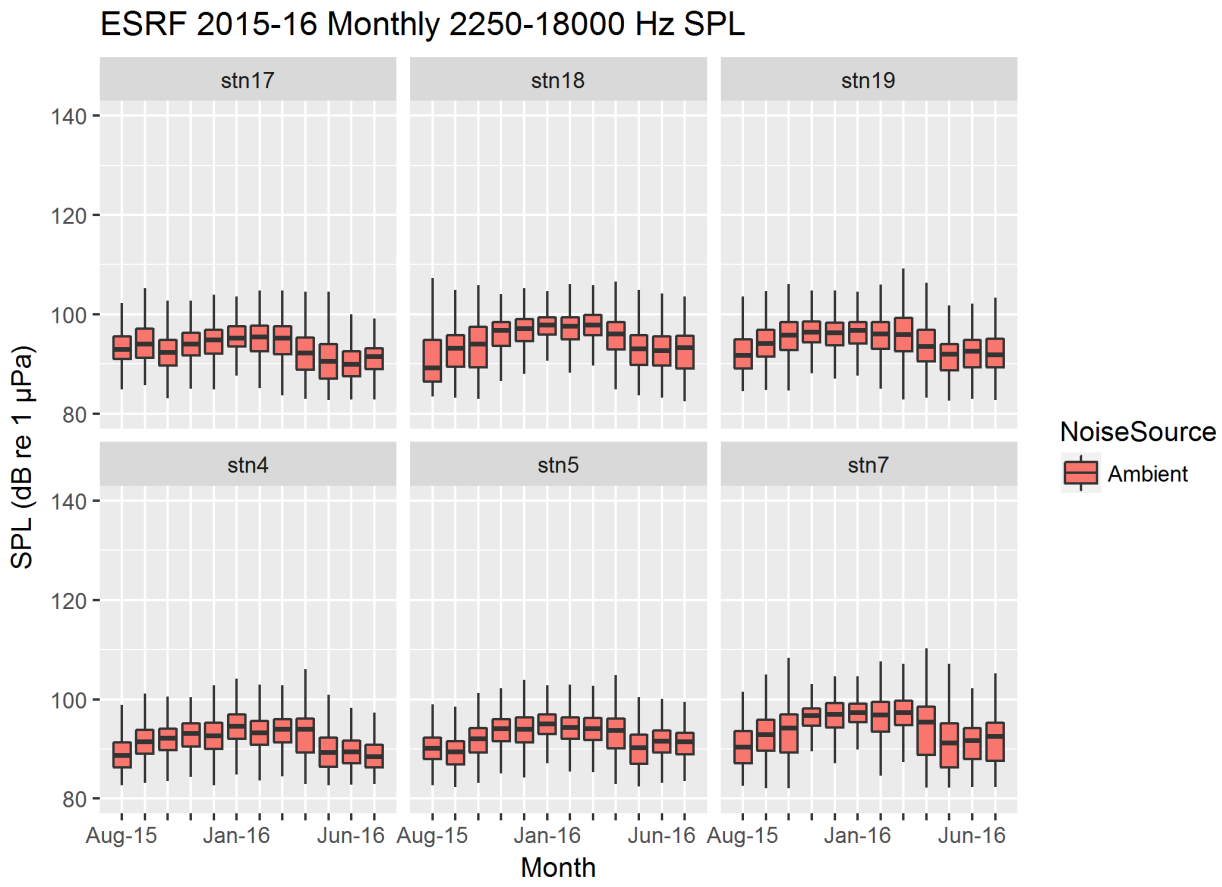

Figure 8. *2250–18000 Hz band*: Distribution of one-minute SPL for selected locations from JASCO's 2015–2016 ESRF data set. Stations 7 and 18 are at <100 m water depth and Stations 4, 5, 17, and 19 are at >1000 m. All measurements were within 10 m of the seabed. Stn 4 and 5 are located off the southwestern Scotian Shelf and represent examples of deep water recordings with and without significant man-made noise sources. Stn 5 is 13 km from Shell's Monteray Jack drilling campaign using the Stena IceMax. Stn 18 is 35 km from the Hibernia platform.

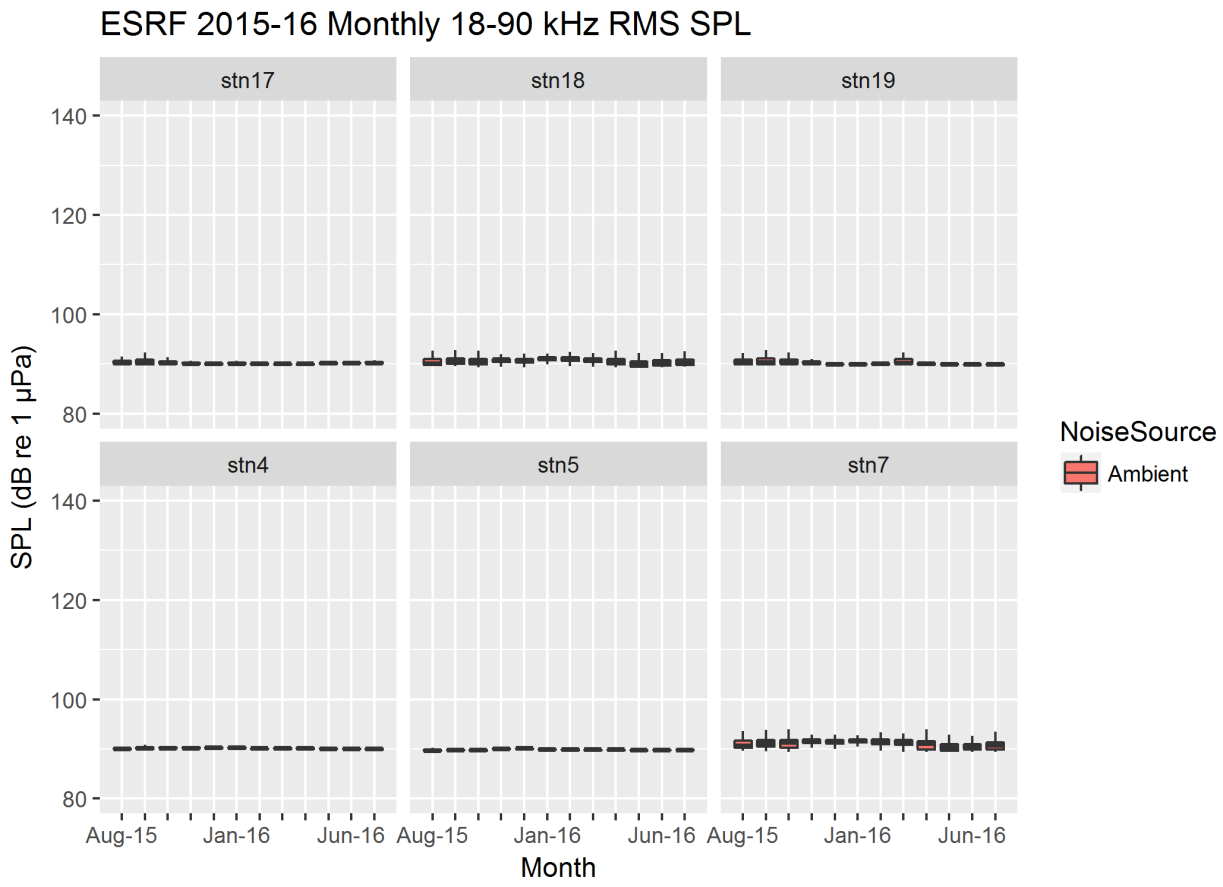

Figure 9. *18000–90,000 Hz band*: Distribution of one-minute SPL for selected locations from JASCO's 2015–2016 ESRF data set. Stations 7 and 18 are at <100 m water depth and Stations 4, 5, 17, and 19 are at >1000 m. All measurements were within 10 m of the seabed. Stn 4 and 5 are located off the southwestern Scotian Shelf and represent examples of deep water recordings with and without significant man-made noise sources. Stn 5 is 13 km from Shell's Monteray Jack drilling campaign using the Stena IceMax. Stn 18 is 35 km from the Hibernia platform.

2.2. Summary of Effects of Sources on the Soundscape

There are four identifiable sources in the Eastern Newfoundland Exploration Drilling Project Area that have long term effects on the soundscape:

1. Fin whales: Fin whales sing from Octoberto March on the Grand Banks. They seem to favour the shallow waters on the Grand Banks compared to the deeper waters off the continental shelf. Their constant notes raise the total sound level in the 10–45 Hz band by 5–10 dB in winter across the Grand Banks and Scotian Shelf. Whales close to a recorder can temporarily increase the one-minute sound levels to 130 or 140 dB re 1 µPa.
2. Platforms: Oil and gas development and production platforms and their associated support vessels increased the SPL in the band of ~40–225 Hz by 15–20 dB at ranges of 35 km from a collection of 3 platforms in shallow water, and 8–10 dB for a single dynamically positioned drill rig 13 km away in deep water. The sound levels in the band of 225–2250 Hz were elevated 5–10 dB in both locations. The platforms are continuous noise sources that cause permanent elevations in the background sound levels.
3. Seismic Surveys: Seismic surveys are known to be one of the most intense sound sources in the ocean, capable of travelling hundreds to thousands of kilometres (McCauley et al. 2000, Gordon et al. 2003, Nieukirk et al. 2012). The seismic surveys detected at Stn 17 and Stn 19 were over 100 km

from the recorders and still a dominant sound source. Seismic array sound's peak frequency is near 50 Hz (Dragoset 1984), however the frequency range increases as the source vessel gets closer to a measurement location. The measurements reported here included energy up to 1 kHz.

4. Ambient: Median sound levels increase 3–5 dB in the winter due to higher wind speeds and storms. The peak frequency band for wind noise is 200–2000 Hz. See Hildebrand (2009) and Cato (2008) for overview of ocean ambient noise and man-made sound sources.

3. Factors Affecting Sound Propagation

The sound levels measured at some distance from a source depend on the source-receiver distance and propagation effects. Sound propagation is influenced by the bathymetry at and around the sound source, the geoacoustic properties of the seafloor, the variation in sound speed in the water as a function of depth, and the spectral characteristics of the noise source. This section details the environmental parameters expected within the Eastern Newfoundland Exploration Drilling Project Area and provides an overview of other propagation effects. Where appropriate, the environmental parameters corresponding to the Scotian Basin Exploration Drilling Project (Zykov 2016) are presented for comparison.

3.1. Bathymetry

Water depths throughout the Eastern Newfoundland Exploration Drilling Project Area were extracted from the SRTM15+ global bathymetry grid, a 30 arc-second grid (~600 × 1800 m at the studied latitude) rendered for the entire globe (Rodríguez et al. 2005). The water depth in the Flemish Pass area varies from 200–300 m in the southwest section (toward the Jeanne D'Arc Basin) to >3000 m northeast of the Flemish Cap (Figure 1). The water depths in the Jeanne D'Arc Basin area range from <80 m on the Grand Banks to more than 2000 m south-east of the Flemish Cap. As explained below, the combined effect of water depth and seabed geoacoustics may strongly influence sound propagation.

3.2. Geoacoustics

When sound propagates through the ocean, the sea surface and ocean floor act as boundaries that reflect, absorb, and scatter the energy. The surface is referred to as a 'pressure-release' interface because the acoustic pressure must be zero. For this to be true, the surface reflects the sound with equal amplitude and opposite phase. The reflected direction is perpendicular to the sea surface, and, therefore, if the surface is tilted by wave action it has a scattering effect that increases with frequency. A hard seabed is a different type of boundary that does not move, so the particle velocity must be zero. Thus, it reflects sound in phase with the incident energy and the pressure doubles. However, most seabeds are not perfect reflectors. Generally, seabeds are modelled as viscous fluids where a portion of the sound energy is reflected and the remainder penetrates the sediment. The amount of reflection and transmission depends on the angle of incidence, bottom roughness, as well as the density and porosity of the material. Less dense materials, such as clays and silts, allow more sound to penetrate. Harder materials like sand and gravel reflect most of the incident sound. When there are layers of less dense sediment over more dense materials, such as bedrock, the sound can reflect off the lower layers and re-enter the water column. Soft materials like clays can also refract and trap sound, as well as absorb and attenuate it. Clearly the sea-bed geoacoustics are an important environmental parameter for understanding and predicting acoustic propagation.

On the Grand Banks continental shelf, through the Flemish Pass, and in the southern Orphan Basin, the shallow sedimentary layers consist of thick grey muds (silt mixed with 10–30% sand and 20–40% clay) with varying amounts of debris and sand bed horizons (Huppertz 2007). The shallow depths (~1100 m) and narrow banks of the Flemish Pass trap sediment deposits from the continental shelf. The sediment thickness throughout the Eastern Newfoundland Exploration Drilling Project Area is >2500 m, reaching ~4000 m in Flemish Pass (Divins 2007, Géli et al. 2007).

Three generic geoacoustic profiles were constructed for the region, based on water depth. A thick layer of silt/mud is assumed for all profiles. The average grain size of the silt was assumed to decrease with increasing water depth. Representative grain sizes and porosity were used in the grain-shearing model proposed by Buckingham (2005) to estimate the geoacoustic parameters that would be required by sound propagation models. Tables 2–4 list the geoacoustic parameters derived for numeric modelling.

These profiles are similar to those used in the Scotian Basin Exploraton Drilling Project (Zykov 2016), for which the sound sources were located on the continental slope, where a thick (~600 m) clay deposit is found.

Table 2. *Shallow water (Site A, ~300 m)*: Geoacoustic parameters derived for Eastern Newfoundland Exploration Drilling Project Area.

Depth below seafloor (m)	Material	Density (g/cm^3)	P-wave speed (m/s)	P-wave attenuation (dB/λ)	S-wave speed (m/s)	S-wave attenuation (dB/λ)
0–5	Silt mixed with sand and clay	1.5–1.7	1560–1650	0.40–0.65	200	3.65
5–50		1.7–2.0	1650–1910	0.65–1.15		
50–500		2.0–2.1	1910–2435	1.15–2.00		
>500		2.1	2435	2.00		

Table 3. *Deep water (Site B, ~1500 m)*: Geoacoustic parameters derived for Eastern Newfoundland Exploration Drilling Project Area.

Depth below seafloor (m)	Material	Density (g/cm^3)	P-wave speed (m/s)	P-wave attenuation (dB/λ)	S-wave speed (m/s)	S-wave attenuation (dB/λ)
0–5	Silt mixed with sand and clay	1.5–1.7	1525–1585	0.25–0.40	130	3.65
5–50		1.7–2.0	1585–1775	0.40–0.75		
50–500		2.0–2.1	1775–2100	0.75–1.40		
>500		2.1	2100	1.40		

Table 4. *Very deep water (Site C, ~3000 m)*: Geoacoustic parameters derived for Eastern Newfoundland Exploration Drilling Project Area.

Depth below seafloor (m)	Material	Density (g/cm^3)	P-wave speed (m/s)	P-wave attenuation (dB/λ)	S-wave speed (m/s)	S-wave attenuation (dB/λ)
0–5	Silt mixed with sand and clay	1.5–1.7	1505–1555	0.20–0.30	85	3.65
5–50		1.7–2.0	1555–1700	0.30–0.50		
50–500		2.0–2.1	1700–1920	0.50–1.00		
>500		2.1	1920	1.00		

3.3. Sound Speed Profiles

As a rule of thumb, sound is 'lazy': It wants to travel as the slowest possible speed. When there is a depth variation in the sound speed, the sound will be refracted toward the depth with the lowest sound speed. The sound speed is a function of the temperature, salinity and pressure (depth) and can vary by tens of meters-per-second from the surface to the seabed.

Sound speed profiles in the Eastern Newfoundland Exploration Drilling Project Area were derived from temperature and salinity profiles from the U.S. Naval Oceanographic Office's Generalized Digital Environmental Model V 3.0 (GDEM; Teague et al. 1990, Carnes 2009). GDEM provides an ocean climatology of temperature and salinity for the world's oceans on a latitude-longitude grid with 0.25° resolution, with a temporal resolution of one month, based on global historical observations from the U.S. Navy's Master Oceanographic Observational Data Set (MOODS). The climatology profiles include 78 fixed depth points to a maximum depth of 6800 m (where the ocean is that deep). The GDEM temperature-salinity profiles were converted to sound speed profiles according to Coppens (1981).

Mean monthly sound speed profiles were derived from the GDEM profiles for the entire year for a central location in the Eastern Newfoundland Exploration Drilling Project Area (47°30′ N, 46°30′ W; Figure 9a). For comparison purposes, the mean monthly sound speed profiles for the Scotian Basin Exploration Drilling Project (Zykov 2016) are also presented (Figure 9b).

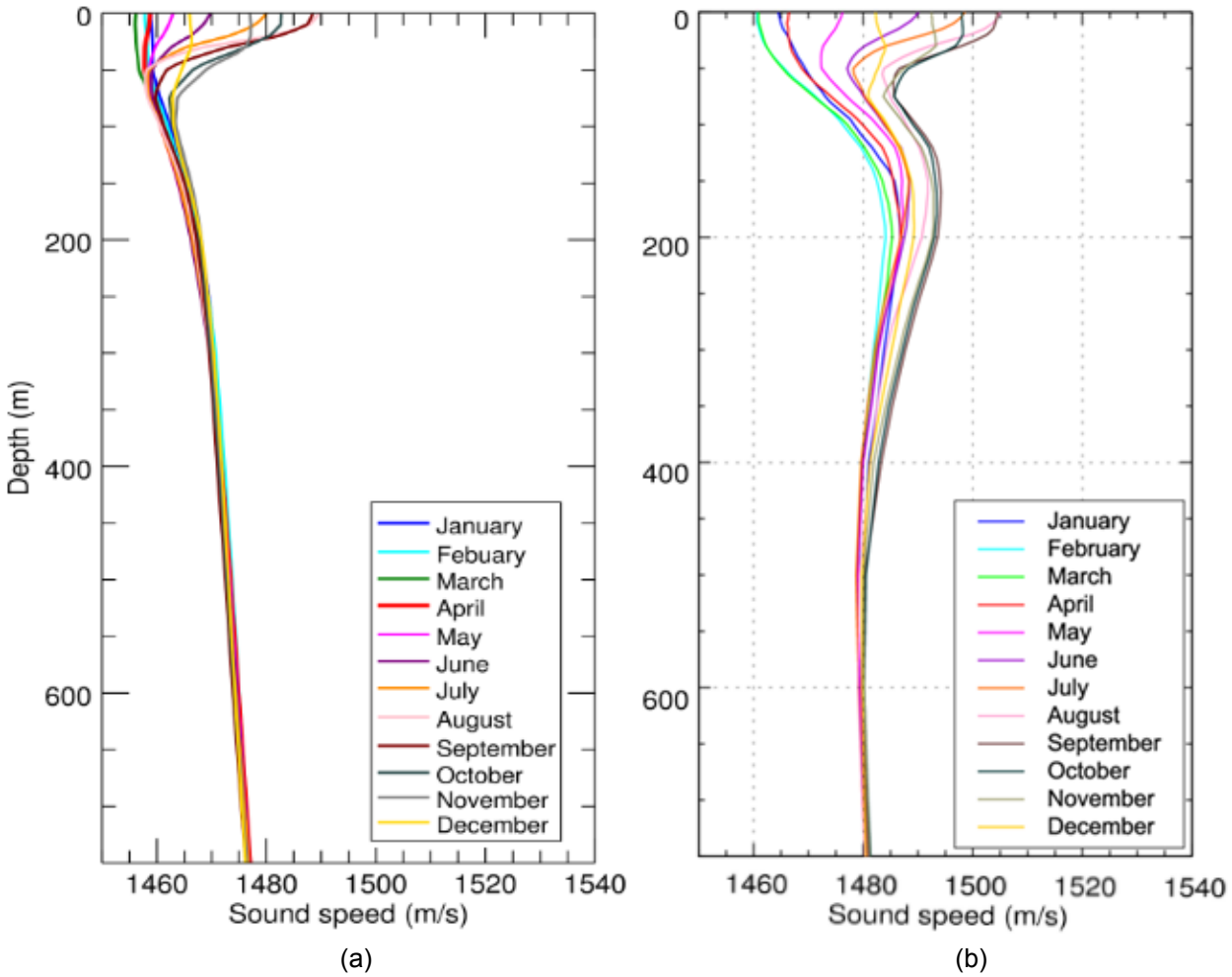

Figure 10. Mean monthly sound speed profiles for the a) Eastern Newfoundland Exploration Drilling Project Area and b) Scotian Basin Exploration Drilling Project (Zykov 2016), derived from data obtained from *GDEM V 3.0* (Teague et al. 1990, Carnes 2009).

The upper portion of the sound speed profile in the Eastern Newfoundland Exploration Drilling Project Area (Figure 9a) varies between isovelocity (January to March) and downward refracting (June to November), down to a depth of ~50–75 m. The sound will tend to refract toward the surface in January-March, but toward the sound speed minimum at 50–75 m in June-November There is little temporal variation in the profiles at depths greater than ~100 m. The sound speed increases slightly with depth, which will refract sound toward the sea surface, promoting long-range sound propagation.

In contrast, the sound speed profile from the Scotian Basin Exploration Drilling program (Figure 9b) results in more complex propagation effects. In winter, there is a strong sound speed minimum in the top 200 m of the water column that supports long range propagation. Below 200 m, there is a second sound speed minimum that tends to confine sound closer to the seabed where it is attenuated through spreading and absorption. In summer, there is a weaker sub-surface sound speed minimum near 50 m, and a stronger deep sound channel minimum. Thus, the sounds of the Scotian Basin drilling program were expected to be 120 dB re 1 µPa 150 km away in winter, and ~50 km away in summer.

The sound speed profile in the Eastern Newfoundland Exploration Drilling Project Area is weakly upward refracting throughout most of the water column. We expect that the effects of the sound speed profile on sound propagation will be between the two conditions modelled for the Scotian Basin project. In the Eastern Newfoundland Exploration Drilling Project Area, we expect less change in propagation conditions throughout the year than were predicted for the Scotian Basin.

3.4. Propagation Effects

Sound propagation in the ocean is a complex process that depends on several factors. Sound levels from an omnidirectional point source in the water column are reduced with range, a process known as *geometric spreading*. Before the sound emanating from the point source reaches the seabed or sea surface boundaries, waves propagate in a spherical pattern. In this case, the received levels at a recorder located a distance R from the source are $20\log R$ dB lower than the levels measured at 1 m from the source. This is known as spherical geometric spreading. Once the waves interact with the sea surface and seabed, propagation in the form of cylindrical waves takes place, leading to cylindrical geometric spreading with a lower range-dependent decay of $10\log R$ dB. Spherical and cylindrical spreading factors provide rules of thumb for quick assessment of the expected levels from a given source. However, more realistic scenarios must consider other factors related to losses at the seabed and sea surface, source frequency spectrum, and environment.

In general, sound levels at short ranges are higher in shallow waters compared to deep waters. This is because in deep waters (and at ranges less than a water depth), sound levels are determined by acoustic arrivals from the source and perhaps from energy bouncing off the air-water interface, while for shallow environments at the same range, sound levels can increase due to contributions from multiple bounces off the seabed. The opposite situation can also be experienced at far ranges (i.e., several water depths for both deep and shallow waters): for shallow waters there are significant losses in acoustic energy due to multiple bounces off the seabed, while for deep waters there are comparatively less interactions of the acoustic wave with the seabed. These general trends must be applied with caution, due to the high complexity of the ocean waveguide.

In addition to the environmental parameters (bathymetry, sound speed profile, and seabed geoacoustics), the frequency content of the sound plays an important role in how it propagates in the ocean. For example, acoustic energy is attenuated by molecular absorption in seawater. The volumetric sound absorption is quantified by an attenuation coefficient, expressed in units of decibels per kilometre (dB/km). This absorption coefficient depends on the temperature, salinity, and pressure of the water, as well as the sound frequency. In general, the absorption coefficient increases with the square of the frequency (i.e., low frequencies are less affected). The absorption of acoustic wave energy has a noticeable effect (>0.05 dB/km) at frequencies above 1 kHz. For example, at 10 kHz the absorption loss over 10 km distance can exceed 10 dB, as computed according to the formulae of François and Garrison (1982a, b). Another mechanism of absorption in the water column is scattering, which results from the sound wave interacting with non-homogeneities (such as air bubbles) and with the rough boundaries at

the air-sea and sea-seabed interfaces. Acoustic energy lost due to scattering is also frequency-dependent, with most noticeable effect when the scatterer is of the same size or larger than the sound wavelength. Therefore, low frequencies are less affected by scattering compared to sounds at high frequencies.

Despite low frequencies being less affected by absorption and scattering, there are other mechanisms that yield the opposite effect (i.e., supporting propagation of sounds at higher frequencies). For example, propagation through a surface duct only applies to frequencies above a certain cut-off. When sound has strong frequency components above this cut-off, acoustic energy is trapped in the surface channel. This trapped energy does not interact with the seabed, so it propagates to farther ranges. Low-frequency sounds, on the other hand, tend to interact with the seabed and are attenuated as they propagate through the seabed sediment.

4. Source Levels

4.1. Semisubmersible Platform, Drillship, and Support Vessel

The source levels associated with drill rigs and support vessels can be estimated based on the platform's number of propellers DP thrusters, their diameter, revolution rate, and number of blades. The source spectrum can be estimated based on the generic spectrum suggested by Brown (1977).

For this project, we considered the semisubmersible platforms West Hercules and West Aquarius (Seadrill). Table 5 provides their parameters. At the time of this preliminary study, the nominal propeller speed and the number of blades were unavailable for the Seadrill vessels. The acoustic spectrum of a semisubmersible platform of similar characteristics–SeaDrill's West Sirius–has been previously modelled (Zykov 2016) and can provide a reference of the expected source levels. Based on the similarity in thruster power, propeller diameter, and number of thrusters, it is expected that the West Hercules/West Aquarius will exhibit similar source levels as those from the West Sirius.

If a drillship is required, the Stena Carron is a representative vessel, which has an identical DP system to the Deep Ocean Clarion drillship that was also included in Zykov (2016).

At the time of this preliminary study, the type of support vessel that may be used in the Project was unknown. The estimates of acoustic source levels and sound spectrum for the support vessel were based on the Damen platform supply vessel 3300CD (Zykov 2016). This vessel design has been in service for 5–7 years, including on the Scotian Basin Exploration Drilling Project. It has a similar power plant and thruster configuration to other platform supply vessels. The vessel's specifications are presented in Table 5.

Table 5. Propulsion system specification of semisubmersible drilling units, drillships, and a supply vessel. The specification for units considered in previous studies of similar operations (Zykov 2016) are shown in blue.

Sound source		Propeller diameter (m)	Nominal propeller speed (rpm)	Max. power (kW)	Number of thrusters	Thruster model	Number of blades	Acoustic source depth* (m)
Semisubmersible unit	West Hercules/ West Aquarius	3.5	NA	3500	8	Rolls Royce, specific model N/A	N/A	21.25
	West Sirius	3.5	177	3800	8	UUC355	4	18
Drillship unit	Deep Ocean Clarion (equivalent to Stena Carron)	4.1	157	5500	6	UUC455	4	9.95
Damen platform supply vessel 3300CD	Main thrusters	2.3	250	2000	2	N/A (azimuthal)	4	5
	Bow thrusters	1.7	290	750	2	N/A (tunnel)	4	5

* Draft-1/2 propeller diameter
N/A means the data were "Not Available" at the time of this preliminary study.

Sound spectra and broadband source levels for the Clarion, West Sirius, and Damen units are expected to be representative of the levels for the Eastern Newfoundland Exploration Drilling Project. Figure 10 provides the estimated source spectra of individual thrusters of models UUC335 (West Sirius), UUC455 (Clarion), and the bow/aft thrusters for the Damen. Source levels for acoustic modelling at far ranges (i.e., where multiple thrusters can be approximated as an equivalent single monopole) were obtained by including the total number of thrusters per vessel (Zykov 2016), resulting in the following broadband levels:

- Deep Ocean Clarion drillship: 196.7 dB re 1 µPa @ 1 m,
- West Sirius semi-submersible platform: 196.7 dB re 1 µPa @ 1 m,
- Damen support vessel: 188.6 dB re 1 µPa @ 1 m.

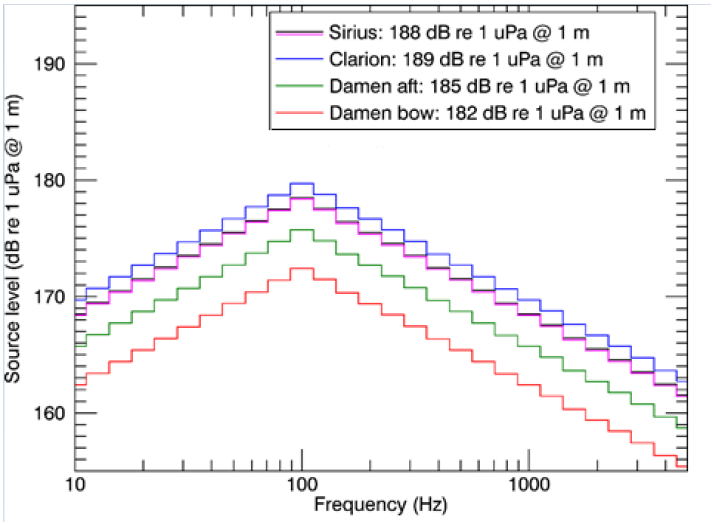

Figure 11. Estimated sound spectra from cavitating propellers of individual thrusters (Zykov 2016). Broadband SPL for each thruster type are provided in the legend.

4.2. VSP Source Array

The activities planned for this operation include Vertical Seismic Profiling (VSP) surveys, which typically use arrays with 3–6 sound source elements with volumes between 150–250 in^3. As a conservative estimate, a 6-element array with 250 in^3 airguns (1500 in^3 total firing volume), such as the Schlumberger's Hypercluster Air Gun Array, was assumed. This array consists of two triangular 3-element airgun clusters, separated 1.7 m, with a central tow depth of 5 m (Figure 11, Table 6).

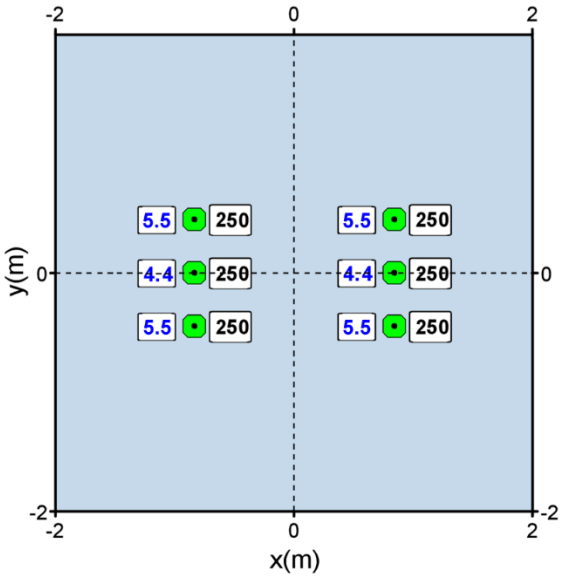

Figure 12. Layout of the modelled airgun array (1500 in^3 total firing volume, 5 m depth), composed of 6 airguns. Labels with black numbers indicate airgun firing volume in cubic inches. The labels with blue numbers indicate the depth of the gun relative to the sea surface.

Table 6. Relative airgun positions within the 1500 in³ airgun array.

Gun	*x* (m)	*y* (m)	*z* (m)	Volume (in^3)
1	0	-0.85	4.4	250
2	-0.445	-0.85	5.5	250
3	0.445	-0.85	5.5	250
4	0	0.85	4.4	250
5	-0.445	0.85	5.5	250
6	0.445	0.85	5.5	250

The source levels and directivity of the airgun array were predicted using JASCO's Airgun Array Source Model (AASM, Appendix A), which accounts for:

- Array layout.
- Volume, tow depth, and firing pressure of each airgun.
- Interactions between different airguns in the array.

The horizontal overpressure signatures and corresponding power spectrum levels for the 1500 in^3 airgun array, at depth of 5 m (to the vertical centre of the gun clusters), are shown in Figure 12 and Table 7 for the broadside (perpendicular to the tow direction) and endfire (parallel to the tow direction) directions. The signatures consist of a strong primary peak related to the initial firing of the airguns, followed by a series of pulses associated with bubble oscillations. Most energy is produced at frequencies below 400 Hz (Figure 12b). The spectrum contains peaks and nulls resulting from interference among airguns in the array, where the frequencies at which they occur depend on the volumes of the airguns and their locations within the array. The horizontal 1/3-octave-band directivities are shown in Figure 13.

For this array, energy is expected to be concentrated in the frequency band 10 to 315 Hz, with broadband SEL of 222.6 dB re 1 µPa^2 @ 1 m (broadside) and 222.4 dB re 1 µPa^2 @ 1 m (endfire).

For comparison purposes, the VSP array used in the Scotian Basin Exploration Drilling Project (Zykov 2016) was the Schlumberger Dual Magnum 2400 in^3 airgun source array at depth 4.5 m. This airgun array consists of four triangular clusters with in-line separations of 2 m; the two external clusters are assemblies of three 250 in³ elements and the two internal clusters are assemblies of three 150 in³ elements. AASM modelling of this 2400 in³ array yielded broadband SEL of 224.7 dB re 1 µPa^2 @ 1 m (broadside) and 224.1 dB re 1 µPa^2 @ 1 m (endfire), with most of its energy in the frequency band 10 to 200 Hz.

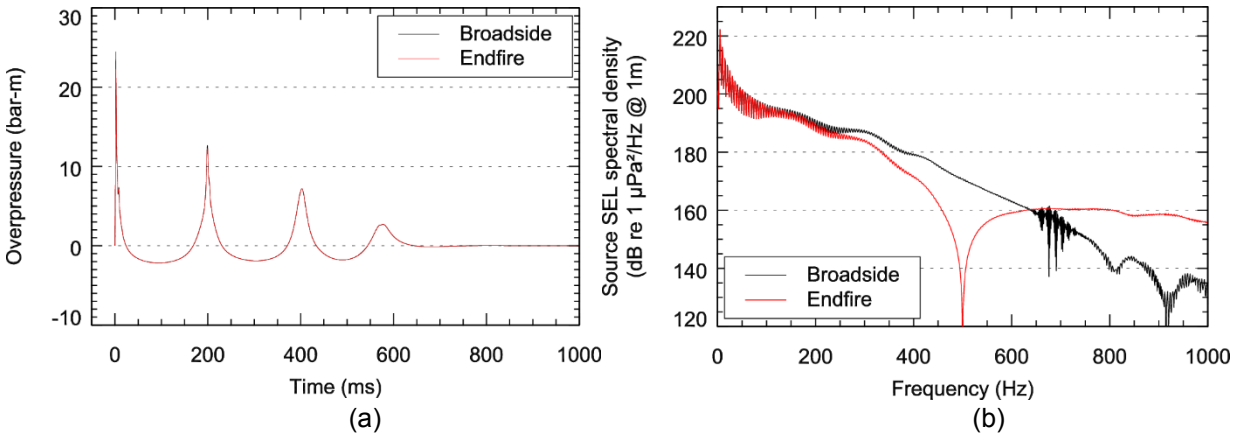

Figure 13. Predicted a) overpressure signature and b) power spectrum in the broadside and endfire (horizontal) directions for the 1500 in^3 array. Surface ghosts (effects of the pulse reflection at the water surface) are not included in these signatures as they are accounted for by the MONM propagation model.

Table 7. Horizontal source level specifications (10–2000 Hz) for the 1500 in^3 seismic airgun array at 5 m depth, computed with AASM in the broadside and endfire directions. Surface ghost effects are not included as they are accounted for by the MONM propagation model.

Direction	Zero-to-peak SPL (dB re 1 µPa @ 1 m)	SEL (dB re 1 µPa^2 @ 1 m)		
		0.01–2 kHz	0.01–1 kHz	1–2 kHz
Broadside	247.8	222.6	222.6	169.5
Endfire	247.0	222.4	222.4	179.2

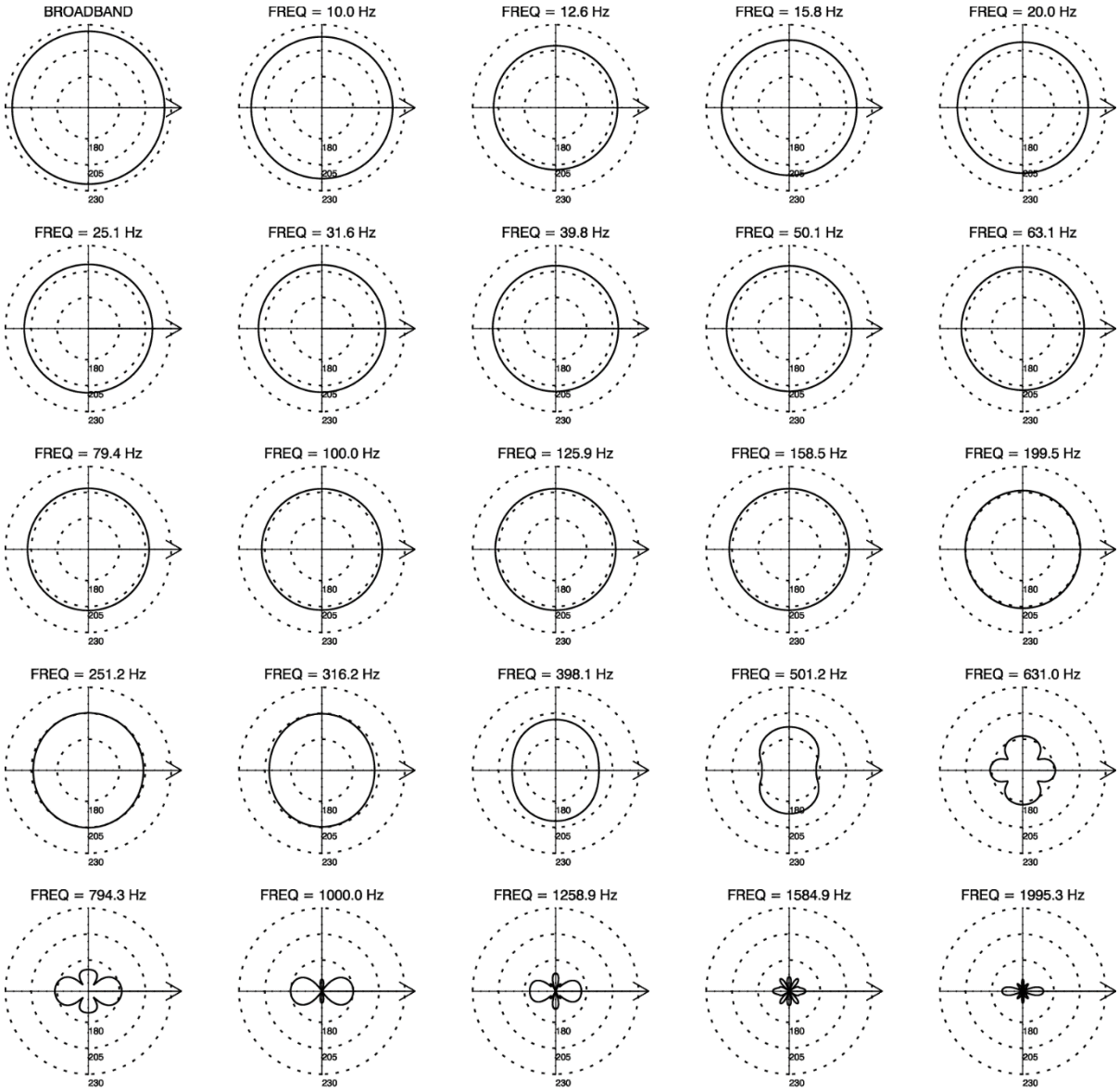

Figure 14. Horizontal directivity of the 1500 in^3 array. Source levels (dB re 1 µPa^2·s) in 1/3-octave-bands. The 1/3-octave-band centre frequencies are indicated above each plot.

5. Conclusion

The year-long data set collected in 2015–2016 provides new information on the ambient soundscape in the Eastern Newfoundland Exploration Drilling Project Area. In general, the ambient sound levels are higher in winter due to fin whales and the effects of higher winds and sea states. Within ranges on the order of 10–40 km from oil and gas platforms, the sounds from the human activities are dominant sound sources for the band of 45–2250 Hz. The effects extend to longer ranges in shallow waters. When present, seismic sources increase the mean monthly sound pressure level by 20 dB or more over large areas.

Accurate assessment of the joint impact of parameters, such as sound speed profile, bathymetry, geoacoustics, and source spectra, can only be achieved by rigourous acoustic propagation modelling. However, the following statements are likely to hold:

- Due to similarities in source levels, seabed geoacoustics, and sound speed profiles, the modelling work previously done at the Scotian Basin (2790 m depth) provides a good reference for the expected sound levels at Sites B and C (1500 and 3000 m depth, respectively) of the current Project. Therefore, distances to thresholds for scenarios involving a drillship/semisubmersible platform with or without a supporting vessel at Sites B and C will be similar to those for the Scotian Basin modelling (Site A from Zykov 2016). The 120 dB re 1 µPa SPL threshold is expected to be reached at maximum distances R_{max} >150 km in winter and R_{max} ~51.6 km in summer.
- Based on the rationale in Section 3.1, for Site A (and in general, for operation sites at shallow water) distances to thresholds corresponding to high levels (e.g., SPL thresholds of 180–190 dB re 1 µPa) are expected to be longer than those modelled for the Scotian Basin Exploration Drilling Project. The opposite would be expected for lower sound level thresholds (e.g., SPL of 120 dB re 1 µPa).
- The most conservative winter sound speed profile for this Project exhibits a weaker surface channel compared to the February profile used in the Scotian Basin modelling. Therefore, the surface channel is not expected to be as conductive to sound, and it will likely yield shorter distances to thresholds.
- Differences in the summer and winter profiles are not as substantial as those in the Scotian Basin area; therefore, distances to thresholds are likely to be more similar in summer and winter in the Eastern Newfoundland Exploration Drilling Project Area than they were at the Scotia Basin site
- Distance to thresholds related to the seismic VSP measurements are likely to be smaller than those from Scotian Basin, due to broadband levels that are ~2 dB lower for this Project's proposed array. This is also based on the observation that both arrays exhibit similar frequency content, with most energy at frequencies < 315 Hz.

Glossary

1/3-octave-band
Non-overlapping passbands that are one-third of an octave wide (where an octave is a doubling of frequency). Three adjacent 1/3-octave-bands comprise one octave. One-third-octave-bands become wider with increasing frequency. Also see octave.

90%-energy time window
The time interval over which the cumulative energy rises from 5% to 95% of the total pulse energy. This interval contains 90% of the total pulse energy. Symbol: T_{90}.

90% sound pressure level (90% SPL)
The root-mean-square sound pressure levels calculated over the 90%-energy time window of a pulse. Used only for pulsed sounds.

absorption
The conversion of acoustic energy into heat, which is captured by insulation.

ambient noise
All-encompassing sound at a given place, usually a composite of sound from many sources near and far (ANSI S1.1-1994 R2004), e.g., shipping vessels, seismic activity, precipitation, sea ice movement, wave action, and biological activity.

attenuation
The gradual loss of acoustic energy from absorption and scattering as sound propagates through a medium.

azimuth
A horizontal angle relative to a reference direction, which is often magnetic north or the direction of travel. In navigation it is also called bearing.

background noise
Total of all sources of interference in a system used for the production, detection, measurement, or recording of a signal, independent of the presence of the signal (ANSI S1.1-1994 R2004). Ambient noise detected, measured, or recorded with a signal is part of the background noise.

bandwidth
The range of frequencies over which a sound occurs. Broadband refers to a source that produces sound over a broad range of frequencies (e.g., seismic airguns, vessels) whereas narrowband sources produce sounds over a narrow frequency range (e.g., sonar) (ANSI/ASA S1.13-2005 R2010).

broadband sound level
The total sound pressure level measured over a specified frequency range. If the frequency range is unspecified, it refers to the entire measured frequency range.

broadside direction
Perpendicular to the travel direction of a source. Compare with endfire direction.

cavitation
A rapid formation and collapse of vapor cavities (i.e., bubbles or voids) in water, most often caused by a rapid change in pressure. Fast-spinning vessel propellers typically cause cavitation, which creates a lot of noise.

compressional wave
A mechanical vibration wave in which the direction of particle motion is parallel to the direction of propagation. Also called primary wave or P-wave.

continuous sound
A sound whose sound pressure level remains above ambient sound during the observation period (ANSI/ASA S1.13-2005 R2010). A sound that gradually varies in intensity with time, for example, sound from a marine vessel.

decibel (dB)
One-tenth of a bel. Unit of level when the base of the logarithm is the tenth root of ten, and the quantities concerned are proportional to power (ANSI S1.1-1994 R2004).

endfire direction
Parallel to the travel direction of a source. See also broadside direction.

far-field
The zone where, to an observer, sound originating from an array of sources (or a spatially-distributed source) appears t o radiate from a single point. The distance to the acoustic far-field increases with frequency.

fast-average sound pressure level
The time-averaged sound pressure levels calculated over the duration of a pulse (e.g., 90%-energy time window), using the leaky time integrator from Plomp and Bouman (1959) and a time constant of 125 ms. Typically used only for pulsed sounds.

frequency
The rate of oscillation of a periodic function measured in cycles-per-unit-time. The reciprocal of the period. Unit: hertz (Hz). Symbol: *f*. 1 Hz is equal to 1 cycle per second.

geoacoustic
Relating to the acoustic properties of the seabed.

hertz (Hz)
A unit of frequency defined as one cycle per second.

hydrophone
An underwater sound pressure transducer. A passive electronic device for recording or listening to underwater sound.

impulsive sound
Sound that is typically brief and intermittent with rapid (within a few seconds) rise time and decay back to ambient levels (NOAA 2013, ANSI S12.7-1986 R2006). For example, seismic airguns and impact pile driving.

non-impulsive sound
Sound that is broadband, narrowband or tonal, brief or prolonged, continuous or intermittent, and typically does not have a high peak pressure with rapid rise time (typically only small fluctuations in decibel level) that impulsive signals have (ANSI/ASA S3.20-1995 R2008). For example, marine vessels, aircraft, machinery, construction, and vibratory pile driving (NIOSH 1998, NOAA 2015).

octave
The interval between a sound and another sound with double or half the frequency. For example, one octave above 200 Hz is 400 Hz, and one octave below 200 Hz is 100 Hz.

peak pressure level (PK)
The maximum instantaneous sound pressure level, in a stated frequency band, within a stated period. Also called zero-to-peak pressure level. Unit: decibel (dB).

phocid
A common term used to describe all members of the family Phocidae. These true/earless seals are more adapted to in-water life than are otariids, which have more terrestrial adaptations. Phocids use their hind flippers to propel themselves. Phocids are one of the three main groups in the superfamily Pinnipedia; the other two groups are otariids and walrus.

pinniped
A common term used to describe all three groups that form the superfamily Pinnipedia: phocids (true seals or earless seals), otariids (eared seals or fur seals and sea lions), and walrus.

point source
A source that radiates sound as if from a single point (ANSI S1.1-1994 R2004).

power spectrum density
The acoustic signal power per unit frequency as measured at a single frequency. Unit: $\mu Pa^2/Hz$, or $\mu Pa^2 \cdot s$.

power spectral density level
The decibel level ($10\log_{10}$) of the power spectrum density, usually presented in 1 Hz bins. Unit: dB re 1 $\mu Pa^2/Hz$.

pressure, acoustic
The deviation from the ambient hydrostatic pressure caused by a sound wave. Also called overpressure. Unit: pascal (Pa). Symbol: *p*.

pressure, hydrostatic
The pressure at any given depth in a static liquid that is the result of the weight of the liquid acting on a unit area at that depth, plus any pressure acting on the surface of the liquid. Unit: pascal (Pa).

received level
The sound level measured at a receiver.

rms
root-mean-square.

shear wave
A mechanical vibration wave in which the direction of particle motion is perpendicular to the direction of propagation. Also called secondary wave or S-wave. Shear waves propagate only in solid media, such as sediments or rock. Shear waves in the seabed can be converted to compressional waves in water at the water-seabed interface.

signature
Pressure signal generated by a source.

sound
A time-varying pressure disturbance generated by mechanical vibration waves travelling through a fluid medium such as air or water.

sound exposure
Time integral of squared, instantaneous frequency-weighted sound pressure over a stated time interval or event. Unit: pascal-squared second ($Pa^2 \cdot s$) (ANSI S1.1-1994 R2004).

sound exposure level (SEL)
A cumulative measure related to the sound energy in one or more pulses. Unit: dB re 1 $\mu Pa^2 \cdot s$. SEL is expressed over the summation period (e.g., per-pulse SEL [for airguns], single-strike SEL [for pile drivers], 24-hour SEL).

sound intensity
Sound energy flowing through a unit area perpendicular to the direction of propagation per unit time.

sound pressure level (SPL)
The decibel ratio of the time-mean-square sound pressure, in a stated frequency band, to the square of the reference sound pressure (ANSI S1.1-1994 R2004).

For sound in water, the reference sound pressure is one micropascal (p_0 = 1 µPa) and the unit for SPL is dB re 1 µPa:

$$\mathrm{SPL} = 10\log_{10}\left(p^2 / p_0^2\right) = 20\log_{10}\left(p / p_0\right)$$

Unless otherwise stated, SPL refers to the root-mean-square sound pressure level. See also 90% sound pressure level and fast-average sound pressure level. Non-rectangular time window functions may be applied during calculation of the rms value, in which case the SPL unit should identify the window type.

sound speed profile
The speed of sound in the water column as a function of depth below the water surface.

source level (SL)
The sound level measured in the far-field and scaled back to a standard reference distance of 1 metre from the acoustic centre of the source. Unit: dB re 1 µPa @ 1 m (sound pressure level) or dB re 1 $\mu Pa^2 \cdot s$ (sound exposure level).

spectrum
An acoustic signal represented in terms of its power (or energy) distribution compared with frequency.

surface duct
The upper portion of a water column within which the sound speed profile gradient causes sound to refract upward and therefore reflect off the surface resulting in relatively long range sound propagation with little loss.

transmission loss (TL)
The decibel reduction in sound level between two stated points that results from sound spreading away from an acoustic source subject to the influence of the surrounding environment. Also called propagation loss.

wavelength
Distance over which a wave completes one oscillation cycle. Unit: meter (m). Symbol: λ.

Literature Cited

[NIOSH] National Institute for Occupational Safety and Health. 1998. *Criteria for a recommended standard: Occupational noise exposure*. Document Number 98-126. U.S. Department of Health and Human Services, NIOSH, Cincinnati, Ohio. 122 pp.

[NMFS] National Marine Fisheries Service. 2016. *Technical Guidance for Assessing the Effects of Anthropogenic Sound on Marine Mammal Hearing: Underwater Acoustic Threshold Levels for Onset Permanent and Temporary Threshold Shifts*. U.S. Department of Commerce, NOAA. NOAA Technical Memorandum NMFS-OPR-55. 178 pp. http://www.nmfs.noaa.gov/pr/acoustics/Acoustic%20Guidance%20Files/opr-55_acoustic_guidance_tech_memo.pdf.

[NOAA] National Oceanic and Atmospheric Administration. 2013. *Draft guidance for assessing the effects of anthropogenic sound on marine mammals: Acoustic threshold levels for onset of permanent and temporary threshold shifts*, December 2013, 76 pp. Silver Spring, Maryland: NMFS Office of Protected Resources. http://www.nmfs.noaa.gov/pr/acoustics/draft_acoustic_guidance_2013.pdf.

[NOAA] National Oceanic and Atmospheric Administration. 2015. *Draft guidance for assessing the effects of anthropogenic sound on marine mammal hearing: Underwater acoustic threshold levels for onset of permanent and temporary threshold shifts*, July 2015, 180 pp. Silver Spring, Maryland: NMFS Office of Protected Resources. http://www.nmfs.noaa.gov/pr/acoustics/draft%20acoustic%20guidance%20July%202015.pdf.

ANSI S12.7-1986. R2006. *American National Standard Methods for Measurements of Impulsive Noise*. American National Standards Institute, New York.

ANSI S1.1-1994. R2004. *American National Standard Acoustical Terminology*. American National Standards Institute, New York.

ANSI/ASA S1.13-2005. R2010. *American National Standard Measurement of Sound Pressure Levels in Air*. American National Standards Institute and Acoustical Society of America, New York.

ANSI/ASA S3.20-1995. R2008. *American National Standard Bioacoustical Terminology*. American National Standards Institute and Acoustical Society of America, New York.

Brown, N.A. 1977. Cavitation noise problems and solutions. *Proceedings International Symposium on Shipboard Acoustics*: 18.

Buckingham, M.J. 2005. Compressional and shear wave properties of marine sediments: Comparisons between theory and data. *Journal of the Acoustical Society of America* 117(1): 137-152. http://link.aip.org/link/?JAS/117/137/1.

Carnes, M.R. 2009. *Description and Evaluation of GDEM-V 3.0*. Document Number NRL Memorandum Report 7330-09-9165. US Naval Research Laboratory, Stennis Space Centre, MS. 21 pp.

Cato, D.H. 2008. Ocean ambient noise: Its measurement and its significance to marine animals. *Proceedings of the Institute of Acoustics* 30(5): 1-9.

Coppens, A.B. 1981. Simple equations for the speed of sound in Neptunian waters. *Journal of the Acoustical Society of America* 69(3): 862-863. http://link.aip.org/link/?JAS/69/862/1.

Divins, D.L. 2007. Total sediment thickness of the world's oceans & marginal seas. National Geophysical Data Centre, National Oceanic and Atmospheric Administration, US Department of Commerce. http://www.ngdc.noaa.gov/mgg/sedthick/sedthick.html (Accessed May 2007).

Dragoset, W.H. 1984. A comprehensive method for evaluating the design of airguns and airgun arrays. *Proceedings, 16th Annual Offshore Technology Conference* Volume 3, May 7-9, 1984. OTC 4747, Houston, Houston. 75–84 pp.

François, R.E. and G.R. Garrison. 1982a. Sound absorption based on ocean measurements: Part I: Pure water and magnesium sulfate contributions. *Journal of the Acoustical Society of America* 72(3): 896-907.

François, R.E. and G.R. Garrison. 1982b. Sound absorption based on ocean measurements: Part II: Boric acid contribution and equation for total absorption. *Journal of the Acoustical Society of America* 72(6): 1879-1890.

Géli, L., J. Cochran, T. Lee, J. Francheteau, C. Labails, C. Fouchet, and D. Christie. 2007. Thermal regime of the Southeast Indian Ridge between 88°E and 140°E: Remarks on the subsidence of the ridge flanks. *J. Geophys. Res.* 112(B10): B10101.

Gordon, J., D. Gillespie, J. Potter, A. Frantzis, M.P. Simmonds, R. Swift, and D. Thompson. 2003. A review of the effects of seismic surveys on marine mammals. *Marine Technology Society Journal* 37(4): 16-34. http://www.ingentaconnect.com/content/mts/mtsj/2003/00000037/00000004/art00003.

Hildebrand, J.A. 2009. Anthropogenic and natural sources of ambient noise in the ocean. *Marine Ecology Progress Series* 395: 5-20.

Huppertz, T.J. 2007. *Late Quaternary History of Flemich Pass, Southeast Canadian Continental Margin*. M.Sc. Thesis. Dalhousie University, Halifax, Nova Scotia. 137 pp.

Landro, M. 1992. Modelling of GI gun signatures. *Geophysical Prospecting* 40: 721–747.

Laws, M., L. Hatton, and M. Haartsen. 1990. Computer modelling of clustered airguns. *First Break* 8: 331–338.

Lurton, X. 2002. *An Introduction to Underwater Acoustics: Principles and Applications*. Springer, Chichester, U.K. 347.

MacGillivray, A.O. 2006. *Acoustic Modelling Study of Seismic Airgun Noise in Queen Charlotte Basin*. MSc Thesis. University of Victoria, Victoria, BC. 98 pp.

McCauley, R.D., J. Fewtrell, A.J. Duncan, C. Jenner, M.-N. Jenner, J.D. Penrose, R.I.T. Prince, A. Adihyta, J. Murdoch, et al. 2000. Marine seismic surveys: A study of environmental implications. *Australian Petroleum Production Exploration Association (APPEA) Journal* 40: 692-708.

Melcon, M.L., A.J. Cummins, S.M. Kerosky, L.K. Roche, S.M. Wiggins, and J.A. Hildebrand. 2012. Blue whales respond to anthropogenic noise. *PLoS ONE* 7(2): 1-6. http://www.plosone.org/article/info%3Adoi%2F10.1371%2Fjournal.pone.0032681.

Nieukirk, S.L., D.K. Mellinger, S.E. Moore, K. Klinck, R.P. Dziak, and J. Goslin. 2012. Sounds from airguns and fin whales recorded in the mid-Atlantic Ocean, 1999–2009. *Journal of the Acoustical Society of America* 131(2): 1102-1112.

Plomp, R. and M.A. Bouman. 1959. Relation between Hearing Threshold and Duration for Tone Pulses. *The Journal of the Acoustical Society of America* 31(6): 749-758. http://scitation.aip.org/content/asa/journal/jasa/31/6/10.1121/1.1907781.

Popper, A.N., A.D. Hawkins, R.R. Fay, D.A. Mann, S. Bartol, T.J. Carlson, S. Coombs, W.T. Ellison, R.L. Gentry, et al. 2014. *Sound Exposure Guidelines for Fishes and Sea Turtles: A Technical Report prepared by ANSI-Accredited Standards Committee S3/SC1 and registered with ANSI*. SpringerBriefs in Oceanography, Volume ASA S3/SC1.4 TR-2014. ASA Press. 87 pp.

Racca, R.G. and J.A. Scrimger. 1986. *Underwater Acoustic Source Characteristics of Air and Water Guns*. Document Number DREP Tech. Rep. 06SB 97708-5-7055. Report by JASCO Research Ltd. for Defence Research Establishment Pacific (Canada), Victoria, BC.

Rodríguez, E., C.S. Morris, Y.J.E. Belz, E.C. Chapin, J.M. Martin, W. Daffer, and S. Hensley. 2005. *An Assessment of the SRTM Topographic Products*. Document Number JPL D-31639. Jet Propulsion Laboratory, Pasadena, CA.

Teague, W.J., M.J. Carron, and P.J. Hogan. 1990. A comparison between the Generalized Digital Environmental Model and Levitus climatologies. *Journal of Geophysical Research* 95(C5): 7167-7183.

Ziolkowski, A. 1970. A method for calculating the output pressure waveform from an air gun. *Geophysical Journal of the Royal Astronomical Society* 21(2): 137-161.

Zykov, M.M. 2016. *Modelling Underwater Sound Associated with Scotian Basin Exploration Drilling Project: Acoustic Modelling Report.* Document Number JASCO Document 01112, Version 2.0. Technical report by JASCO Applied Sciences for Stantec Consulting Ltd. http://www.ceaa.gc.ca/050/documents/p80109/116305E.pdf.

Appendix A. JASCO's Airgun Array Source Model

The source levels and directivity of the airgun array were predicted with JASCO's Airgun Array Source Model (AASM; MacGillivray 2006). AASM includes both a low-frequency and a high-frequency module for predicting different components of the airgun array spectrum. The low frequency module is based on the physics of oscillation and radiation of airgun bubbles, as originally described by Ziolkowski (1970), that solves the set of parallel differential equations that govern bubble oscillations. Physical effects accounted for in the simulation include pressure interactions between airguns, port throttling, bubble damping, and generator-injector (GI) gun behaviour discussed by Dragoset (1984), Laws et al. (1990), and Landro (1992). A global optimization algorithm tunes free parameters in the model to a large library of airgun source signatures. These airgun data are measurements of the signatures of Bolt 600/B guns ranging in volume from 5 to 185 in^3 (Racca and Scrimger 1986).

AASM produces a set of notional signatures for each array element based on:

- Array layout
- Volume, tow depth, and firing pressure of each airgun
- Interactions between different airguns in the array

These notional signatures are the pressure waveforms of the individual airguns at a standard reference distance of 1 m; they account for the interactions with the other airguns in the array. The signatures are summed with the appropriate phase delays to obtain the far-field source signature of the entire array in all directions. This far-field array signature is filtered into 1/3-octave-bands to compute the source levels of the array as a function of frequency band and azimuthal angle in the horizontal plane (at the source depth), after which it is considered to be a directional point source in the far field.

A seismic array consists of many sources and the point-source assumption is invalid in the near field where the array elements add incoherently. The maximum extent of the near field of an array (R_{nf}) is:

$$R_{\mathrm{nf}} < \frac{l^2}{4\lambda} \qquad \text{(A-1)}$$

where λ is the sound wavelength and l is the longest dimension of the array (Lurton 2002, §5.2.4). For example, an airgun array length of l = 16 m yields a near-field range of 85 m at 2 kHz and 17 m at 100 Hz. Beyond this R_{nf} range, the array is assumed to radiate like a directional point source and is treated as such for propagation modelling.

The interactions between individual elements of the array create directionality in the overall acoustic emission. Generally, this directionality is prominent mainly at frequencies in the mid-range between tens of hertz to several hundred hertz. At lower frequencies, with acoustic wavelengths much larger than the inter-airgun separation distances, the directionality is small. At higher frequencies, the pattern of lobes is too finely spaced to be resolved and the effective directivity is less.

APPENDIX D

Marine Mammals and Ambient Sound Sources in the Flemish Pass:
Analaysis from 2014 and 2015 Acoustic Recordings
(Maxner et al. 2017)

Marine Mammals and Sound Sources in the Flemish Pass

Analysis from 2014 and 2015 Acoustic Recordings

Submitted to:
Colleen Leeder
Statoil Canada Ltd
Purchse Order: 4503553349 / 08/07/2017

Authors:
Emily Maxner
Bruce Martin
Katie Kowarski

2 November 2017

P001273-002
Document 01456
Version 1.0

JASCO Applied Sciences (Canada) Ltd
Suite 202, 32 Troop Ave.
Dartmouth, NS B3B 1Z1 Canada
Tel: +1-902-405-3336
Fax: +1-902-405-3337
www.jasco.com

Suggested citation:

Maxner, E., B. Martin, and K. Kowarski. 2017. Marine Mammals and Ambient Sound Sources in the Flemish Pass: Analysis from 2014 and 2015 Acoustic Recordings. Document 01456, Version 1.0. Technical report by JASCO Applied Sciences for Statoil Canada Ltd.

Disclaimer:

The results presented herein are relevant within the specific context described in this report. They could be misinterpreted if not considered in the light of all the information contained in this report. Accordingly, if information from this report is used in documents released to the public or to regulatory bodies, such documents must clearly cite the original report, which shall be made readily available to the recipients in integral and unedited form.

Contents

Figures

Tables

Executive Summary

An acoustic recorder was deployed in the Flemish Pass from June-October 2014 and from May-September 2015. The data were analyzed to characterize the baseline soundscape, the presence of marine mammals, and characterize the soundscape during Statoil's 2014-2016 drilling program.

Seismic surveys increased baseline sound levels by 10-35 dB throughout the summer months. Drilling operations by the semi-submersible drill rig *West Hercules* generated sound levels similar to those previously reported for the *Stena IceMAX* off Nova Scotia.

Five confirmed species of marine mammals, plus an unknown number of dolphin species (up to six), were detected acoustically. Baleen whale detections were sparse and occurred predominantly in the late summer and early fall, showing pronounced seasonal variations as a result of changes in vocal behavior, migratory movements, or both. Blue whales were detected once in early August and once in early October in 2014, and three times in early September 2015. Only one fin whale call was detected at the beginning of the study period in 2014, but detections increased in early fall 2015. The occurrence of northern bottlenose whales was sporadic throughout the study period in each year and were acoustically active during seismic surveys. In both years, sperm whale calls occurred continuously throughout the recording. Delphinids, which include pilot whales as well as several species of dolphins, were the most broadly detected class. Noise associated with anthropogenic activities, namely seismic surveys, vessel traffic and oil and gas activities, at times restricted or prevented our ability to detected some species.

1. Introduction

The Canadian Atlantic seaboard is home to a wealth of marine life and the site of diverse human activities, including fishing, shipping, and oil and gas activities. To varying degrees, these anthropogenic activities all contribute to the soundscape of the surrounding waters. In 2014 and 2015, Statoil Canada Limited employed a JASCO Applied Sciences (JASCO) acoustic recorder owned by AMEC for opportunistic acoustic recordings at Statoil's 2014-2016 drilling areas off the Canadian Atlantic coast in the Flemish Pass. We present an analysis of these recordings, focusing on the biological (marine mammal) and anthropogenic (seismic surveys, and oil and gas production activities.

1.1. Soniferous Marine Life and Acoustic Monitoring

Passive acoustic monitoring of marine life relies on the monitored species to produce detectable sound. Several marine taxa produce sounds, including all marine mammals as well as some crustaceans (e.g., snapping shrimp; see Au and Banks 1998), and fish (e.g. Nordeide and Kjellsby 1999, Hawkins et al. 2002, Amorim 2006, Erbe et al. 2015). Neither crustaceans, fish spawning aggregations, or fish choruses were present in the acoustic data.

The biological focus of this study was on marine mammals. Twenty-five cetacean and six pinniped species may be found in the study area (Table 1). The presence of pygmy sperm whales is known only from strandings (Measures et al. 2004). Blainville's beaked whales have stranded in Nova Scotia (Mead 1989) and were observed live once near the Gully Canyon (DFO 2016). Gervais' and True's beaked whales may occur in the study area based on habitat characteristics, but have not been sighted or recorded. A bowhead whale sighted in the Bay of Fundy in 2012 is believed to have been a vagrant individual (http://rightwhales.neaq.org/2012/08/11-bowhead-whale-in-bay-of-fundy.html), so detections of this species, if any, would be rare.

Marine mammals are the main biological contributors to the underwater soundscape. For instance, fin whale songs can raise noise levels in the 18–25 Hz band by 5–10 dB over extended time periods (Delarue et al. 2016). Marine mammals, cetaceans in particular, rely almost exclusively on sound for navigating, foraging, breeding, and communicating (Clark 1990, Edds-Walton 1997, Tyack and Clark 2000). Although species differ widely in their vocal behaviour, most can be reasonably expected to produce sounds on a regular basis and passive acoustic monitoring is therefore increasingly preferred as a cost-effective and efficient survey method. Seasonal and sex- or age-biased differences in sound production as well as signal frequency, source level, and directionality all influence the applicability and success rate of acoustic monitoring to some extent and should therefore be considered for each species.

The acoustic signals of some species are poorly known or unknown, which prevents or complicates the acoustic assessment of their occurrence. This is the case for hooded seals, pygmy sperm whales, and True's beaked whales. While the vocal repertoire of most odontocetes in the area is fairly well known, similarities in the spectral features of their signals generally preclude resolving species identity for most detection events. Exceptions include the tonal signals of killer whales and pilot whales and the clicks of sperm whales, beaked whales, and harbour porpoise. In most cases, baleen whale signals can be reliably identified by species.

Table 1. Cetacean and pinniped species known to occur (or possibly occurring) in the study area and their Committee on the Status of Endangered Wildlife in Canada (COSEWIC) and Species at Risk Act (SARA) status.

Species name	Scientific name	COSEWIC status	SARA status
Baleen whales			
Minke whale	*Balaenoptera acutorostrata*	Not at risk	Not listed
Sei whale	*Balaenoptera borealis*	Data deficient	Not listed
Blue whale	*Balaenoptera musculus*	Endangered	Endangered

Fin whale	*Balaenoptera physalus*	Special concern	Special concern
Humpback whale	*Megaptera novaeangliae*	Not at risk	Special concern
North Atlantic right whale	*Eubalaena glacialis*	Endangered	Endangered
Bowhead whale	*Balaena mysticetus*	Special concern	Endangered
Toothed whales			
Short-beaked common dolphin	*Delphinus delphis*	Not at risk	Not listed
Striped dolphin	*Stenella coeruleoalba*	Not at risk	Not listed
White-beaked dolphin	*Lagenorhynchus albirostris*	Not at risk	Not listed
White-sided dolphin	*Lagenorhynchus acutus*	Not at risk	Not listed
Bottlenose dolphin	*Tursiops truncatus*	Not at risk	Not listed
Risso's dolphin	*Grampus griseus*	Not at risk	Not listed
Killer whale	*Orcinus orca*	Special concern	Not listed
Beluga whale	*Delphinapterus leucas*	Endangered[1]	Threatened[1]
Long-finned pilot whale	*Globicephala melas*	Not at risk	Not listed
Harbour porpoise	*Phocoena*	Special concern	Threatened
Pygmy sperm whale	*Kogia breviceps*	Not at risk	Not listed
Sperm whale	*Physeter macrocephalus*	Not at risk	Not listed
Cuvier's beaked whale	*Ziphius cavirostris*	Not at risk	Not listed
Sowerby's beaked whale	*Mesoplodon bidens*	Special concern	Special concern
Northern bottlenose whale	*Hyperoodon ampullatus*	Endangered[2]	Endangered[2]
Blainville's beaked whale	*Mesoplodon densirostris*	Not at risk	Not listed
Gervais beaked whale	*Mesoplodon europaeus*	Not assessed	Not listed
True's beaked whale	*Mesoplodon mirus*	Not at risk	Not listed
Pinnipeds			
Grey seal	*Halichoerus grypus*	Not at risk	Not listed
Ringed seal	*Phoca hispida*	Not at risk	Not listed
Hooded seal	*Cystophora cristata*	Not at risk	Not listed
Bearded seal	*Erignathus barbatus*	Not assessed	Not listed
Harp seal	*Phoca groenlandica*	Not at risk	Not listed
Harbour seal	*Phoca vitulina*	Not at risk	Not listed
Atlantic walrus	*Odobenus rosmarus*	Special concern	Not listed

[1] Status of the Gulf of St. Lawrence population
[2] Status of the Scotian shelf population

1.2. Ambient Sound Levels

The ambient, or background, sound levels that create the ocean soundscape are comprised of many natural and anthropogenic sources (Figure 1). The main environmental sources of sound are wind, precipitation, and sea ice. Wind-generated noise in the ocean is well-described (e.g., Wenz 1962, Ross 1976), and surf noise is known to be an important contributor to near-shore soundscapes (Deane 2000). In polar regions, sea ice can produce loud sounds that are often the main contributor of acoustic energy

in the local soundscape, particularly during ice formation and break up. Precipitation is a frequent noise source, with contributions typically concentrated at frequencies above 500 Hz. At low frequencies (<100 Hz), earthquakes and other geological events contribute to the soundscape.

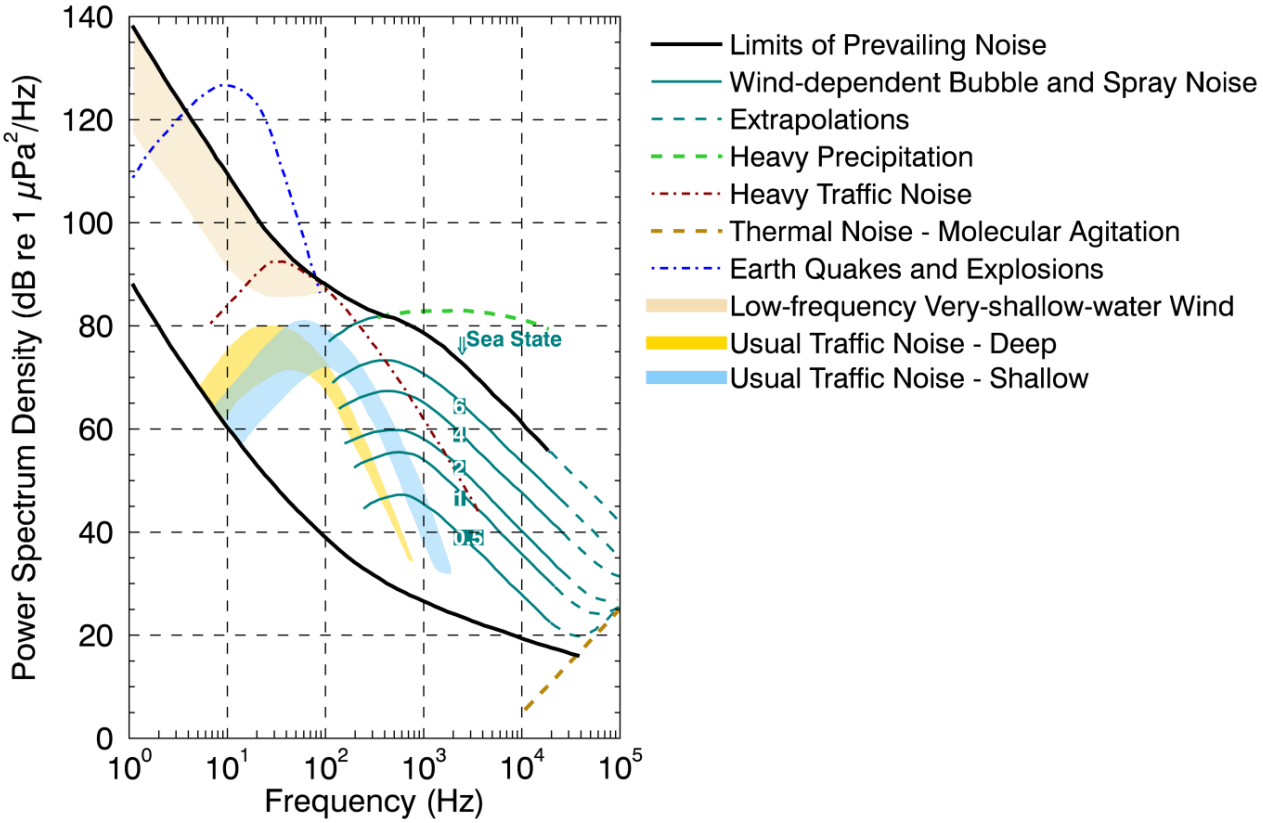

Figure 1. Wenz curves (NRC 2003), describing pressure spectral density levels of marine ambient noise from weather, wind, geologic activity, and commercial shipping, adapted from Wenz (1962).

1.3. Anthropogenic Contributors to the Soundscape

Anthropogenic (human-generated) sound can be a by-product of vessel operations, such as engine noise radiating through vessel hulls and cavitating propulsion systems, or a product of active acoustic data collection with sonar, depth sounding, and seismic surveys. The contribution of anthropogenic sources to the ocean soundscape has increased steadily over the past several decades. The anthropogenic increase is largely driven by greater worldwide amounts of shipping and oil and gas exploration (Hildebrand 2009). Seismic survey sounds have increased significantly following their expansion into deep water, and they can now be detected across ocean basins (Nieukirk et al. 2004). The main anthropogenic contributors to ambient noise in the study area are dynamic positioning vessels and seismic surveys.

1.3.1. Vessel Traffic

There are several major shipping lanes south of the study area. Vessel tracks fan out after leaving the Gulf of St. Lawrence, resulting in constant traffic on the Scotian shelf and in areas south of Newfoundland. A few isolated areas of denser vessel traffic off the coast indicate the location of oil and natural gas extraction platforms and the associated transit of support vessels, as well as areas targeted by seismic surveys and potential fishing hotspots (Figure 2).

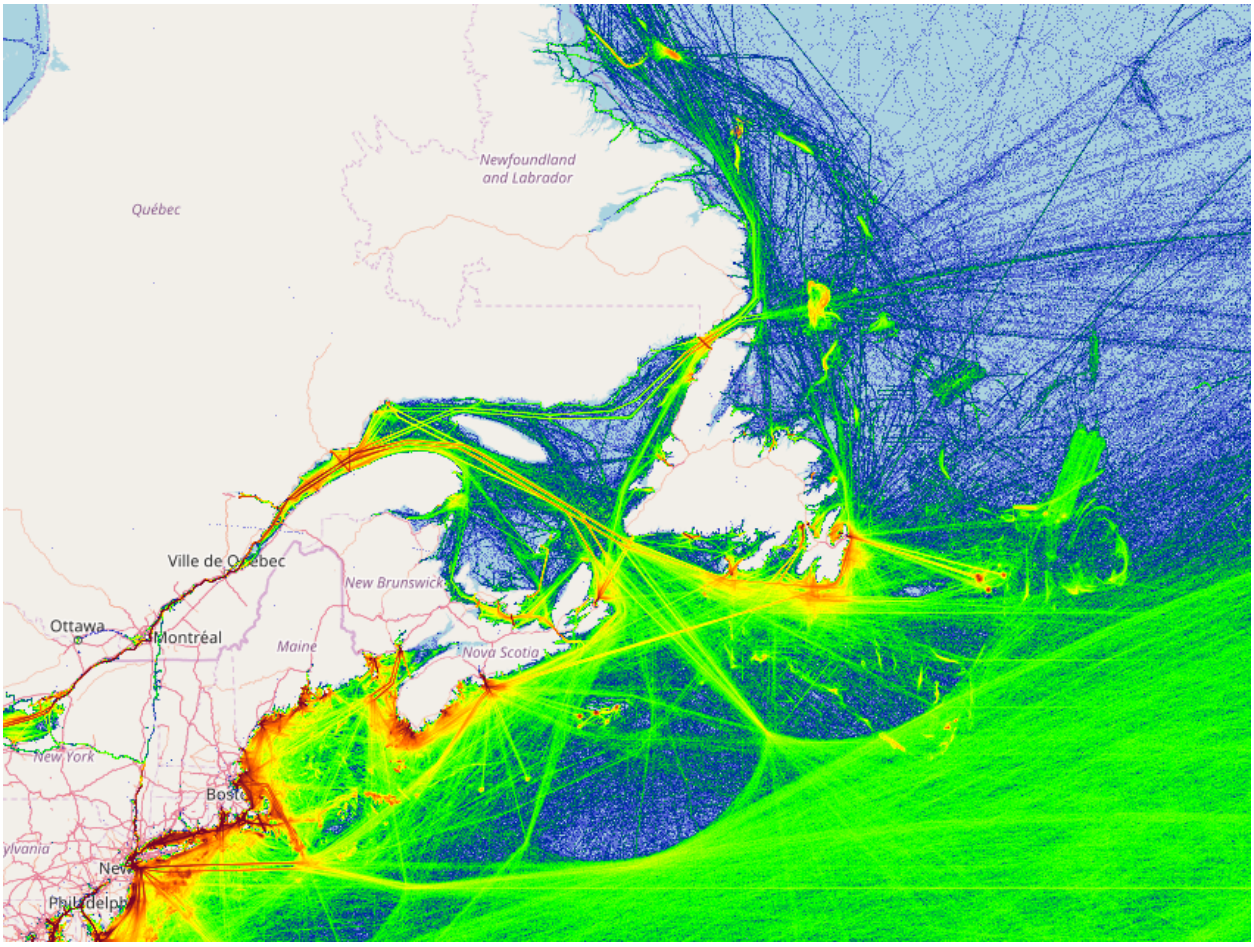

Figure 2. Shipping traffic off the US and Canadian east coast (source: marinetraffic.com; accessed 30 Aug 2017).

1.3.2. Seismic Surveys and Oil and Gas Extraction

Seismic exploration has a long history on Canada's east coast. Increasing in the 1960s, success in both Nova Scotia and Newfoundland in the 1970s and 1980s resulted in an exploration peak in 1983. The next wave of seismic exploration began in 1995 and continued into the 2000s, as 3-D work focused on the Scotian Shelf. In recent years TGS, Petroleum Geo-Services (PGS), Nalcor Energy, and to a lesser extent Shell and BP have undertaken extensive surveys from Nova Scotia to Labrador. Nearly 500,000 km were surveyed across areas under the jurisdiction of the Canada Newfoundland Labrador Offshore Petroleum Board (CNLOPB) during the 2015–2016 fiscal year (Table 2). Figure 3 shows the extent of the surveys conducted by MKI, a joint venture between Nalcor, TGP, and PGS in 2015–2016. There were no seismic surveys conducted in 2015–2016 in areas under the jurisdiction of the Canada Nova Scotia Offshore Petroleum Board (CNSOPB).

In addition to the seismic exploration programs the Statoil 2014-2016 drilling program in the Flemish pass contributed to the soundscape from 4 Nov 2014 to 22 May 2016. The Seadrill *West Hercules* semi-submersible drill rig equipped with 8 Rolls-Royce 3,500 kW azimuthing dynamic positioning thrusters was employed for the drilling operations (Figure 4).

Table 2. Geoscientific programs with fieldwork authorized during 2015–2016 fiscal year.(Source: CNLOPB 2016).

Operator	Program	Region	Distance surveyed (km)
Hibernia Management and Development Company Ltd.	4-D Seismic	Jeanne d'Arc Basin	90,818
Multi Klient Invest	2-D Seismic	Northern Labrador and Northeastern Newfoundland	9,951
Multi Klient Invest	3-D Seismic	Eastern Newfoundland	166,219
Multi Klient Invest	3-D Seismic	Eastern Newfoundland	211,734
Multi Klient Invest	2-D Seismic	Eastern and northeastern Newfoundland	2,483
Multi Klient Invest	2-D Seismic	Southern and southeastern Newfoundland	14,403

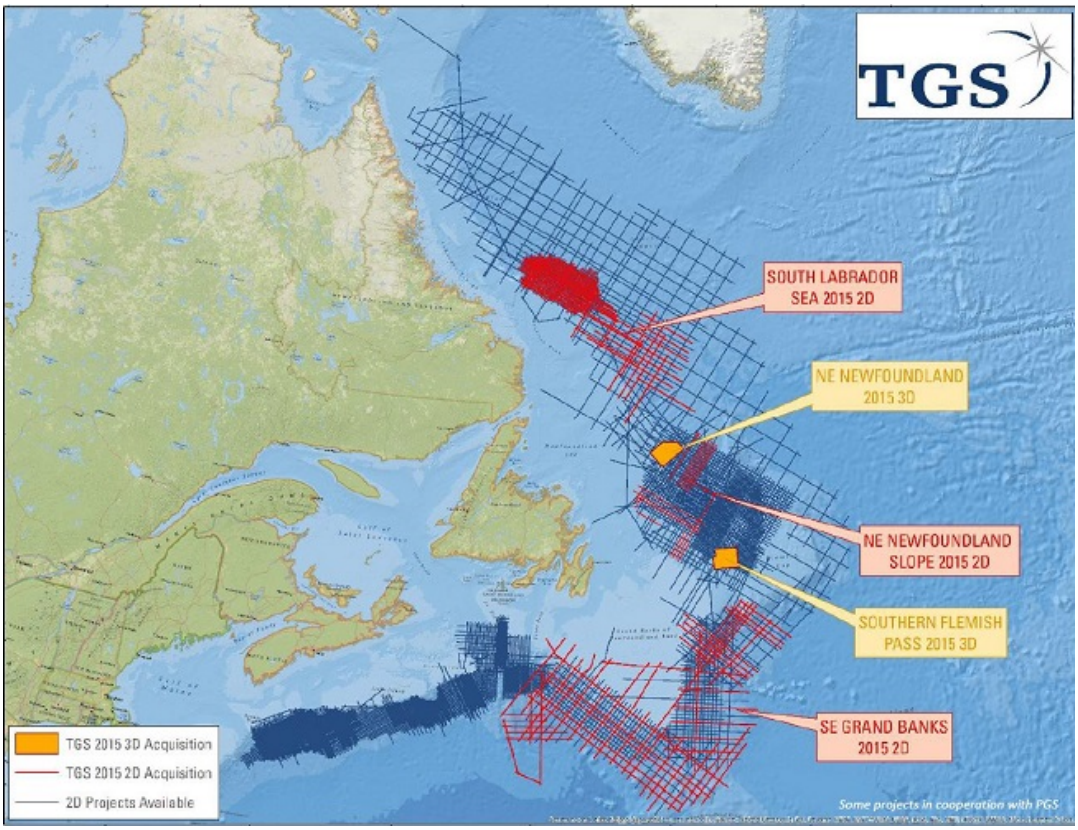

Figure 3. 2015 seismic surveys completed by TGS and PGS and previously available 2-D seismic data in eastern Canadian waters. (Source: Larsen and Ashby 2015; accessed 14 Nov 2016).

Figure 4. Seadrill *West Hercules* semisubmersible drill rig.

2. Methods

2.1. Data Collection

An acoustic recorder (AMAR172) was purchased by AMEC for the Statoil program in 2014 and included in the CM2 current meter mooring. JASCO performed a data download and refurbishment for AMEC prior to the redeployment in 2015.

In August 2015 JASCO deployed an AMAR at Station 19, approximately 230 km north east of the Statoil 2014-2016 drilling area as part of a project sponsored by the Environmental Studies Research Fund (ESRF). These data are included in this report because sounds from the Statiol 2014-2016 drilling program were detected in this data and it serves as a baseline for comparison to the CM2 data.

2.1.1. Mooring Design and Deployment Location

AMEC designed the mooring configuration for a suspended AMAR (Figure 5). The recorded drilling operations was 13.4 km distance to the mooring CM2 (Table 3). The AMAR was deployed twice in the Flemish Pass (CM2 Recorder; Figure 7, Figure 8) from 2 Jun to 9 Oct 2014 and 9 May to 11 Sep 2015 (Table 4). The CM2 deployment recorded the drillilng operations of BdN4 L-76 from 2 May to 11 Sep (Table 3, Figure 8). The AMAR recorded for an average recording duration of four months each year, and was successfully retrieved using an acoustic release.

ESRF Stn 19 mooring (Figure 6, Figure 7) was deployed on 25 August 2015 and retrieved 17 July 2016 in 1280 m of water. The recorder was 209-246 km from the drilling operations until they ceased on 22 May 2016 (Table 3).

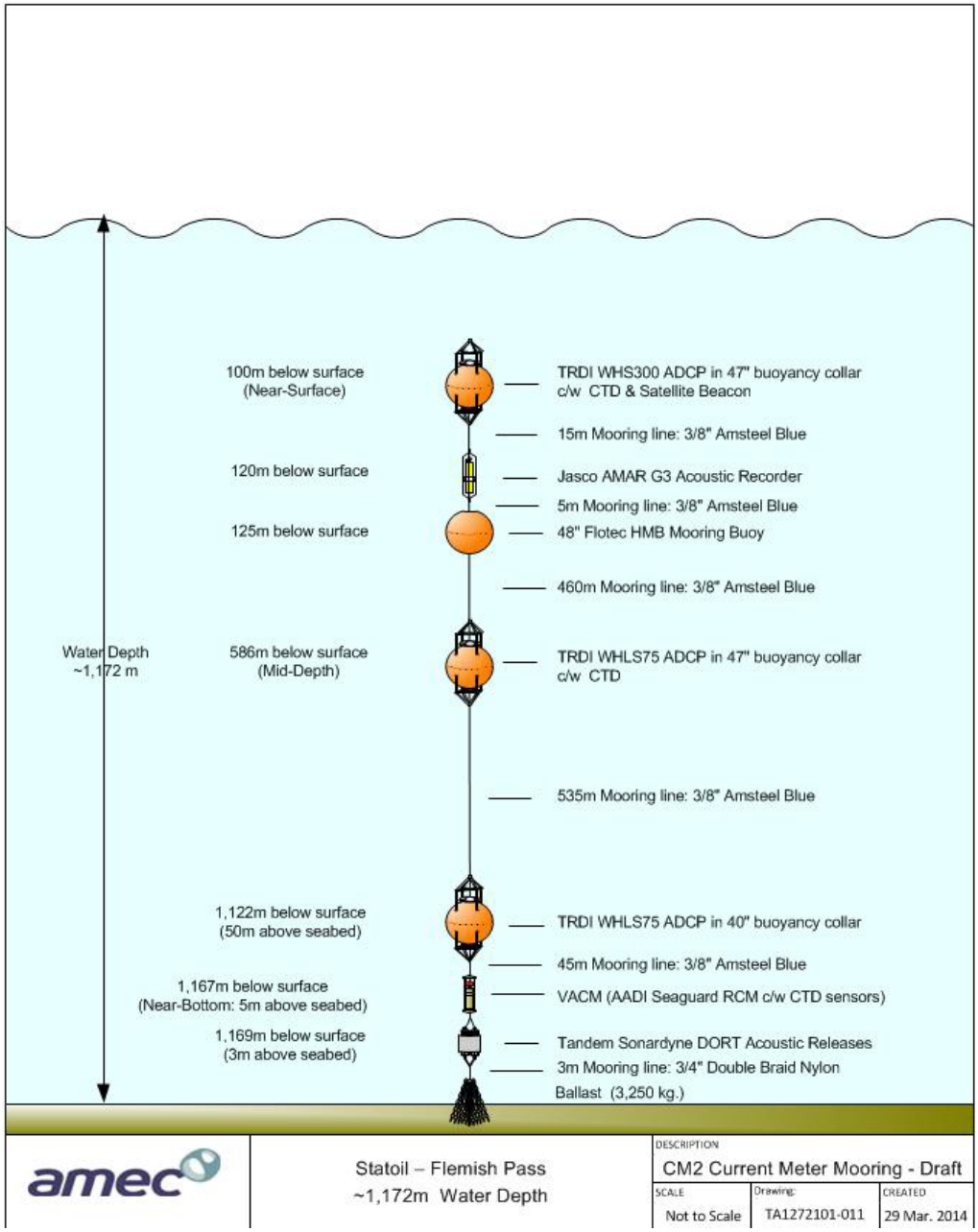

Figure 5. The mooring design used by AMEC.

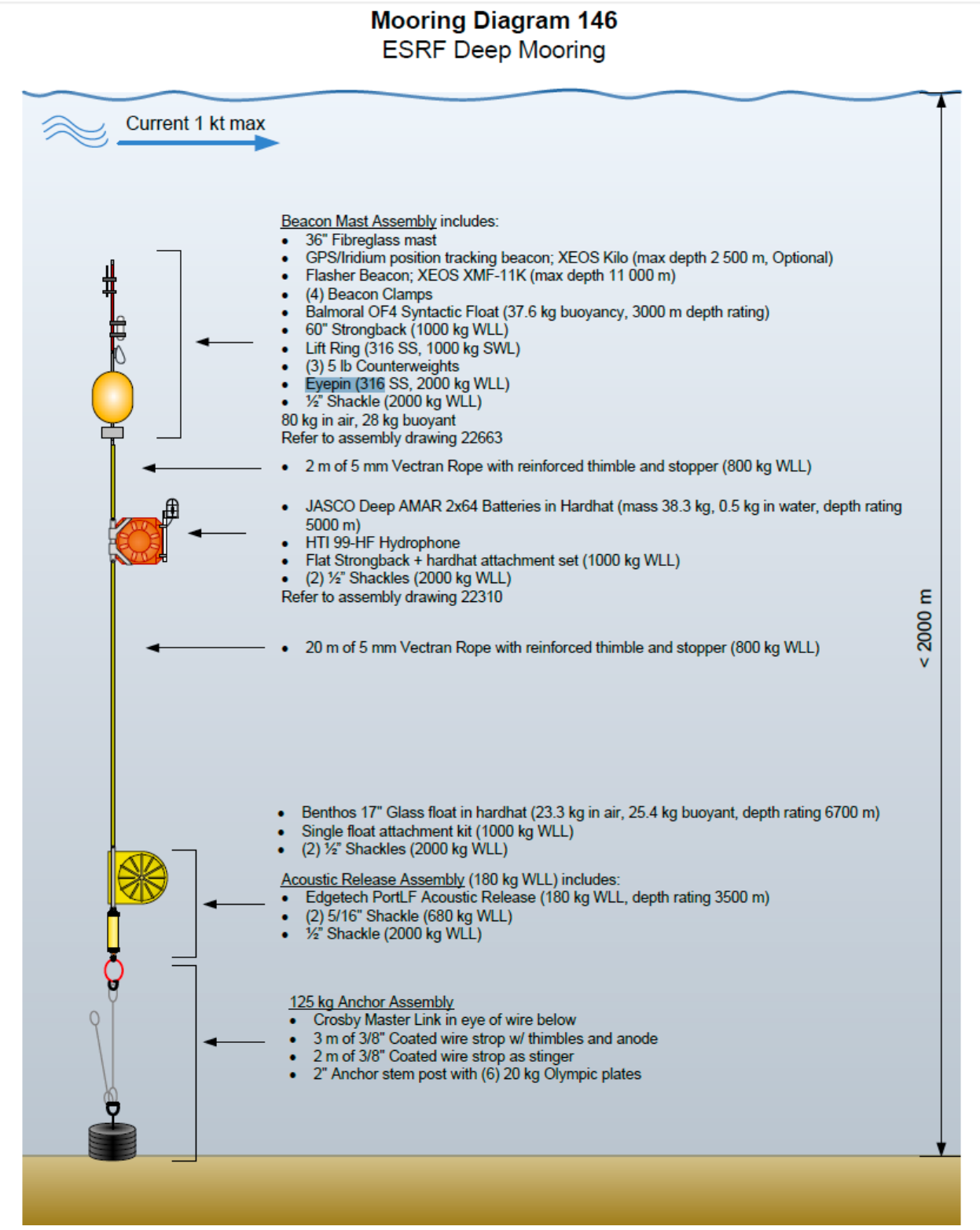

Figure 6. JASCO Mooring 146 employed at ESRF Station 19.

Table 3. The drill rig operation period, location, and distance to the CM2 and Stn19 recorders. Only BdN4 L-76 was recorded at CM2.

Well drilling operation	Rig coordinates (Lat, Long)	Approx. distance to CM2 (km)	Approx. distance to ESRF Stn19 (km)	Operation date
BdN4 L-76	47° 55' 43.9403 N 46° 26' 42.6303 W	13.4	234	2 May to 12 Sep 2015
BdE, B-09	47° 58' 09.8601 N 46° 30' 19.8867 W	Not deployed	230	13–28 Sep 2015 1–31 Dec 2015
Cupids, A-33	49° 02' 08.2606 N 46° 04' 43.9385 W	Not deployed	246	29 Sep - 23 Nov 2015
Fitzroya, A-12	48° 01' 00.1739 N 46° 46' 43.1924 W	Not deployed	209	24–30 Nov 2015
M-62	47° 51' 48.6828 N 46° 25' 19.5067 W	Not deployed	240	31 Mar - 22 May 2016

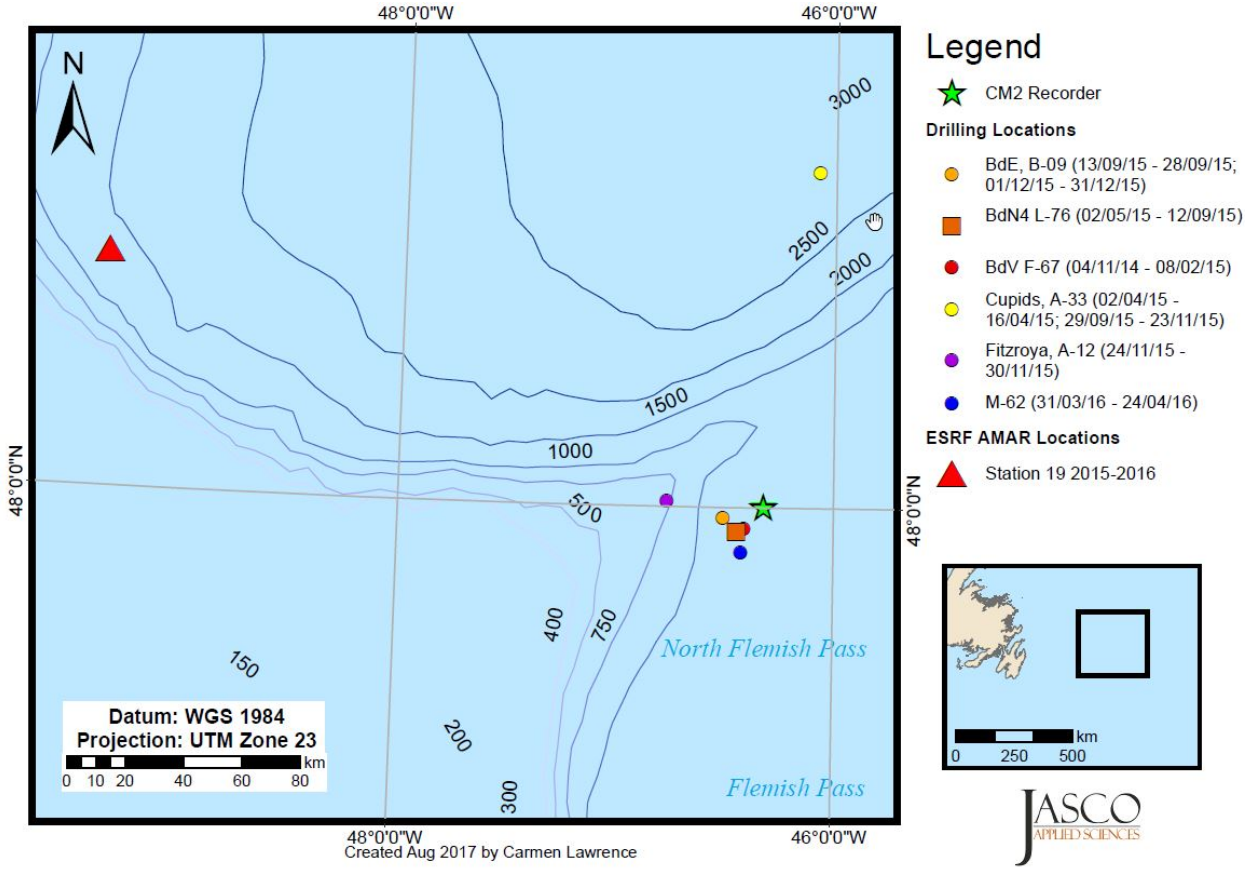

Figure 7. CM2 recorder, ESRF Station 19 recorders, and Statoil 2015-2016 drilling locations off the east cost of Newfoundland.

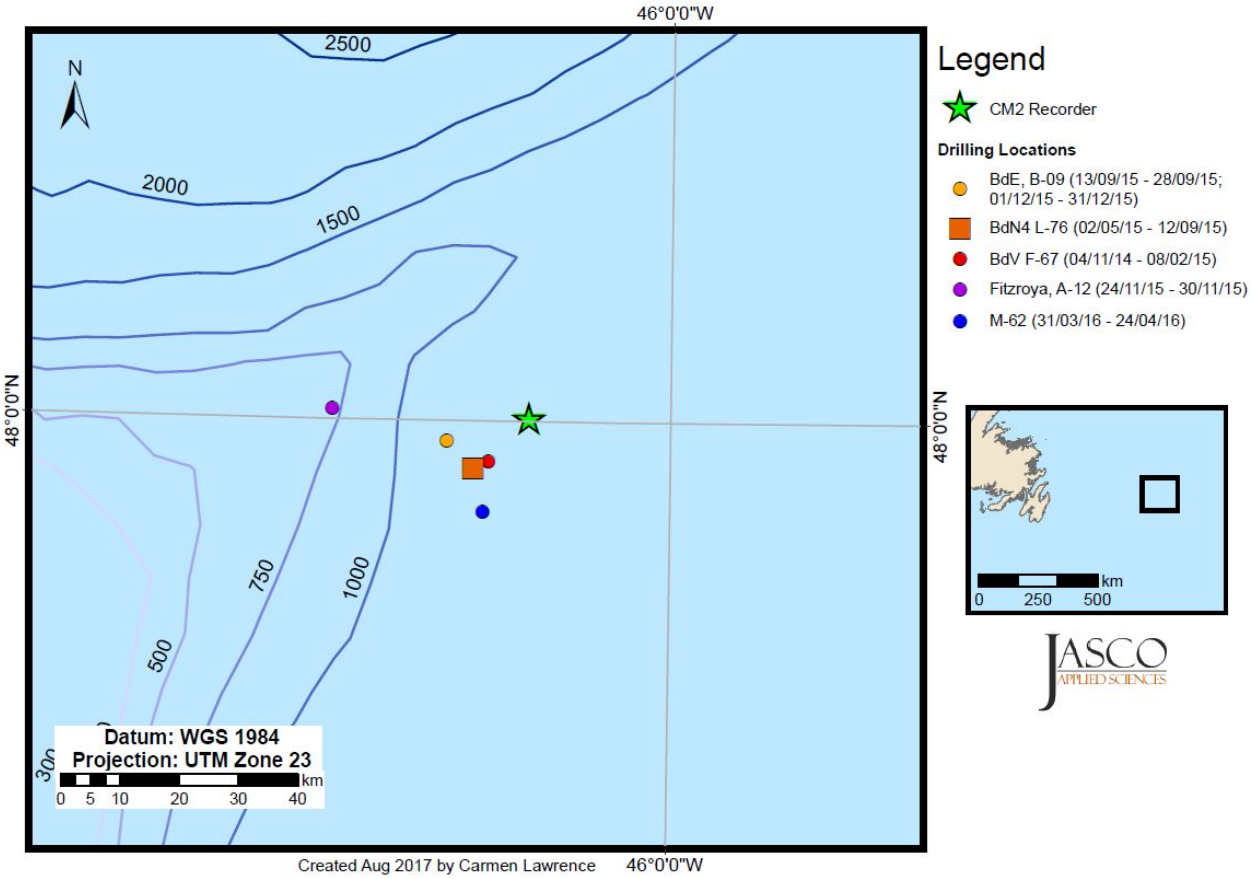

Figure 8. Statoil 2014-2016 drilling sites and CM2 recorder location. The BdN4 L-76 site is highlighted as a square.

Table 4. Operation period, location, and depth of the AMAR deployed in 2014 and 2015 for the Statoil study.

Year	Latitude	Longitude	Depth (m)	Deployment	Retrieval	Duration (days)
2014	44.71155	−63.5874	~1,170	2 Jun 2014	9 Oct 2014	129
2015	49.89104	−47.6597	~1,170	9 May 2015	11 Sep 2015	125

2.1.2. Acoustic Recorders

Underwater sound was recorded with Autonomous Multichannel Acoustic Recorders (AMARs, JASCO). The AMAR on CM2 was fitted with a M8E-35dB omnidirectional hydrophone (GeoSpectrum Technologies Inc.; −164 dB re 1 V/µPa sensitivity). The AMAR hydrophone was protected by a hydrophone cage, which was covered with a cloth shroud to minimize noise artifacts due to water flow. The AMARs operated on a duty cycle. The AMAR sampled on a 15 min duty cycle: 680 s at 16 ksps, then 170 s at 128 ksps, and then 50 s of sleep. The 16 ksps recording channel had a 24-bit resolution with no gain resulting in a spectral noise floor of 24 dB re 1 $\mu Pa^2/Hz$ and could resolve a maximum sound pressure level (SPL) of 171 dB re 1 µPa. The 128 ksps data were recorded at 24-bit resolution with no gain resulting in a spectral noise floor of 18 dB re 1 $\mu Pa^2/Hz$ and could resolve a maximum sound pressure level (SPL) of 171 dB re 1 µPa. The spectral noise floor represents the quietest sounds that can be recorded, and is directly comparable to the Wenz ocean noise spectra (Figure 1). Acoustic data were stored on internal solid-state flash memory.

The AMAR deployed at ESRF Station 19 an HTI-99 hydrophone (Hi-tech Industries; -165 dB re 1 V/µPa sensitivity). The AMAR hydrophone was protected by a hydrophone cage, which was covered with a cloth shroud to minimize noise artifacts due to water flow. The AMARs operated on a duty cycle. The AMAR sampled on a 20 min duty cycle: 680 s at 8 ksps, then 65 s at 250 ksps, and then 455 s of sleep. The 8 ksps recording channel had a 24-bit resolution with 6 dB gain resulting in a spectral noise floor of 32 dB re 1 $\mu Pa^2/Hz$ and could resolve a maximum sound pressure level (SPL) of 165 dB re 1 µPa. The 250 ksps data were recorded at 16-bit resolution with no gain resulting in a spectral noise floor of 32 dB re 1 $\mu Pa^2/Hz$ and could resolve a maximum sound pressure level (SPL) of 171 dB re 1 µPa

2.1.3. Recorder Calibrations

A 42AC pistonphone calibrator (G.R.A.S. Sound & Vibration A/S; Figure 9) was used to verify the sensitivity of the whole recording apparatus—the hydrophone, pre-amplifier, and AMAR. The pressure response of the recording system was verified by placing the pistonphone and its adapter over the hydrophone while the pistonphone produced a known pressure signal on the hydrophone element (a 250 Hz sinusoid at 152.2 dB re 1 µPa). The system sensitivity was measured independently of the software that performed the data analysis. This independently calibrated the analysis software. Calibrations were performed in JASCO's facility before the recorders were shipped. The reading was verified for consistency before data analysis was performed.

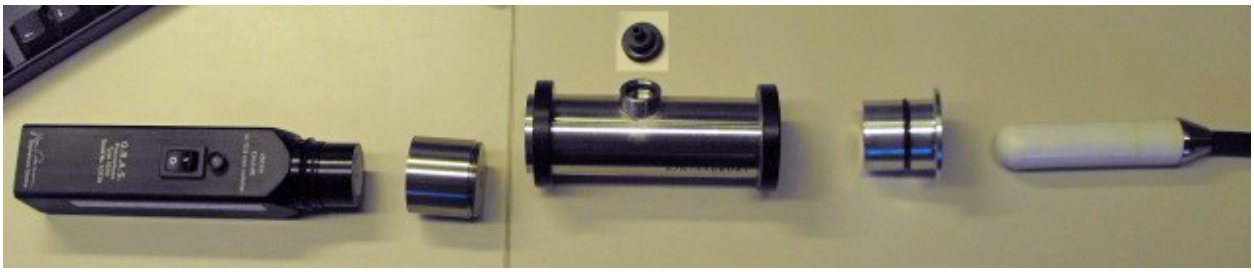

Figure 9. Split view of a G.R.A.S. 42AC pistonphone calibrator with an M15B hydrophone.

2.2. Automated Data Analysis

We use a specialized computing platform for processing acoustic data hundreds of times faster than real-time. The system performs automated analysis of total ocean noise and sounds from vessels, seismic surveys, and (possible) marine mammal calls. Figure 10 outlines the stages of the automated analysis.

We also classify the dominant sound source in each minute of data as "Vessel", "Seismic", or "Ambient". To minimize the influence of anthropogenic sources on ambient sound level estimates, we define ambient levels from individual minutes of data that did not have an anthropogenic detection within one hour on either side of that minute. This results in more accurate estimates of daily sound exposure levels from each source class, cumulative distribution functions of sound pressure levels, and exceedance spectra.

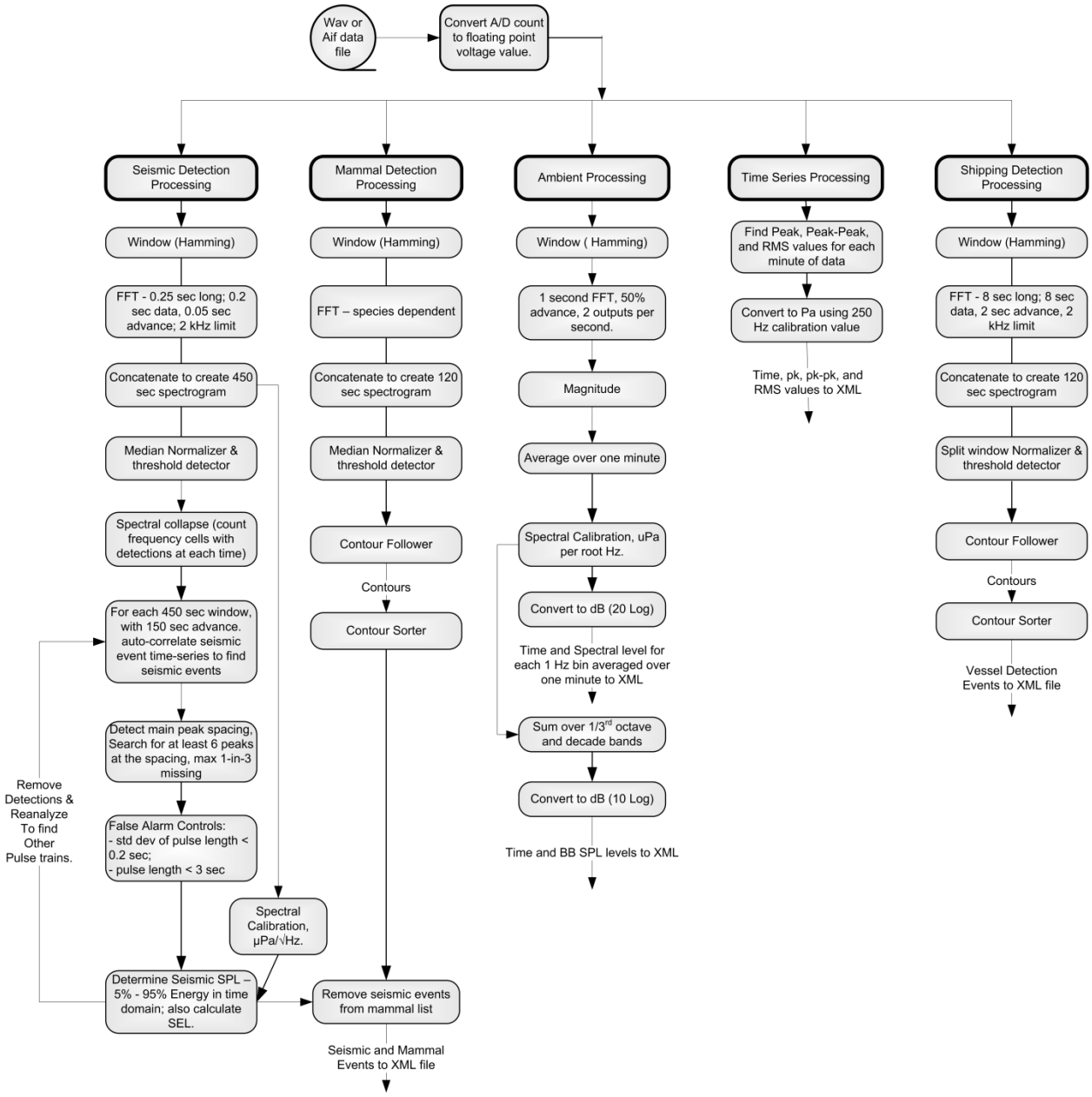

Figure 10. Major stages of the automated acoustic analysis software suite.

2.2.1. Total Ocean Noise and Time Series Analysis

Ambient noise levels at the recording station were examined to document the local baseline underwater sound conditions. In Section 3, ambient noise levels are presented as:

- Statistical distribution of SPL in each 1/3-octave-band. The boxes of the statistical distributions indicate the first (L_{25}), second (L_{50}), and third (L_{75}) quartiles. The whiskers indicate the maximum and minimum range of the data. The solid line indicates the mean SPL, or L_{mean}, in each 1/3-octave.
- Spectral density level percentiles: Histograms of each frequency bin per 1 min of data. The L_{eq}, L_5, L_{25}, L_{50}, L_{75}, and L_{95} percentiles are plotted. The L_5 percentile curve is the frequency-dependent level exceeded by 5% of the 1 min averages. Equivalently, 95% of the 1 min spectral levels are above the 95th percentile curve.

- Broadband and approximate-decade-band SPL over time for these frequency bands: 10 Hz to 8 kHz, 10–100 Hz, 100 Hz to 1 kHz, and 1–63 kHz.
- Spectrograms: Ambient noise at each station was analyzed by Hamming-windowed fast Fourier transforms (FFTs), with 1 Hz resolution and 50% window overlap. The 120 FFTs performed with these settings are averaged to yield 1 min average spectra.
- Daily sound exposure levels (SEL): Computed for the total received sound energy and the detected shipping energy. The SEL is the linear sum of the 1 min SEL. For shipping, the 1 min SEL values are the linear 1 min squared SPL values multiplied by the duration, 60 s. For seismic survey pulses, the 1 min SEL is the linear sum of the per-pulse SEL.

The 50th percentile (median of 1 min spectral averages) can be compared to the well-known Wenz ambient noise curves (Figure 1), which show the variability of ambient spectral levels off the east coast of Canada as a function of frequency of measurements for a range of weather, vessel traffic, and geologic conditions. The Wenz curve levels are generalized and are used for approximate comparisons only (see Section 2.2.1.2).

2.2.1.1. *Sound Levels*

Underwater sound pressure amplitude is measured in decibels (dB) relative to a fixed reference pressure of p_0 = 1 µPa. Because the perceived loudness of sound, especially impulsive noise such as from seismic airguns, pile driving, and sonar, is not generally proportional to the instantaneous acoustic pressure, several sound level metrics are commonly used to evaluate noise and its effects on marine life. We provide specific definitions of relevant metrics used in the accompanying report. Where possible we follow the ANSI and ISO standard definitions and symbols for sound metrics, but these standards are not always consistent.

The zero-to-peak pressure level, or peak pressure level (PK; dB re 1 µPa), is the maximum instantaneous sound pressure level in a stated frequency band attained by an acoustic pressure signal, $p(t)$:

$$PK = 10\log_{10}\left[\frac{\max\left(\left|p^2(t)\right|\right)}{p_0^2}\right] . \qquad (1)$$

$L_{p,pk}$ is often included as criterion for assessing whether a sound is potentially injurious; however, because it does not account for the duration of a noise event, it is generally a poor indicator of perceived loudness.

The sound pressure level (SPL or L_p; dB re 1 µPa) is the root-mean-square (rms) pressure level in a stated frequency band over a specified time window (T, s) containing the acoustic event of interest. It is important to note that SPL always refers to an rms pressure level and therefore not instantaneous pressure:

$$\mathrm{SPL} = 10\log_{10}\left(\frac{1}{T}\int_T p^2(t)dt \Big/ p_0^2\right) . \qquad (2)$$

The SPL represents a nominal effective continuous sound over the duration of an acoustic event, such as the emission of one acoustic pulse, a marine mammal vocalization, the passage of a vessel, or over a fixed duration. Because the window length, T, is the divisor, events with similar SEL, but more spread out in time have a lower SPL.

The SEL (dB re 1 µPa²·s) is a measure related to the acoustic energy contained in one or more acoustic events (*N*). The SEL for a single event is computed from the time-integral of the squared pressure over the full event duration (*T*):

$$\mathrm{SEL} = 10\log_{10}\left(\int_T p^2(t)dt \Big/ T_0 p_0^2\right) \tag{3}$$

where T_0 is a reference time interval of 1 s. The SEL continues to increase with time when non-zero pressure signals are present. It therefore can be construed as a dose-type measurement, so the integration time used must be carefully considered in terms of relevance for impact to the exposed recipients.

SEL can be calculated over periods with multiple events or over a fixed duration. For a fixed duration, the square pressure is integrated over the duration of interest. For multiple events, the SEL can be computed by summing (in linear units) the SEL of the *N* individual events:

$$L_{\mathrm{E,N}} = 10\log_{10}\left(\sum_{i=1}^{N} 10^{\frac{L_{E,i}}{10}}\right) . \tag{4}$$

To compute the SPL(T_{90}) and SEL of acoustic events in the presence of high levels of background noise, equations 3 and 4 are modified to subtract the background noise contribution:

$$L_{\mathrm{p90}} = 10\log_{10}\left(\frac{1}{T_{90}}\int_{T_{90}} (p^2(t) - \overline{n^2})dt \Big/ p_0^2\right) \tag{5}$$

$$L_{\mathrm{E}} = 10\log_{10}\left(\int_T (p^2(t) - \overline{n^2})dt \Big/ T_0 p_0^2\right) , \tag{6}$$

where $\overline{n^2}$ is the mean square pressure of the background noise, generally computed by averaging the squared pressure of a temporally-proximal segment of the acoustic recording during which acoustic events are absent (e.g., between pulses).

Because the SPL(T_{90}) and SEL are both computed from the integral of square pressure, these metrics are related by the following expression, which depends only on the duration of the time window *T*:

$$L_{\mathrm{p}} = L_{\mathrm{E}} - 10\log_{10}(T) \tag{7}$$

$$L_{\mathrm{p90}} = L_{\mathrm{E}} - 10\log_{10}(T_{90}) - 0.458 , \tag{8}$$

where the 0.458 dB factor accounts for the 10% of SEL missing from the SPL(T_{90}) integration time window.

Energy equivalent SPL (dB re 1 µPa) denotes the SPL of a stationary (constant amplitude) sound that generates the same SEL as the signal being examined, $p(t)$, over the same period of time, *T*:

$$L_{\mathrm{eq}} = 10\log_{10}\left(\frac{1}{T}\int_T p^2(t)dt \Big/ p_0^2\right) . \tag{9}$$

The equations for SPL and the energy-equivalent SPL are numerically identical; conceptually, the difference between the two metrics is that the former is typically computed over short periods (typically of one second or less) and tracks the fluctuations of a non-steady acoustic signal, whereas the latter reflects the average SPL of an acoustic signal over times typically of one minute to several hours.

2.2.1.2. *One-Third-Octave-Band Analysis*

The distribution of a sound's power with frequency is described by the sound's spectrum. The sound spectrum can be split into a series of adjacent frequency bands. Splitting a spectrum into 1 Hz wide bands, called passbands, yields the power spectral density of the sound. These values directly compare to the Wenz curves, which represent typical deep ocean sound levels (Figure 1) (Wenz 1962). This splitting of the spectrum into passbands of a constant width of 1 Hz, however, does not represent how animals perceive sound.

Because animals perceive exponential increases in frequency rather than linear increases, analyzing a sound spectrum with passbands that increase exponentially in size better approximates real-world scenarios. In underwater acoustics, a spectrum is commonly split into 1/3-octave-bands, which are one-third of an octave wide; each octave represents a doubling in sound frequency. A very similar measure is to logarithmically divide each frequency decade into 10 passbands, which are commonly misnamed the 1/3-octave-bands rather than deci-decades; we use this naming in the report. The centre frequency of the ith 1/3-octave-band, $f_c(i)$, is defined as:

$$f_c(i) = 10^{i/10}, \tag{10}$$

and the low (f_{lo}) and high (f_{hi}) frequency limits of the ith 1/3-octave-band are defined as:

$$f_{lo} = 10^{-1/20} f_c(i) \quad \text{and} \quad f_{hi} = 10^{1/20} f_c(i). \tag{11}$$

The 1/3-octave-bands become wider with increasing frequency, and on a logarithmic scale the bands appear equally spaced (Figure 11).

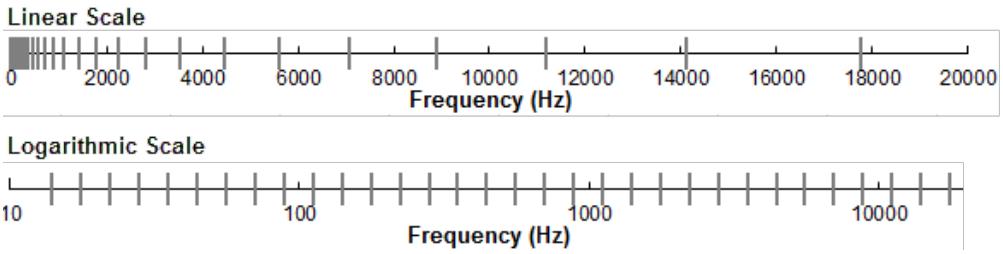

Figure 11. One-third-octave-bands shown on a linear frequency scale and on a logarithmic scale.

The sound pressure level in the ith 1/3-octave-band $(L_b^{(i)})$ is computed from the power spectrum $S(f)$ between f_{lo} and f_{hi}:

$$L_b^{(i)} = 10 \log_{10} \left(\int_{f_{lo}}^{f_{hi}} S(f) df \right). \tag{12}$$

Summing the sound pressure level of all the 1/3-octave-bands yields the broadband sound pressure level:

$$\text{Broadband SPL} = 10 \log_{10} \sum_i 10^{L_b^{(i)}/10}. \tag{13}$$

Figure 12 shows an example of how the 1/3-octave-band sound pressure levels compare to the power spectrum of an ambient noise signal. Because the 1/3-octave-bands are wider with increasing frequency, the 1/3-octave-band SPL is higher than the power spectrum, especially at higher frequencies. 1/3-octave-band analysis is applied to both continuous and impulsive noise sources. For impulsive sources, the 1/3-octave-band SEL is typically reported.

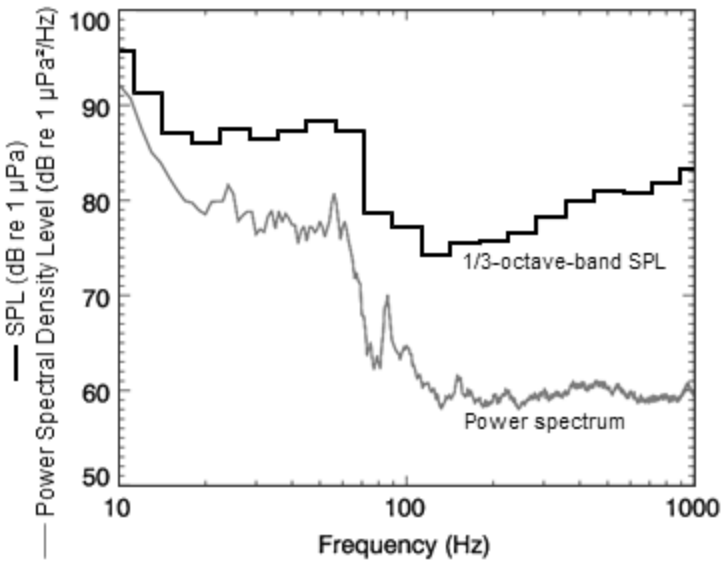

Figure 12. A power spectrum and the corresponding 1/3-octave-band sound pressure levels of example ambient noise shown on a logarithmic frequency scale. Because the 1/3-octave-bands are wider with increasing frequency, the 1/3-octave-band SPL is higher than the power spectrum.

2.2.2. Vessel Noise Detection

Vessels are detected in two steps:

1. Detect constant, narrowband tones produced by a vessel's propulsion system and other rotating machinery (Arveson and Vendittis 2000). These sounds are also referred to as tonals. We detect the tonals as lines in a 0.125 Hz resolution spectrogram of the data.
2. Assess the rms SPL for each minute in the 100–315 Hz frequency band. Figure 13 shows an example with a bandwidth of 40–315 Hz, which commonly contains most sound energy produced by mid-sized to large vessels; however, for this study, most of the energy below 100 Hz is likely due to seismic noise. Background estimates of the shipping band SPL and broadband SPL are then compared to their median values over the 12 h window, centred on the current time.

Vessel detections are defined by three criteria:

- The SPL in the shipping band is at least 3 dB above the median.
- At least 3 shipping tonals (0.125 Hz bandwidth) are present.
- The SPL in the shipping band is within 12 dB of the broadband SPL (Figure 13).

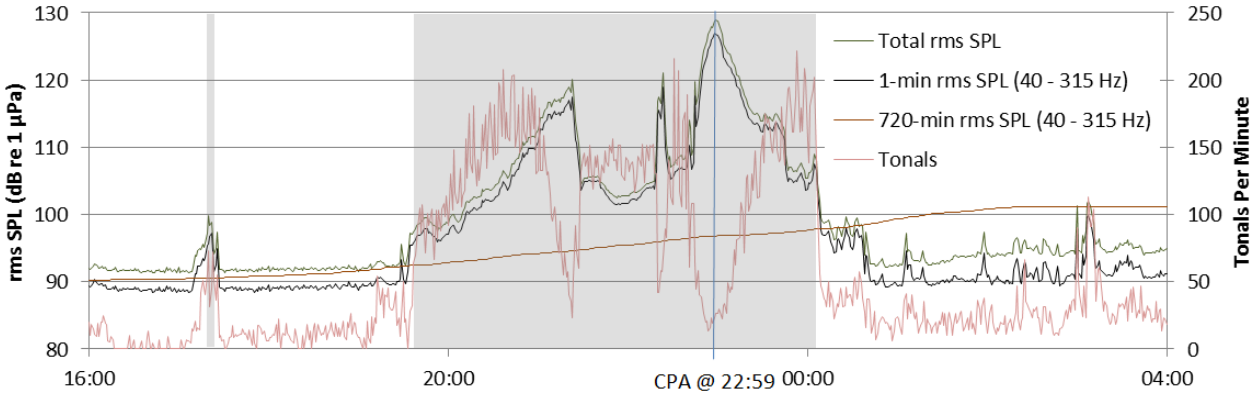

Figure 13. Example of broadband and 40–315 Hz band SPL, as well as the number of tonals detected per minute as a ship approached a recorder, stopped, and then departed. The shaded area is the period of shipping detection. Fewer tonals are detected at the ship's closest point of approach (CPA) at 22:59 because of masking by broadband cavitation noise and due to Doppler shift, that affects the tone frequencies.

2.2.3. Seismic Survey Event Detection

Seismic pulse sequences are detected using correlated spectrogram contours. We calculate spectrograms using a 300 s long window with 4 Hz frequency resolution and a 0.05 s time resolution (Reisz window). All frequency bins are normalized by their medians over window the 300 s window. The detection threshold is three times the median value at each frequency. Contours are created by joining the time-frequency bins above threshold in the 7–1000 Hz band using a 5 × 5 bin kernel. Contours 0.2–6 s in duration with a bandwidth of at least 60 Hz are retained for further analysis.

An "event" time series is created by summing the normalized value of the frequency bins in each time step that contained detected contours. The event time series is auto-correlated to look for repeated events. The correlated data space is normalized by its median and a detection threshold of 3 is applied. Peaks larger than their two nearest neighbours are identified, and the peaks list is searched for entries with a set repetition interval. The allowed spacing between the minimum and maximum time peaks is 4.8 to 65 s, which captures the normal range of seismic pulse periods. Where at least six regularly spaced peaks occur, the original event time series is searched for all peaks that match the repetition period within a tolerance of 0.25 s. The duration of the 90% SPL window of each peak is determined from the originally sampled time series, and pulses more than 3 s long are rejected.

2.2.4. Marine Mammal Detection

We apply automated analysis techniques to detect sounds from odontocetes, mysticetes, and pinnipeds in the acoustic data. Targeted signals for odontocetes are echolocation clicks and tonal whistles. Echolocation clicks are high-frequency with impulses ranging from 5 to over 150 kHz (Au et al. 1999, Mohl et al. 2000), while the whistles are commonly between 1 and 20 kHz (Steiner 1981b, Rendell et al. 1999). Baleen whale and pinniped calls are lower in frequency and range predominantly between 15 Hz and 4 kHz (Berchok et al. 2006, Risch et al. 2007). The detectors are applied to the 128 ksps data (audio bandwidth up to 65 kHz for ~2 min of every 15 min).

2.2.4.1. *Click Detection*

We apply an automated click detector/classifier to the high-frequency data to detect clicks from sperm whales, beaked whales, porpoise, and delphinids (Figure 14). This detector/classifier is based on the zero-crossings in the acoustic time series. Zero-crossings are the rapid oscillations of a click's pressure waveform above and below the signal's normal level (e.g., Figure 14). Clicks are detected by the following steps (Figure 14):

1. The raw data is high-pass filtered to remove all energy below 8 kHz. This removes most energy from other sources such as shrimp, vessels, wind, and cetacean tonal calls, while allowing the energy from all marine mammal click types to pass.
2. The filtered samples are summed to create a 0.5 ms rms time series. Most marine mammal clicks have a 0.1–1 ms duration.
3. Possible click events are identified with a Teager-Kaiser energy detector.
4. The maximum peak signal within 1 ms of the detected peak is found in the high-pass filtered data.
5. The high-pass filtered data is searched backwards and forwards to find the time span where the local data maxima are within 12 dB of the maximum peak. The algorithm allows for two zero-crossings to occur where the local peak is not within 12 dB of the maximum before stopping the search. This defines the time window of the detected click.
6. The classification parameters are extracted. The number of zero crossings within the click, the median time separation between zero crossings, and the slope of the change in time separation between zero crossings are computed. The slope parameter helps to identify beaked whale clicks, as beaked whale clicks increase in frequency (upsweep).
7. The Mahalanobis distance between the extracted classification parameters and the templates of known click types is computed. The covariance matrices for the known click types, computed from thousands of manually identified clicks for each species, are stored in an external file. Each click is classified as a type with the minimum Mahalanobis distance, unless none of them are less than the specified distance threshold.

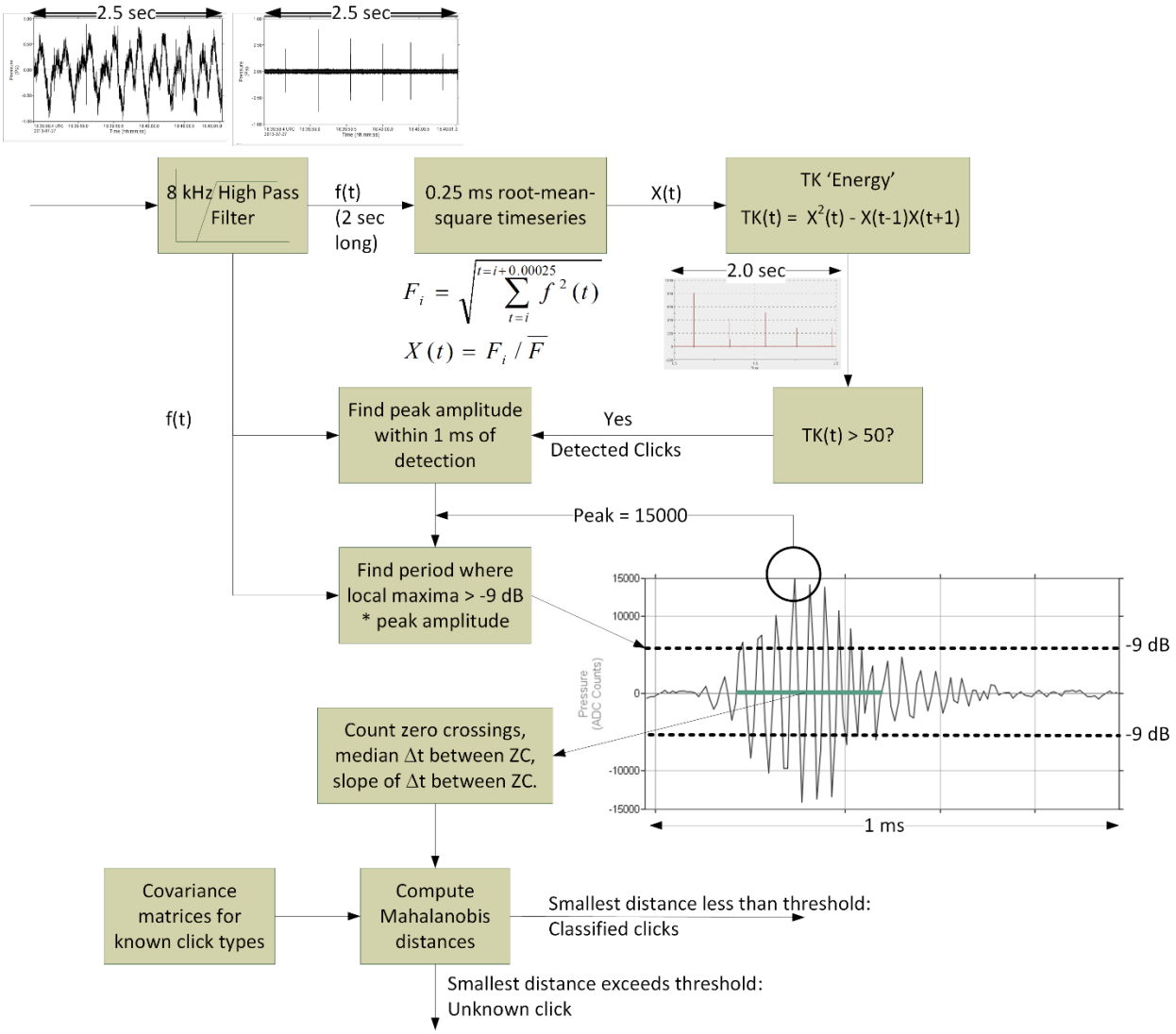

Figure 14. The click detector/classifier and a 1-ms time-series of four click types.

2.2.4.2. *Tonal Call Detection*

The tonal call detector identifies data likely to contain marine mammal moans, songs, and whistles. Tonal calls are detected by the following steps:

1. Spectrograms of the appropriate resolution for each mammal call type that are normalized by the median value in each frequency bin for each detection window (Table 5) are created.
2. Adjacent bins are joined and contours are created via a contour-following algorithm (Figure 15).
3. A call sorting algorithm determines if the contours match the definition of a mammal call type (Table 6).

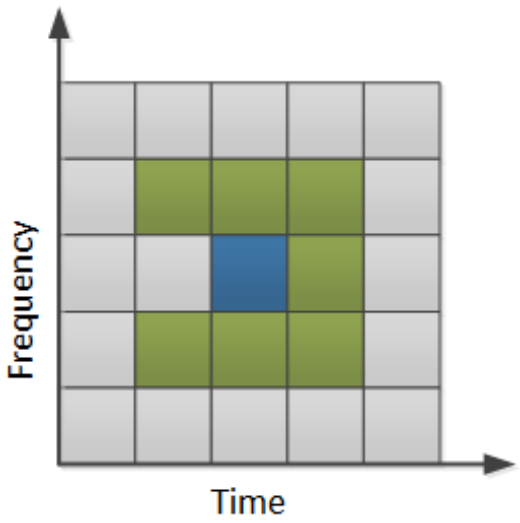

Figure 15. Illustration of the search area used to connect spectrogram bins. The blue square represents a bin of the binary spectrogram equalling 1 and the green squares represent the potential bins it could be connected to. The algorithm advances from left to right so grey cells left of the test cell need not be checked.

Table 5. Fast Fourier Transform and detection window settings used to detect tonal calls of marine mammal species expected in the data. Values are based on JASCO's experience and empirical evaluation on a variety of data sets.

Possible species	Call type	FFT			Detection window (s)	Detection threshold
		Resolution (Hz)	Frame length (s)	Timestep (s)		
Pilot whales	Whistle	16	0.03	0.015	5	3
Dolphin	Whistle	64	0.015	0.005	5	3
Humpback whales	Moan	4	0.2	0.05	5	3
Blue whales	Infrasonic moan	0.125	2	0.5	120	4
Fin whales	20-Hz note	1	0.2	0.05	5	4
Sei whales	Downsweep	3.25	0.2	0.035	5	3.5

Table 6. Call sorter definitions for the tonal calls of cetacean species expected in the area.

Possible species	Call type	Frequency (Hz)	Duration (s)	Bandwidth (Hz)	Other detection parameters
Pilot whales	Whistle	1,000–10,000	0.5–5	>300	Minimum frequency <5,000 Hz
Dolphin	Whistle	4,000–20,000	0.3–3	>700	Maximum instantaneous bandwidth = 5,000 Hz
Humpback whales	Moan	100–700	0.5–5	>50	Maximum instantaneous bandwidth = 200 Hz
Blue whales	Infrasonic moan	15–22	8–30	1–5	Minimum frequency <18 Hz
Sei whales	Downsweep	20–150	0.5–1.7	19–120	Maximum instantaneous bandwidth = 100 Hz Sweep rate = −100 to −6 Hz/s
Fin whales	20 Hz downsweep	8–40	0.3–3	>6	Minimum frequency <17 Hz Sweep rate = −100 to 0 Hz/s

2.2.4.3. *Validation of Automated Detectors*

Automated detectors are often developed and tested with example data files that contain a range of vocalisation types and representative background noise conditions. However, test files normally cannot cover the full range of possible conditions. Therefore, a selection of files must be manually validated to check the detector performance in the specific conditions of each recorder. For each recorder and for each species or call type, a sample of files containing low, medium, and high numbers of detections was reviewed. Files that contained early or late automated detections were primarily selected to help bound the period of occurrence of a species/call type. The automated detector results were checked to evaluate the true presence or absence of each species, as well as vessels and other anthropogenic signals. These validated results were fed to a maximum likelihood estimation (grid search) algorithm that maximised the probability of detection and minimised the number of false alarms using the 'F-score':

$$F = \frac{(1+\beta^2)P * R}{(\beta^2)P + R}; P = \frac{TP}{TP + FP}; R = \frac{TP}{TP + FN}$$

where *TP* (true positive) is the number of correctly detected files, *FP* (false positive) is the number of files that are false detections, and *FN* (false negatives) is the number of files with missed detections. *P* is the classifier's precision, representing the proportion of detected calls that are true positives. A *P* value of 0.9 means that 90% of the detections are correctly classified, but says nothing about whether all calls in the dataset were identified. *R* is the classifier's recall, representing the proportion of calls in the dataset that are detected by the detector. An *R* value of 0.8 means that 80% of all calls in the dataset were detected, but says nothing about how many classifications were wrong. Thus, a perfect detector/classifier would have *P* and *R* values equal to 1. An F-score is a combined measure of *P* and *R* where an F-score of 1 indicates perfect performance–all events are detected with no false alarms. The algorithm determines a classification threshold for each species that maximizes the F-score. Table 7 shows the dependence of the classification threshold on the *β*-parameter and its effect on the precision and recall of the detector and classifier system. *β* is the relative weight between the recall and precision. Here, we have made precision more important than recall as a *β* of 0.5 means the recall has half the weight of the precision.

Table 7. Effects of changing the F-score β-parameter on the classification threshold, precision, and recall for the odontocete clicks.

β	Classification threshold	Precision $P = \frac{TP}{TP + FP}$	Recall $R = \frac{TP}{TP + FN}$	F-score
2	25	0.87	0.95	0.93
0.5	50	0.91	0.91	0.91

Detection time series based on the restrictions above are plotted using JASCO's ADPT software and critically reviewed. Questionable detections based on time of year and location or overlap with the detection period of other species are manually reviewed and removed from the plots if they are found to be false. The detector performance metrics presented in Section 3.4.1 are based on the fully revised and edited results as shown in the detection time series. Detections are also presented as spatial plots showing the number of detections at each station over selected periods.

3. Results

3.1. Total Soundscapes

The objective of this analysis was identification of the sound sources contributing to the recordings at CM2 in 2014 before the start of the Statoil 2014-2016 drilling program and in 2015 during the drilling program. Recordings made 230 km from the drilling program provide contextual information. The main contributors were seismic surveys, fin whales and the *West Hercules* semi-submersible drill rig. This section provides and overview of the measured sound levels. Section 3.2 provides a summary of when vessels were detectable at CM2. Section 3.3 discusses the nature and occurance of the seismic sounds detected at CM2, and 3.4 documents the detections of marine mammals.

Long-term spectral averages along with median band-level time series figures (Figure 16) provide an overview of the time and frequency evolution in the soundscape. In 2014 the soundscape at CM2 was dominated by a relatively close seismic survey. In 2015 CM2 recorded both the *West Hercules* drilling operations and a distant seismic survey. ESRF STN 19 recorded seismic survey sounds until November 2015, and beginning again in June 2016. The winter period of 15 Nov 15 – 1 Jun 16 was representative of a normal ambient soundscape for this region with the *West Hercules* being faintly detectable (Figure 16). Fin whale mating choruses were a dominant sound source in the band of 18-25 Hz from November – March, and were detectable in September and October (Figure 16).

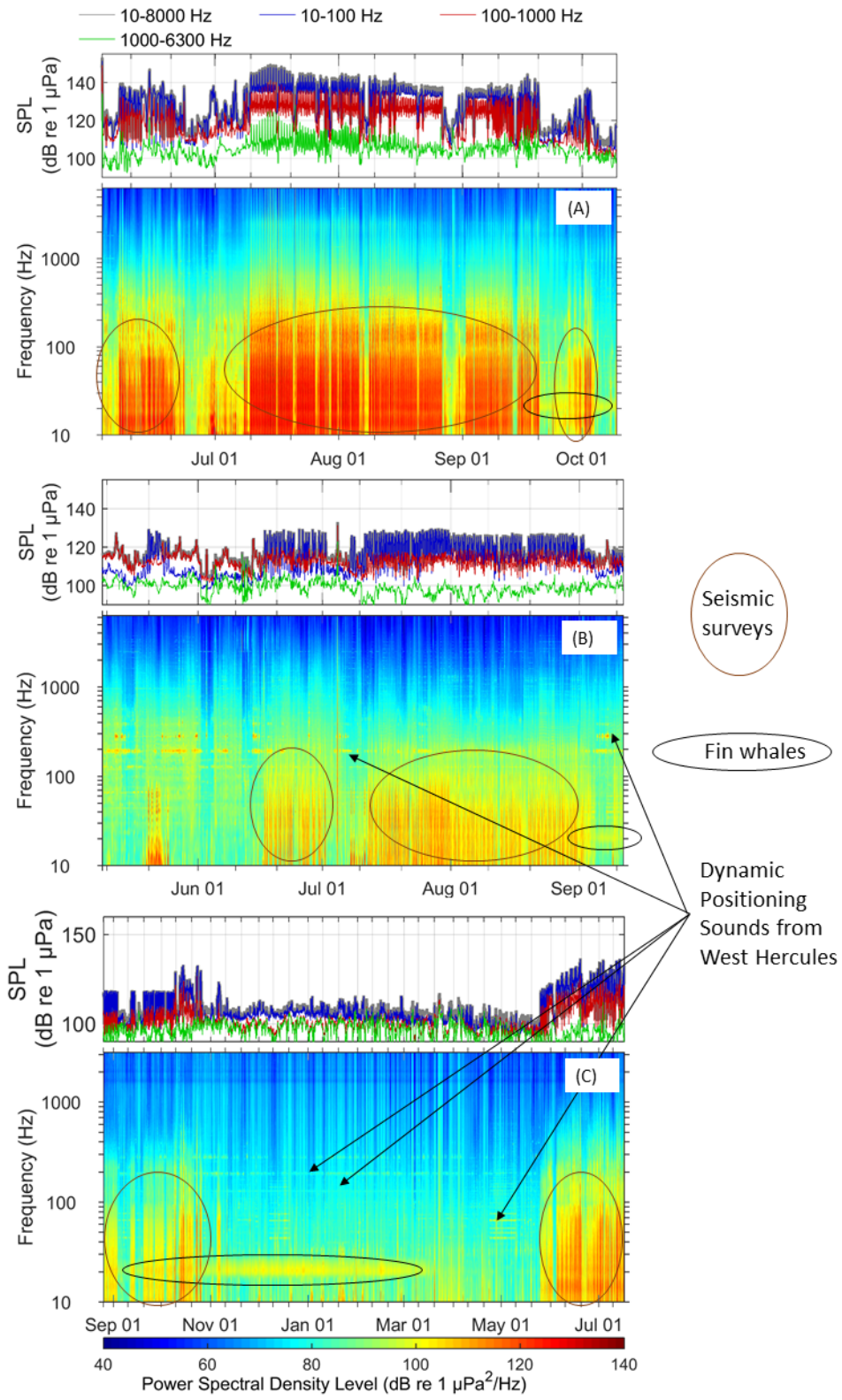

Figure 16. Summary of each recorder's acoustic data. (A) CM2 2014, (B) CM2 2015 and (C) ESRF Stn 19 (Aug 15-Jul 16). For each station the top figure is the median hourly in-band SPL and bottom is the long-term spectral average of the measured sound. On the long-term spectral averages the sounds from seismic surveys, fin whales and the *West Hercules* are annotated.

Band-level box and whisker plots provide a statistical representation of the magnitude of the sound levels recorded (Figure 17). The maximum and minimum broadband SPL measured in 2014 were 165.8 and 104.9 dB re 1 µPa, respectively, and 148.3 and 102.4 dB re 1 µPa in 2015. At ESRF STN 19 the values were 139.5 and 90.5 (Figure 17). The median SPL at ESRF STN 19 of 107.5 dB re 1 µPa is representative of the level measured in most northern deep water ocean locations far from shipping lanes and industrial activity. The seismic survey increased the median levels measured at CM2 to 130 dB re 1 µPa in 2014 and 117 dB re 1 µPa in 2015 (a 10 dB increase in SPL is 10 times louder). In all cases the 10-100 Hz band contained the most energy. This is the band associated with seismic surveys and large shipping. In the winter, it is also associated with fin whale mating choruses.

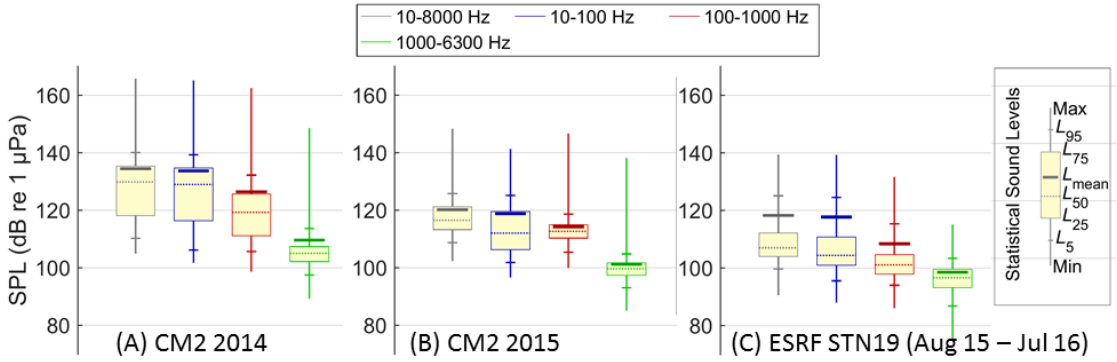

Figure 17. Comparison of the broadband and decade band 1-minute sound pressure levels for (A) CM2 2014, (B) CM2 2015 and (C) ESRF Stn 19 (Aug 15-Jul 16).

Power spectral density and 1/3-octave-band distribution plots (Figure 18) can be directly compared to the Wenz plots (Figure 1) and provide more detailed spectral distribution information than the long-term spectral averages and box-and-whisker plots. In 2014, noise from seismic activity caused the noise between 30 to 250 Hz to exceed the expected limits of prevailing noise for the L_{75} percentile curve, or for 75% of the time (Figure 18). The maximum sound levels were measured during a period of seismic activity. Similarly in 2015, anthropogenic noise between 40–250 Hz L_{50} exceeded expected limits of prevailing noise (Figure 18) (Wenz 1962). These noise levels were likely caused by the thrusters of the drill rig *West Hercules* (see Section 4.1).

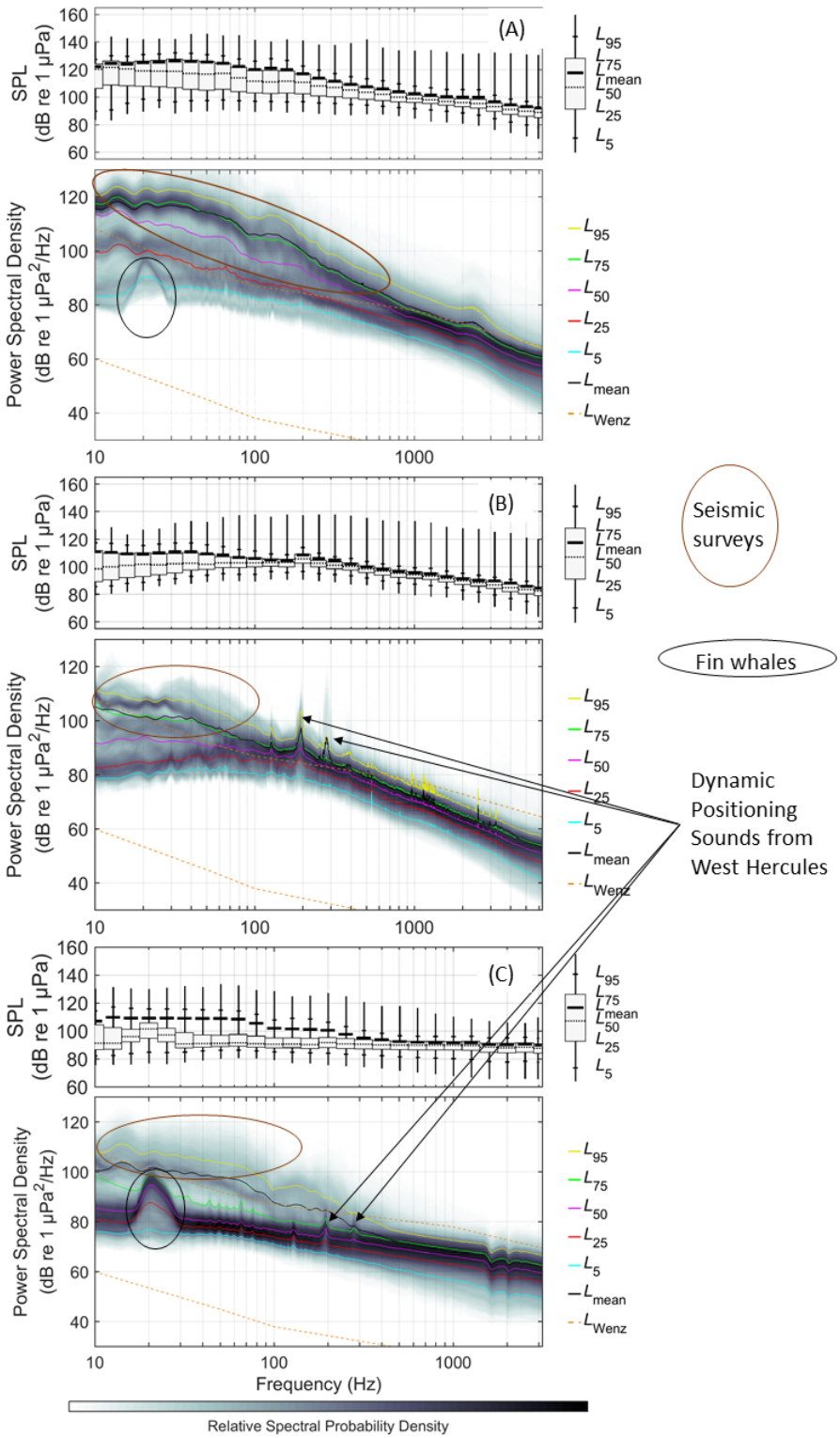

Figure 18. Summary of spectral content of each recorder's acoustic data. (A) CM2 2014, (B) CM2 2015 and (C) ESRF Stn 19. For each station the top figure shows a box-and-whisker plot for the 1/3-octave-band SPLs, and bottom shows the power spectral density percentiles and probability density (grayscale) of 1-min PSD levels compared to the limits of prevailing noise (Wenz 1962). The signatures of seismic surveys, fin whales and the *West Hercules* are annotated.

The daily sound exposure level integrates the total sound energy at a receiver location and is believed to be a good predictor of possible temporary threshold shifts in marine life hearing if it is high enough (([NMFS] National Marine Fisheries Service 2016)). Noise associated with a seismic survey was the main contributor to the daily SEL in 2014, which was up to 35 dB higher than daily SEL recorded at ESRF STN 19 in the absence of seismic surveys (Figure 19). At CM2 in 2015 seismic surveys and vessel noise were the main contributors to the daily SEL, which was 10-15 dB higher than the levels measured at ESRF STN 19 without seismic surveys (Figure 19). The daily SEL associated with seismic surveys in 2015 and 2016 were higher at ESRF STN 19 than what was recorded at CM2. The daily SEL at ESRF STN 19 rose in the winter due to both fin whales and increase wind and wave activity (Figure 19, Figure 18).

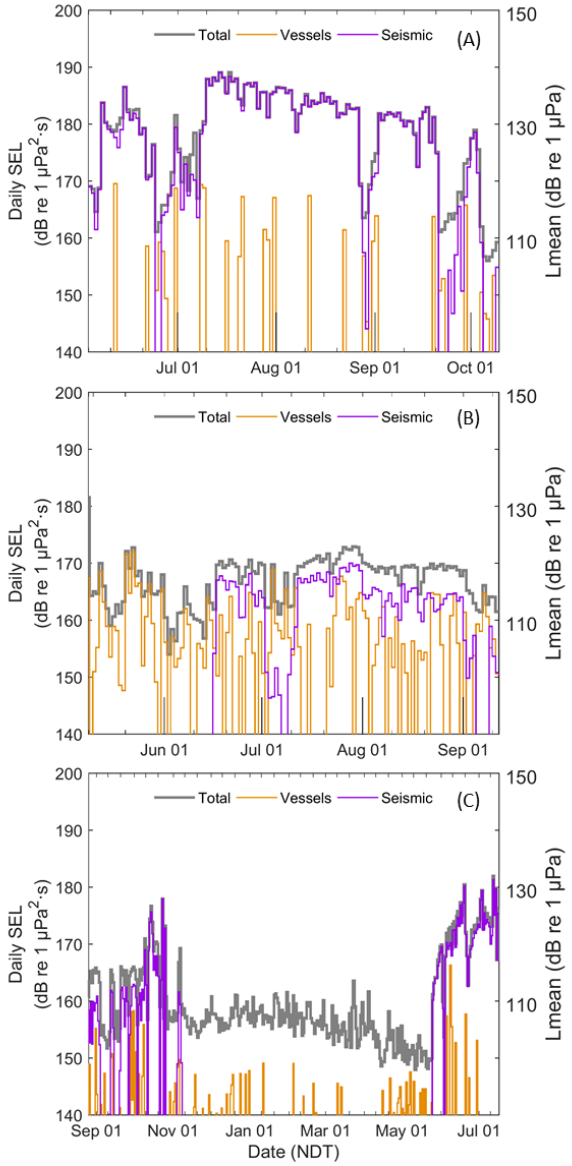

Figure 19. Total, vessel, and seismic-associated daily SEL and equivalent continuous noise levels (L_{mean}). (A) CM2 2014, (B) CM2 2015 and (C) ESRF Stn 19 (Aug 16 – Jul 16). The detectors described in Sections 2.2.2 and 2.2.3 were used to identify the periods when seismic surveys and vessel were the dominant sound sources. In 2015 there were multiple simultaneous surveys which are difficult for the detector to properly distinguish, leading to less energy assigned to the seismic source than was actually in the water.

3.2. Vessel Detections

Vessels were detected using the automated detection algorithm described in Section 2.2.2. Vessel detections denote closest points of approach (CPA) to the recorder, by hour (Figures 20 and 21). The second year of the study had the most vessel detections, which agrees with the known presence of the vessels supporting the Statiol 2014-2016 drilling program (Figure 21). Note that the shipping detector will not detect the constant energy from the drill rig thrusters.

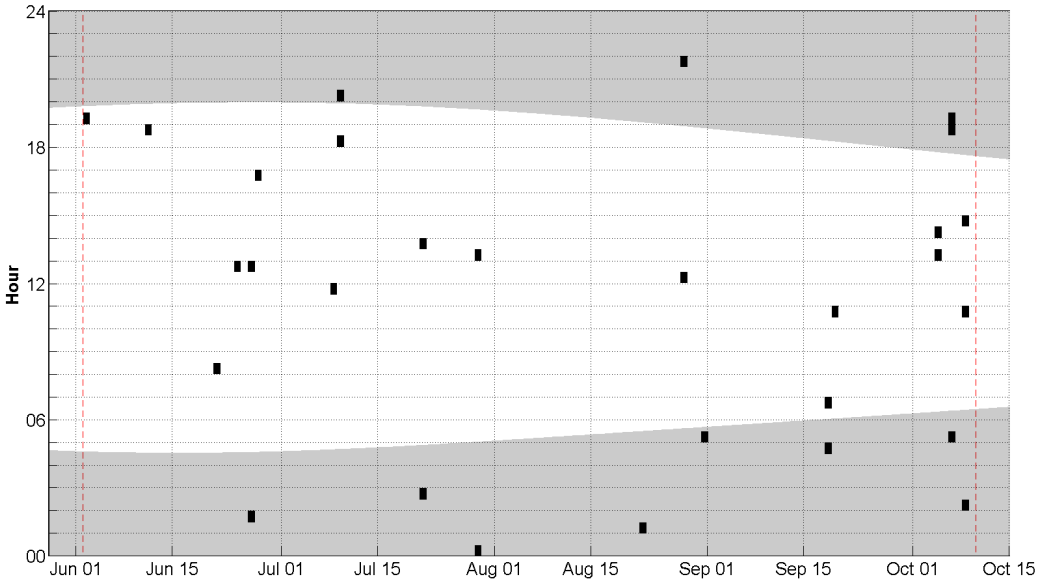

Figure 20. Vessel detections each hour (vertical axis) compared to date (horizontal axis) in the Flemish Pass from 2 Jun to 9 Oct 2014. Shaded areas indicate periods of darkness. The red dashed lines indicate AMAR deployment and retrieval dates.

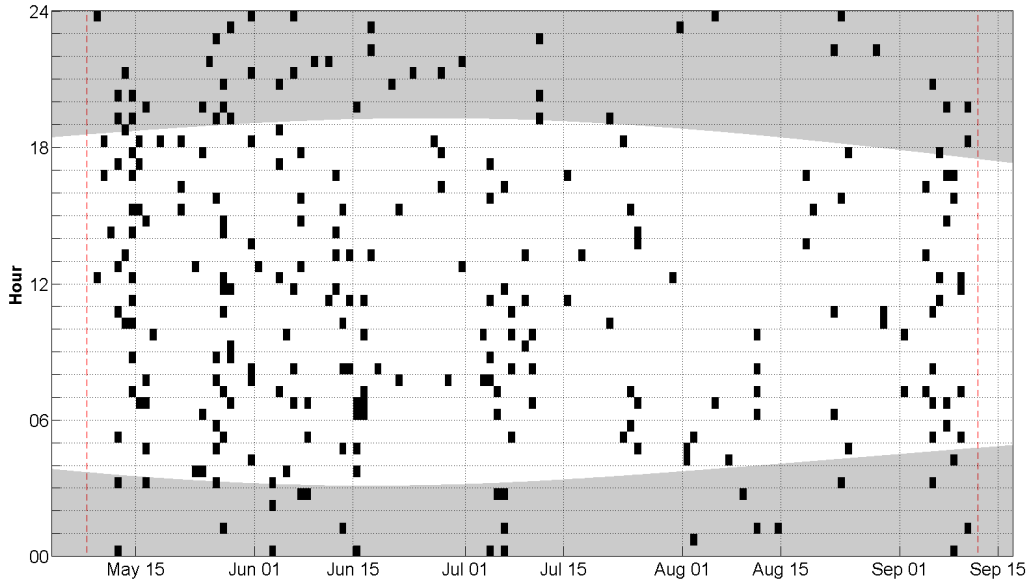

Figure 21. Vessel detections each hour (vertical axis) compared to date (horizontal axis) in the Flemish Pass from 9 May to 11 Sep 2015. Shaded areas indicate periods of darkness. The red dashed lines indicate AMAR deployment and retrieval dates.

3.3. Seismic Survey Sounds

Seismic survey sounds were detected using the automated detection algorithm described in Section 2.2.3. In 2014, seismic noise was the main contributor to the total SEL and had more hours with seismic detections (Figure 22) compared to the distant seismic detected in 2015 (Figure 23). Figures 18 and 19 show the effects of the seismic surveys on the mean daily SPL and power spectral densities.

Propagation of airgun signals in deep waters is highly complex, with different frequencies contributing to the received energy at different ranges and depths. Small changes in the range of the source, the sound speed profile, or the source or receiver depth significantly change the sound levels (Figures 24 and 25). Typical 2D and 3D seismic survey generate one impulse every 10-12 seconds. The multiple impulsive arrivals shown in Figure 24 and Figure 25 are the result of the sound reflecting off the seabed and sea surface multiple times. This number of multi-path arrivals increases with distance between the source and receiver. In the case of Figure 25 the arrivals continue for 8 seconds, a pattern JASCO has previously observed in waters 800 m deep off Greenland. The multipath arrivals tend to have lower amplitudes in deeper waters and for environments with softer bottoms.

Notably in 2015, seismic noise was distant and an example of multiple seismic surveys displaying close and distant seismic noise source is shown in Figure 26.

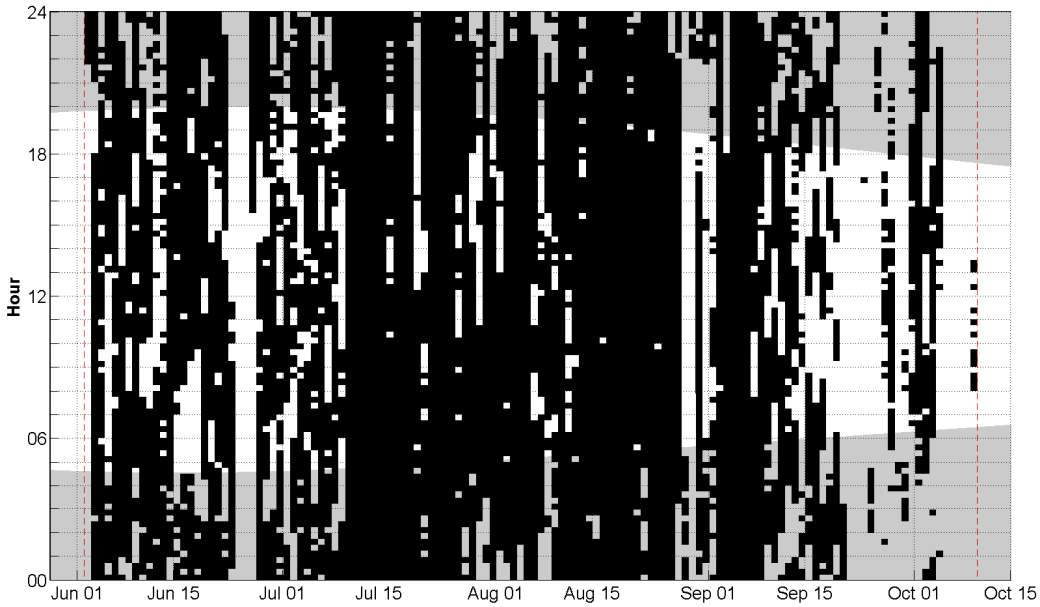

Figure 22. Seismic detections each hour (vertical axis) versus date (horizontal axis) in the Flemish Pass from 2 Jun to 9 Oct 2014. Shaded areas indicate periods of darkness. The red dashed lines indicate AMAR deployment and retrieval dates.

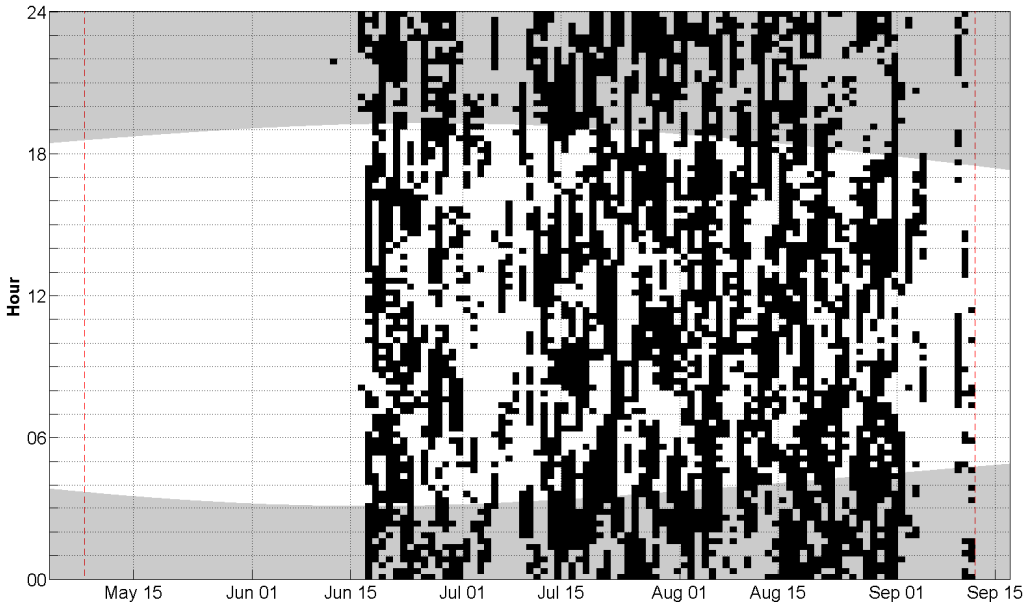

Figure 23. Seismic detections each hour (vertical axis) versus date (horizontal axis) in the Flemish Pass from 9 May to 11 Sep 2015. Shaded areas indicate periods of darkness. The red dashed lines indicate AMAR deployment and retrieval dates.

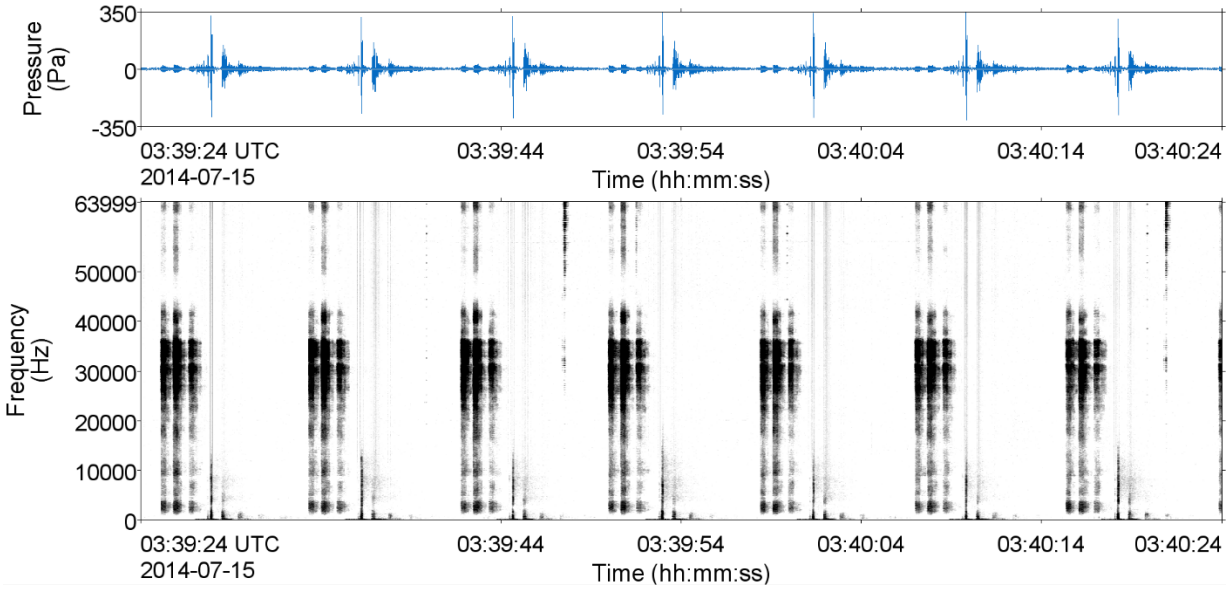

Figure 24. (Top) Pressure signature and (bottom) spectrogram of multibeam seismic pulses from an airgun array on 15 Jul 2014 (2 Hz frequency resolution, 0.128 s frame size, 0.032 s time step, and Hamming window).

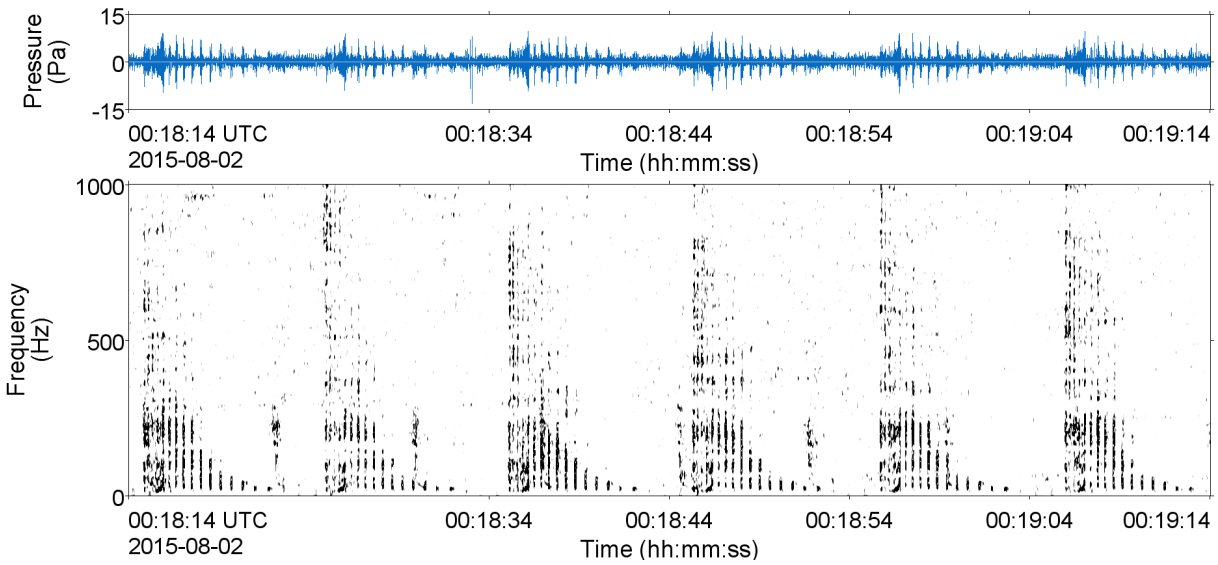

Figure 25. (Top) Pressure signature and (bottom) spectrogram of seismic pulses from an airgun array on 2 Aug 2015 (2 Hz frequency resolution, 0.128 s frame size, 0.032 s time step, and Hamming window).

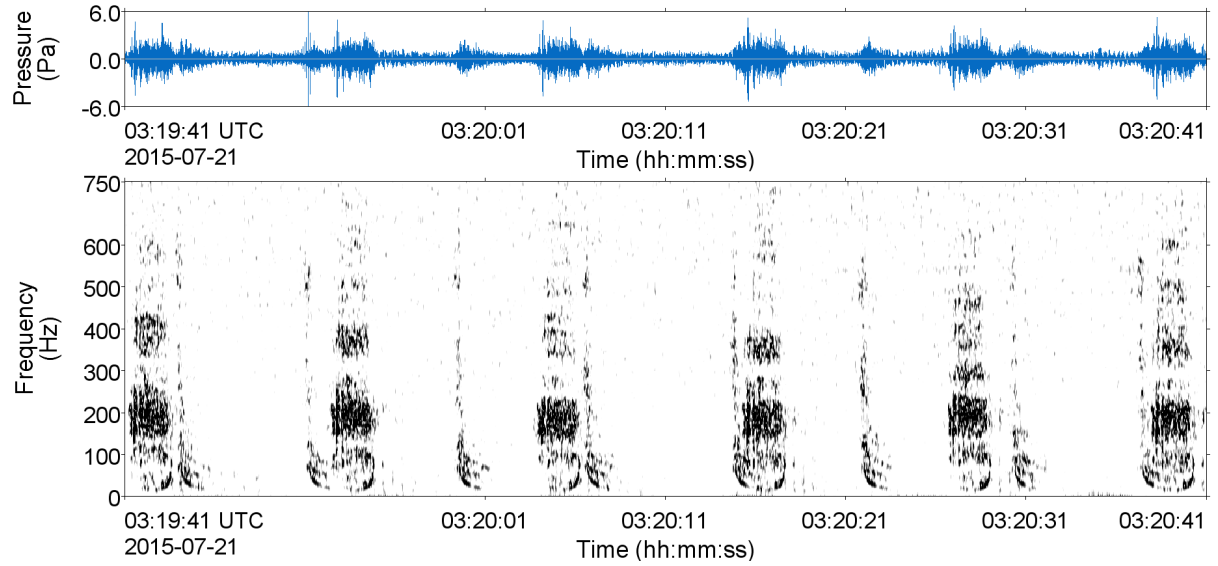

Figure 26. (Top) Pressure signature and (bottom) spectrogram of two seismic surveys on 21 Jul 2015 (2 Hz frequency resolution, 0.128 s frame size, 0.032 s time step, and Hamming window).

3.4. Marine Mammals

The acoustic presence of marine mammals was identified automatically by JASCO's detectors (Section 2.2.4.3), and 5% of the acoustic data was verified by the manual analysis. Detectors and analysts found the 63 kHz acoustic recordings contained sounds from blue, fin, long-finned pilot, northern bottlenose, and sperm whales, as well as dolphins.

3.4.1. Detector Performance

Detector performance varied across species and call types. Except for northern bottlenose whale clicks, pilot whale whistles, and blue whale moans, the detector precision was generally high. It ranged from 0.80 (sperm whales) to 1 (fin whale), indicating that 80 to 100% of files containing calls were correctly detected and classified (Table 8). The lower the precision value, the higher the proportion of non-target signals included in the results. The poor precision for the blue whale moan, pilot whale whistle and northern bottlenose whale click detectors can be attributed to interfering noises consistently falsely triggering the detectors. For pilot whales, false detections were triggered by airgun sounds, vessel noise, and other delphinid whistles. For sperm and northern bottlenose whales, false detections were triggered by airgun sounds, vessel noise (particularly echosounders), and loud delphinid clicks.

Manual validation indicated that detection thresholds were needed for all species identified, except for unknown dolphin/pilot whale clicks (Table 8). These thresholds raised the precision, but lowered the recall values of the detectors. Except for the moderately high-performing dolphin whistle (R = 0.69) and click (R = 0.68) detectors, detector recall values were low to moderate, ranging from 0.13 for fin whales to 0.54 for sperm whales (Table 8). The consistently lower R than P in our detectors reflects the bias of our analysis protocol in favour of precision over recall. A low recall may translate into missing detection events, defined as a string of consecutive files (one or more) with detections of a given species, completely, or missing some files within a detection event. The ultimate effect of a low recall is likely a combination of both scenarios, although the relative contribution of each will depend on species, season, and interfering sound sources at a location. When the primary measure of interest is daily presence of a species, detectors with high precision and lower recall generally provide accurate results with low false alarms.

To compare results across years, the detection count thresholds were calculated using validated detections from both 2014 and 2015. For northern bottlenose, pilot, fin and blue whales, the manual rather than the automated detections will be presented in the following sections.

Table 8. Classification thresholds determined from validating the automated detector outputs. The classification thresholds are the minimum number of detected calls/file required to be confident in that detections are not false alarms. The precision (P), recall (R), and F-score (F) before the threshold is applied (original) and after (threshold) is shown.

File analyzed	Species/call	$P_{original}$	$R_{original}$	Classification threshold	$P_{threshold}$	$R_{threshold}$	$F_{threshold}$
353 files at 2 min 128 ksps	Dolphin whistle	0.90	0.69	1	0.90	0.69	0.85
	Delphinid click	0.79	0.92	40	0.98	0.68	0.90
	Sperm whales	0.55	0.85	17	0.80	0.54	0.73

3.4.2. Odontocetes

3.4.2.1. Northern Bottlenose Whales

The northern bottlenose whale detector was unreliable, as it was falsely triggered by dolphin clicks and high-frequency sperm whale clicks. Therefore, results from manual analysis are presented here and represent a minimum estimate of acoustic occurrence. Clicks classified as northern bottlenose whales had a centroid frequency between 25 and 30 kHz and a smooth upswept contour, ranging in frequency from 20–50 kHz (Figures 27 and 28) (Hooker and Whitehead 2002, Wahlberg et al. 2012).

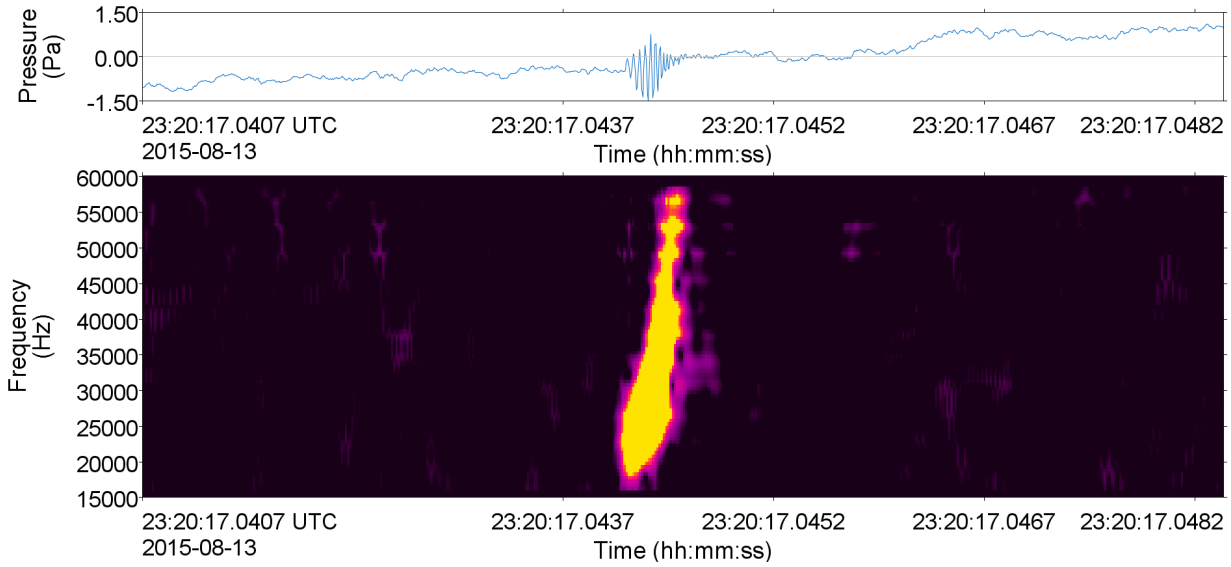

Figure 27. Spectrogram of a northern bottlenose whale click recorded on 13 Aug 2015 (512 Hz frequency resolution, 0.26 ms time window, 0.02 ms time step, Hamming window).

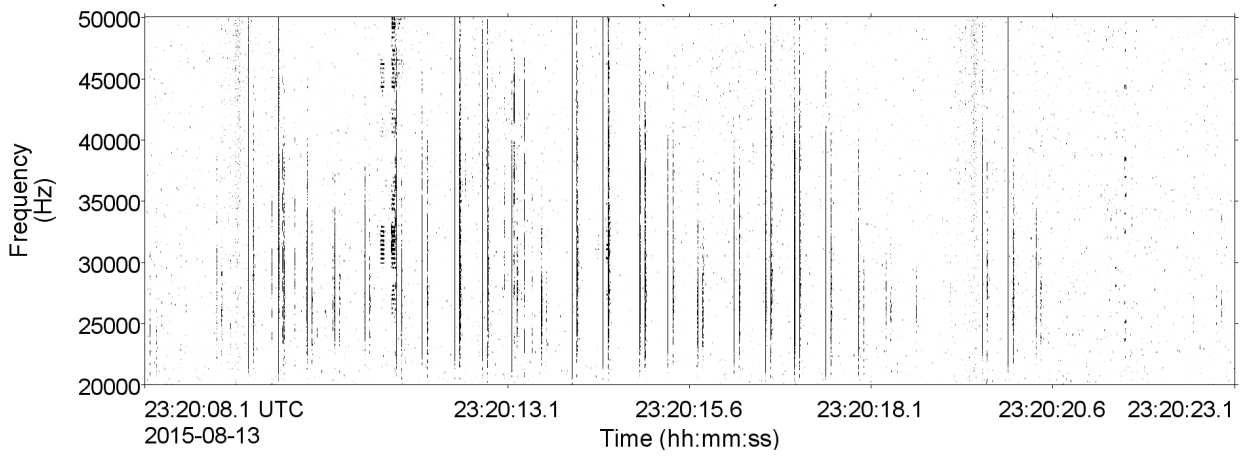

Figure 28. Spectrogram of northern bottlenose whale click trains recorded at 13 Aug 2015 (64 Hz frequency resolution, 0.01 s time window, 0.005 s time step, Hamming window). The window length is 15 s.

Northern bottlenose whale clicks were sporadic throughout the recording period in each year. In 2014, detections occurred from mid-June to mid-July. Additionally, there were detections on one day in mid-August and one in late September (Figure 29, Table 9). In 2015, Two detections occurred in June, while 9 days in July contained northern. Detections also occurred on 4–5 days in both August and September (Figure 30, Table 9).

Table 9. Northern bottlenose whales: Summary of manually validated acoustic detections.

Year	Deployment	First detection	Last detection	Record end	Number of days with manual detections
2014	2 Jun	12 Jun	26 Sep	9 Oct	9
2015	9 May	9 Jun	8 Sep	11 Sep	19

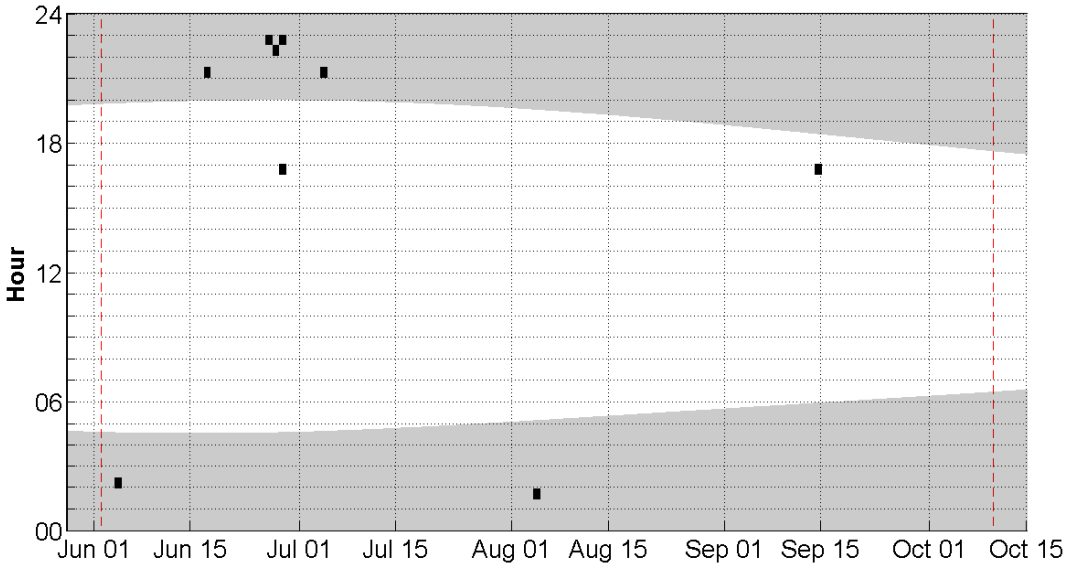

Figure 29. Manual validation of daily and hourly occurrence of northern bottlenose whale clicks recorded in the Flemish Pass from 2 Jun to 9 Oct 2014. Shaded areas indicate periods of darkness. The red dashed lines indicate AMAR deployment and retrieval dates.

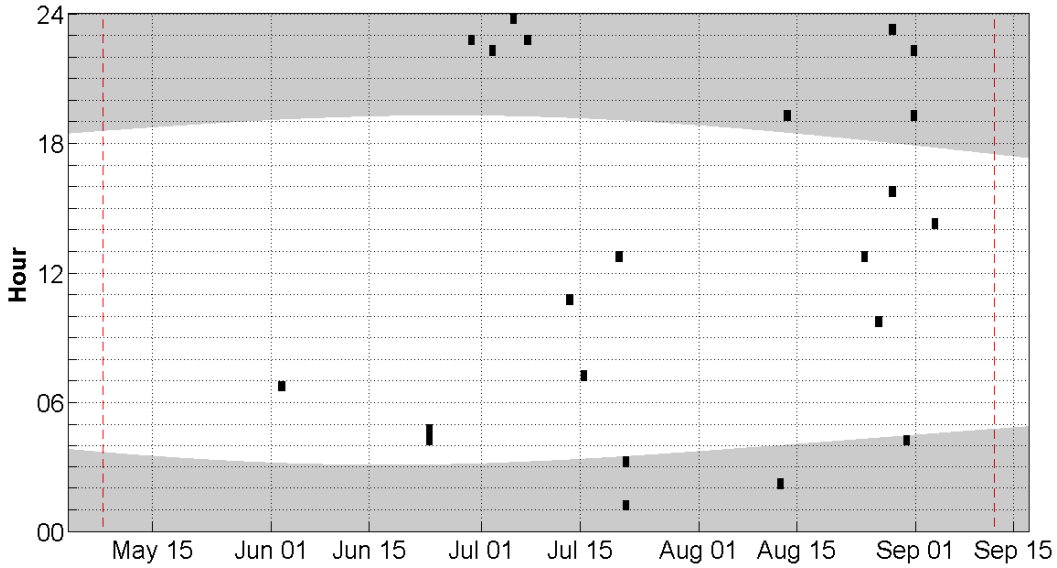

Figure 30. Manual validation of daily and hourly occurrence of northern bottlenose whale clicks recorded in the Flemish Pass from 9 May to 11 Sep 2015. Shaded areas indicate periods of darkness. The red dashed lines indicate AMAR deployment and retrieval dates.

3.4.2.2. *Delphinids*

Unlike most odontocetes that are only known to produce clicks, delphinids produce both impulsive (click) and tonal (whistle) sounds that show less species-level specificity than other marine mammal signals and are therefore more difficult to distinguish acoustically. Here, we present results for pilot whales and unidentified dolphins, species groups that can be confidently distinguished based on their tonal signals (Steiner 1981b, Rendell et al. 1999). The tonal calls of pilot whales have energy at frequencies as low as 1.0 kHz and whistles with acoustic energy concentrated below 5–6 kHz. The main energy in tonal calls of unidentified dolphins is greater than 6 kHz. Because of the overlap in spectral features of tonal signals from the different dolphin species expected in the study area (Steiner 1981a) and the expected but unquantified variability of these signals around the few described call types, we were unable to distinguish dolphin calls by species in most cases.

Delphinid clicks show even less species-specificity than tonal signals, partially because of their directionality and the associated degradation of their spectral features when recorded at increasing angles away from the longitudinal axis of the calling animal. The following subsections present pilot whale and dolphin whistle detections, as well as delphinid click detections.

3.4.2.2.1. Pilot Whales

Pilot whale whistles (Figure 31) were distinguished from dolphin whistles based frequency. Detections generally occurred during summer, June to September (Figures 32 and 33). Pilot whale calls were sparsely detected on 10% of the recording days in 2014, and increased to 15% in 2015 (Table 10). The pilot whale detector had a low recall of 32%, reflecting the ability of manual analysts to identify whistles too faint for the automated detector (Table 8). Thus, the results presented here are the manually validated pilot whale whistles.

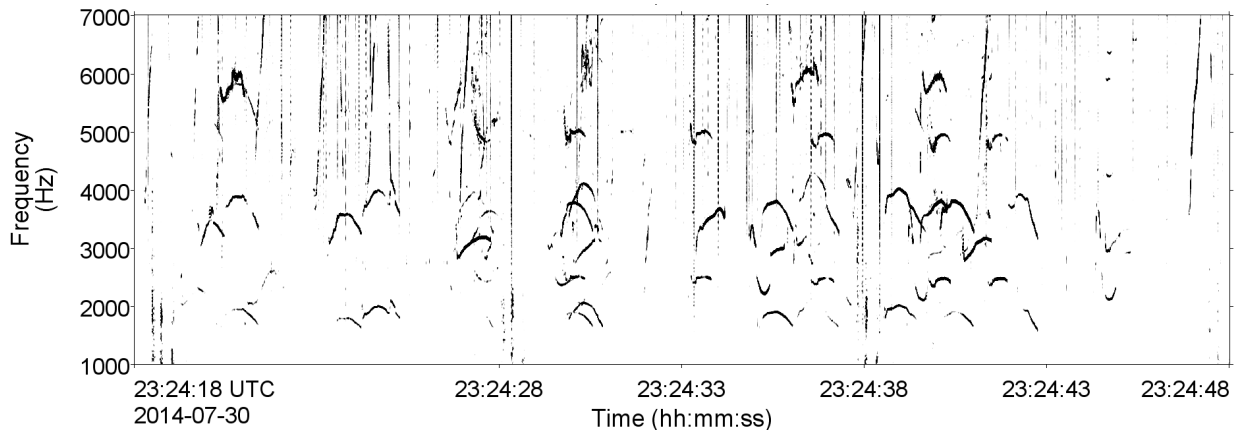

Figure 31. Spectrogram of pilot whale whistles recorded on 30 Jul 2014 (4 Hz frequency resolution, 0.05 s time window, 0.01 s time step, Hamming window). The window length is 30 s.

Table 10. Pilot whales: Summary of manually validated acoustic detections.

Year	Deployment	First detection	Last detection	Record end	Number of days with manual detections
2014	2 Jun	3 Jun	7 Oct	9 Oct	13
2015	9 May	14 May	3 Sep	11 Sep	19

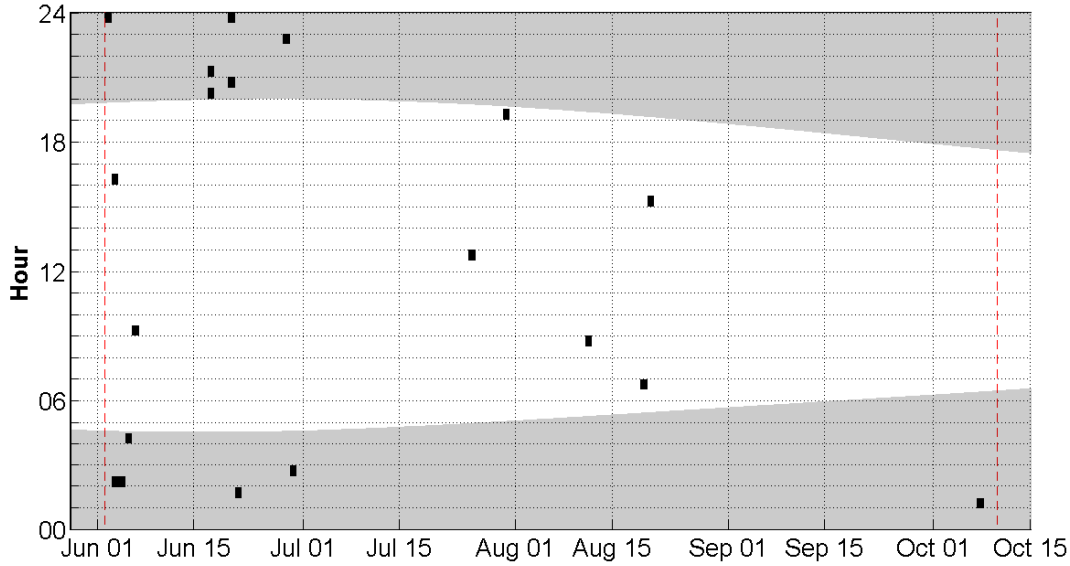

Figure 32. Manual validation of daily and hourly occurrence of pilot whale whistles recorded in the Flemish Pass from 2 Jun to 9 Oct 2014. Shaded areas indicate periods of darkness. The red dashed lines indicate AMAR deployment and retrieval dates.

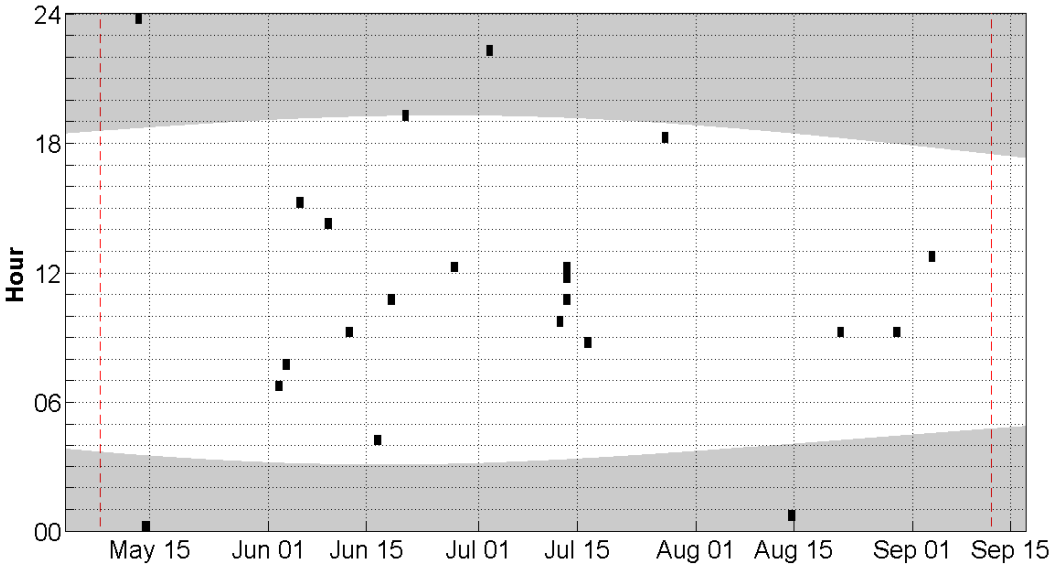

Figure 33. Manual validation of daily and hourly occurrence of pilot whale whistles recorded in the Flemish Pass from 9 May to 11 Sep 2015. Shaded areas indicate periods of darkness. The red dashed lines indicate AMAR deployment and retrieval dates.

3.4.2.2.2. Small Dolphins

The detector performed well for small dolphin whistles (Figure 34) and delphinid clicks (Figures 35 and 36, Table 8). Ninety percent of whistle detections and almost 100% of click detections presented here are accurately classified. The whistle results likely include other acoustic signals such a high-frequency components of pilot whale whistles.

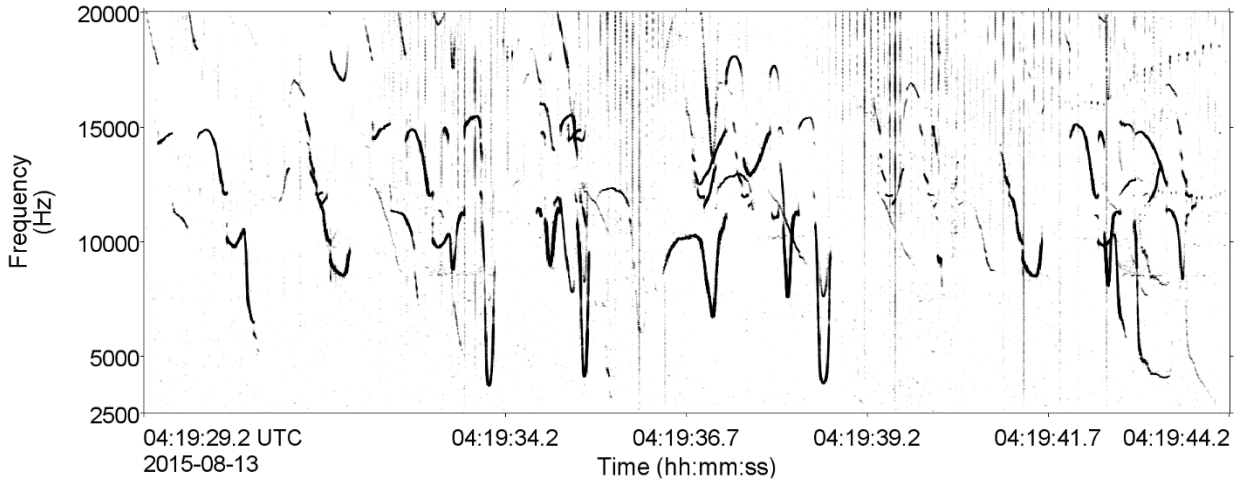

Figure 34. Spectrogram of unidentified dolphin whistles recorded on 13 Aug 2015 (4 Hz frequency resolution, 0.05 s time window, 0.01 s time step, Hamming window). The window length is 15 s.

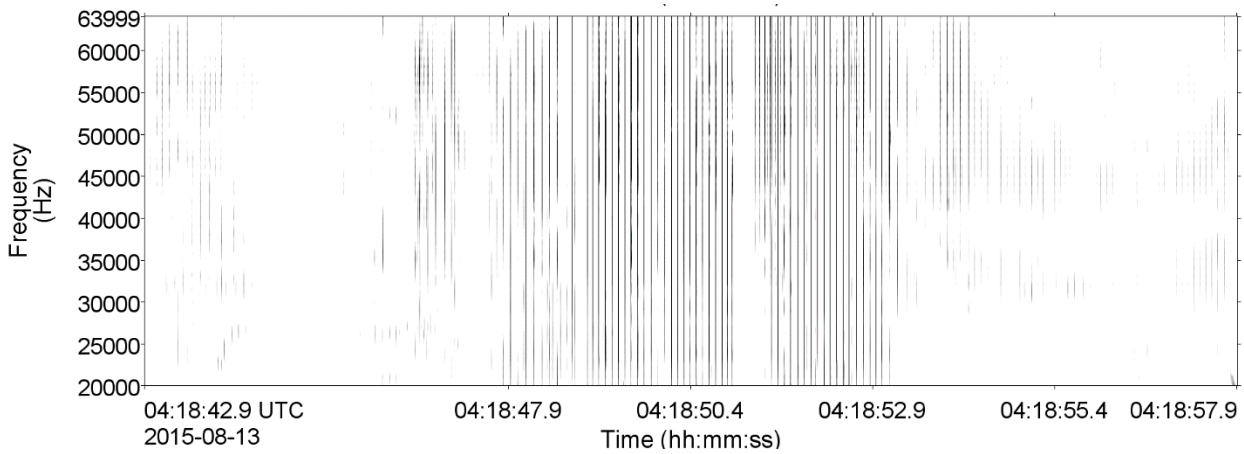

Figure 35. Spectrogram of unidentified dolphin click trains recorded on 13 Aug 2016 (128 Hz frequency resolution, 0.001 s time window, 0.0005 s time step, Hamming window). The window length is 15 s.

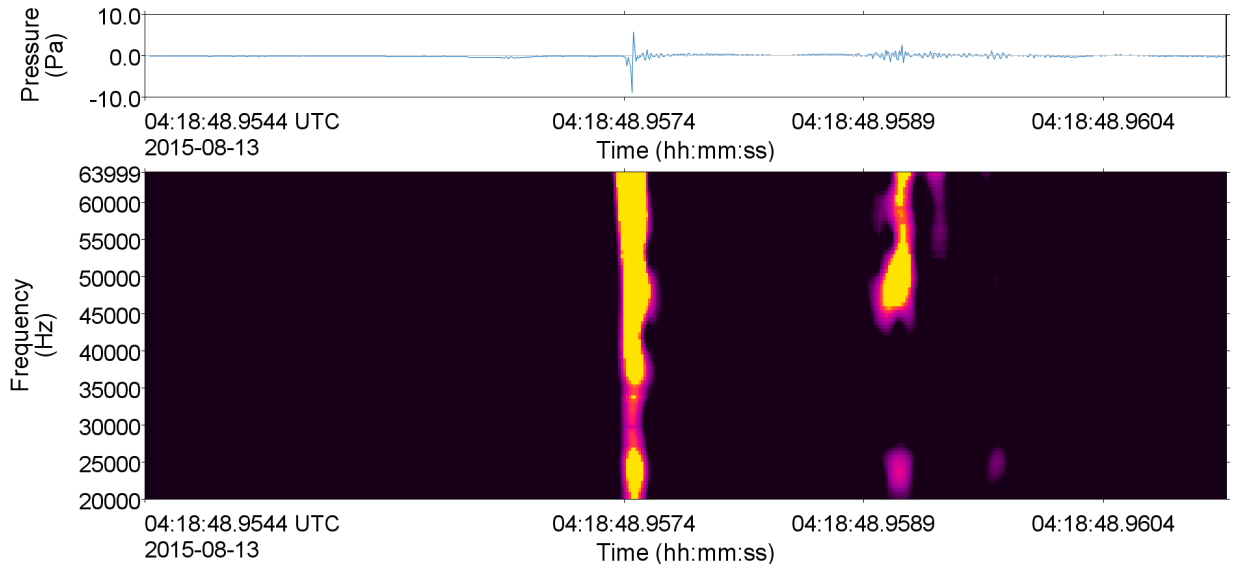

Figure 36. Spectrogram of unidentified dolphin click recorded on 29 Jun 2014 (512 Hz frequency resolution, 0.26 ms time window, 0.02 ms time step, Hamming window).

Clicks and whistles produced by delphinids occurred on ~30% of the recording days (Tables 11 and 12). The number of click detections in 2014 was almost double that of 2015 (Table 11). The opposite is true for whistles detected, as the number of detections in 2015 almost doubles those detected in 2014 (Table 12). Unlike dolphin whistles that were detected throughout the day (Figures 37 and38), delphinid clicks showed a diel pattern, occurring more often at night than in the day (Figures 39 and 40).

Table 11. Delphinid clicks: Summary of automated acoustic detections.

Year	Deployment	First detection	Last detection	Record end	Number of days with manual detections	Number of detections
2014	2 Jun	12 Jun	9 Oct	9 Oct	50	40,852
2015	9 May	9 Jun	10 Sep	11 Sep	36	26,268

Table 12. Dolphin whistles: Summary of automated acoustic detections.

Year	Deployment	First detection	Last detection	Record end	Number of days with manual detections	Number of detections
2014	2 Jun	3 Jun	9 Oct	9 Oct	50	1,598
2015	9 May	14 May	10 Sep	11 Sep	40	2,460

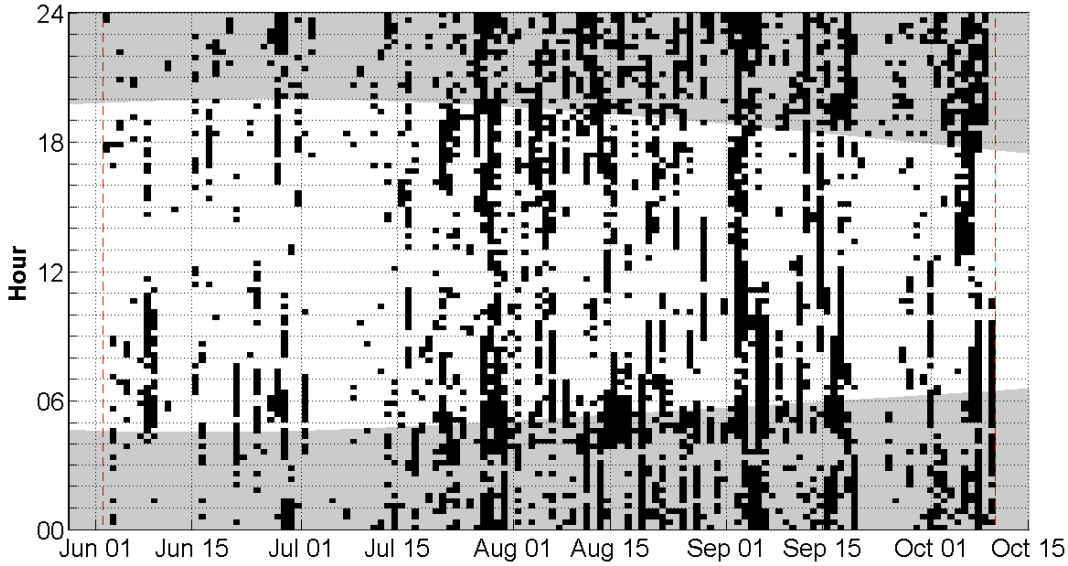

Figure 37. Daily and hourly occurrence of dolphin whistles recorded in the Flemish Pass from 2 Jun to 9 Oct 2014. Shaded areas indicate periods of darkness. The red dashed lines indicate AMAR deployment and retrieval dates.

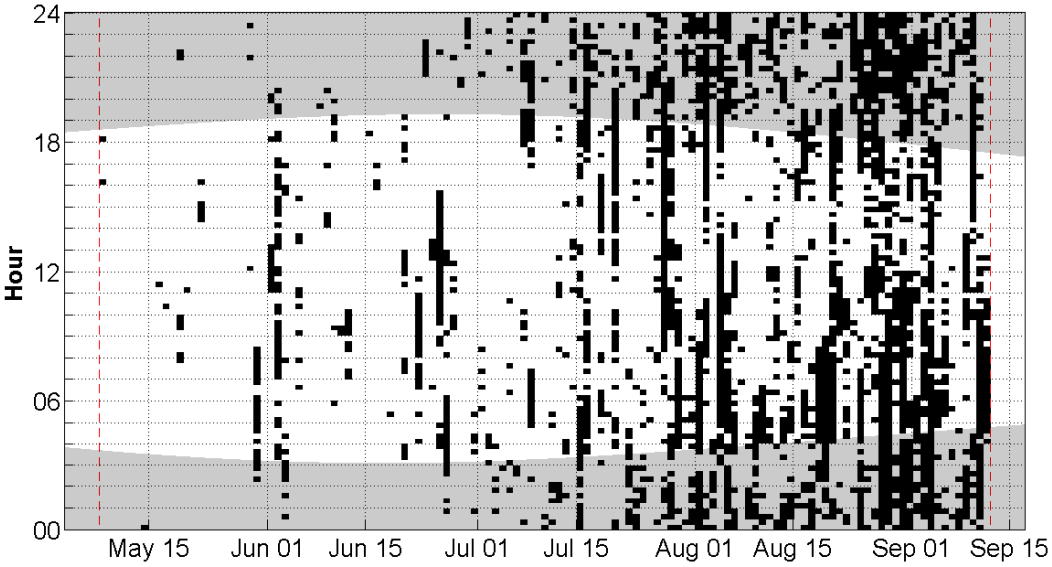

Figure 38. Daily and hourly occurrence of dolphin whistles recorded in the Flemish Pass from 9 May to 11 Sep 2015. Shaded areas indicate periods of darkness. The red dashed lines indicate AMAR deployment and retrieval dates.

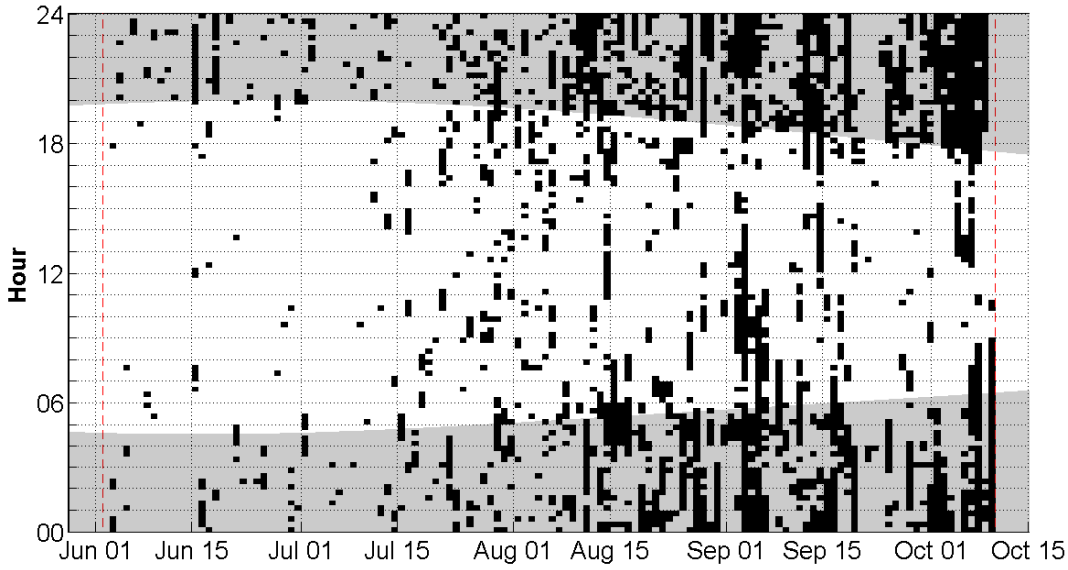

Figure 39. Daily and hourly occurrence of dolphin clicks recorded in the Flemish Pass from 2 Jun to 9 Oct 2014. Shaded areas indicate periods of darkness. The red dashed lines indicate AMAR deployment and retrieval dates.

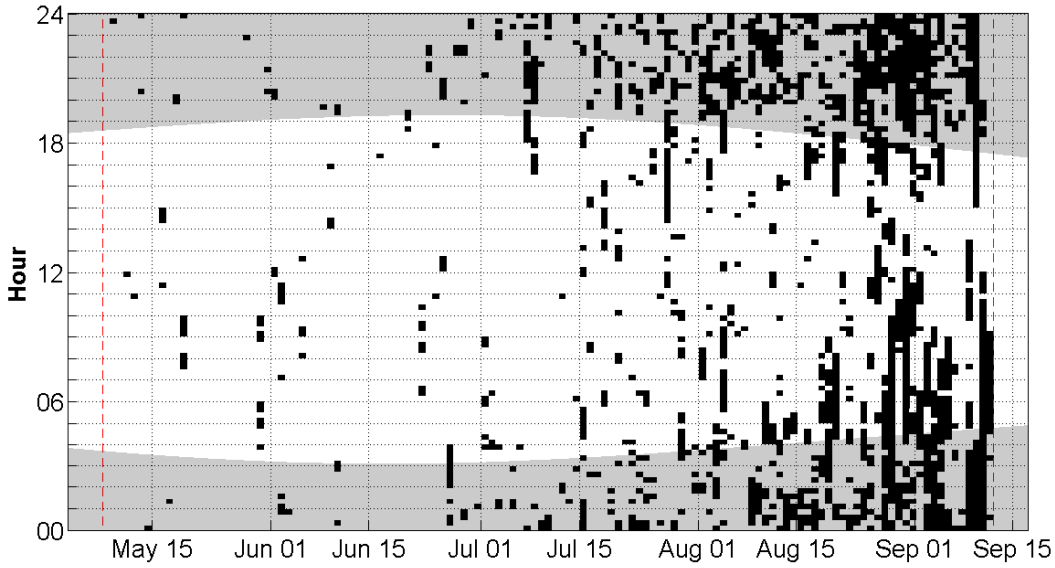

Figure 40. Daily and hourly occurrence of dolphin clicks recorded in the Flemish Pass from 9 May to 11 Sep 2015. Shaded areas indicate periods of darkness. The red dashed lines indicate AMAR deployment and retrieval dates.

3.4.2.3. *Sperm Whales*

Sperm whale clicks (Figure 41) were detected consistently throughout the study period in both years (Table 13, Figures 42 and 43). Sperm whale detections were expected in the deep waters of the Flemish Pass along the shelf break. Sperm whale clicks were accurately classified (P = 80%), but the results underestimate the true presence of the species, as the detector missed over 50% of clicks. This could be the result of the high-frequency targeted by the detector (centre frequency ≥8 kHz), whereas most clicks were faint (<8 kHz) or masked by anthropogenic noise.

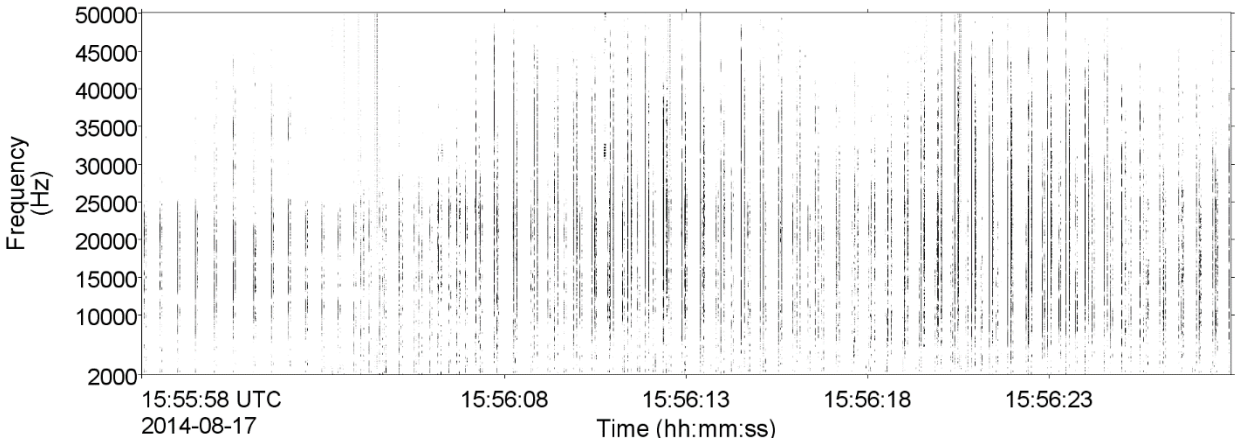

Figure 41. Spectrogram of sperm whale clicks recorded on 17 Aug 2014 (64 Hz frequency resolution, 0.01 s time window, 0.005 s time step, Hamming window). The window length is 30 s.

Table 13. Sperm whales: Summary of automated acoustic detections.

Year	Deployment	First detection	Last detection	Record end	Number of days with manual detections	Number of detections
2014	2 Jun	3 Jun	6 Oct	9 Oct	37	6,517
2015	9 May	9 May	10 Sep	11 Sep	37	6,089

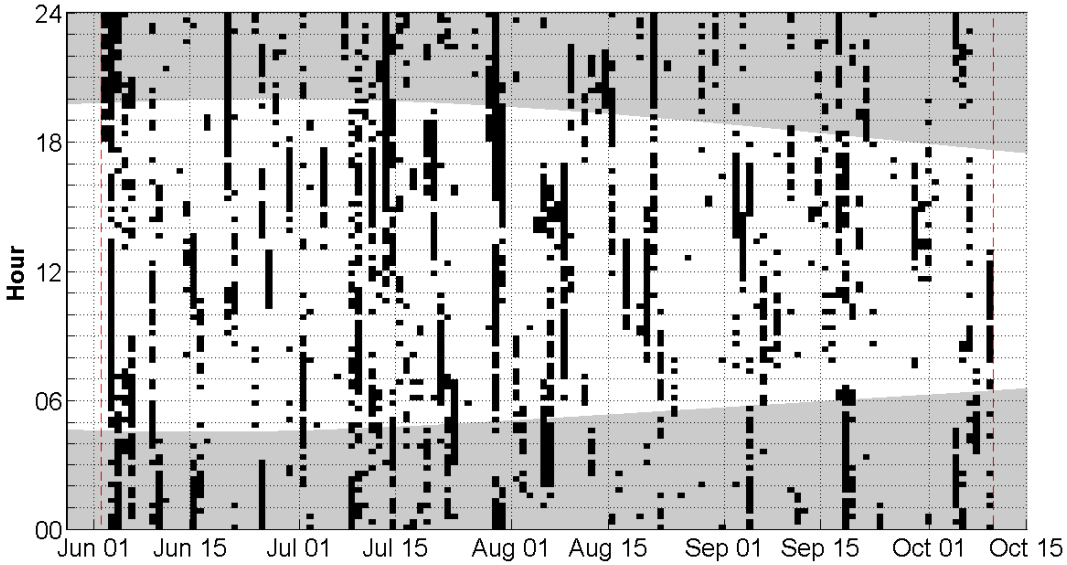

Figure 42. Daily and hourly occurrence of sperm whale clicks recorded in the Flemish Pass from 2 Jun to 9 Oct 2014. Shaded areas indicate periods of darkness. The red dashed lines indicate AMAR deployment and retrieval dates.

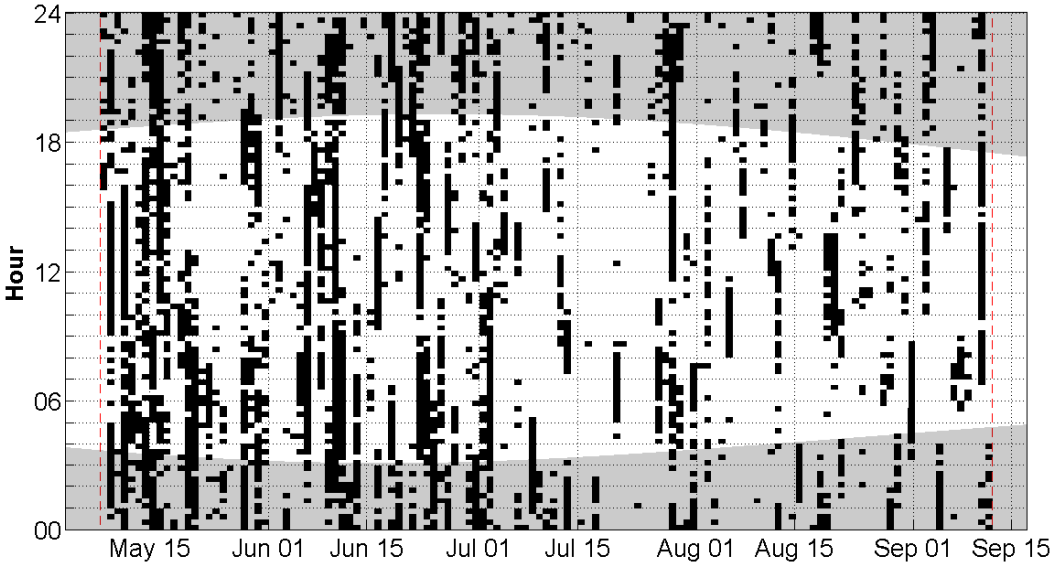

Figure 43. Daily and hourly occurrence of sperm wale clicks recorded in the Flemish Pass from 9 May to 11 Sep 2015. Shaded areas indicate periods of darkness. The red dashed lines indicate AMAR deployment and retrieval dates.

3.4.3. Mysticetes

3.4.3.1. *Blue Whales*

Infrasonic blue whale calls were manually detected in the Flemish Pass in both years of the study (Figure 44) (Mellinger and Clark 2003). This call type is produced in late summer, fall, and winter. Calls were detected on 7 Aug and 2 Oct 2014 (Table 14). While most automated detections occurred in mid-May through mid-June during the 2015 deployment, none of these calls were validated as truly produced by blue whales. Seismic and vessel noise triggered the detector, thus, only manual validated results are presented here. Validated detections occurred on 2 Sep and ended 10 Sep 2015 (Table 14).

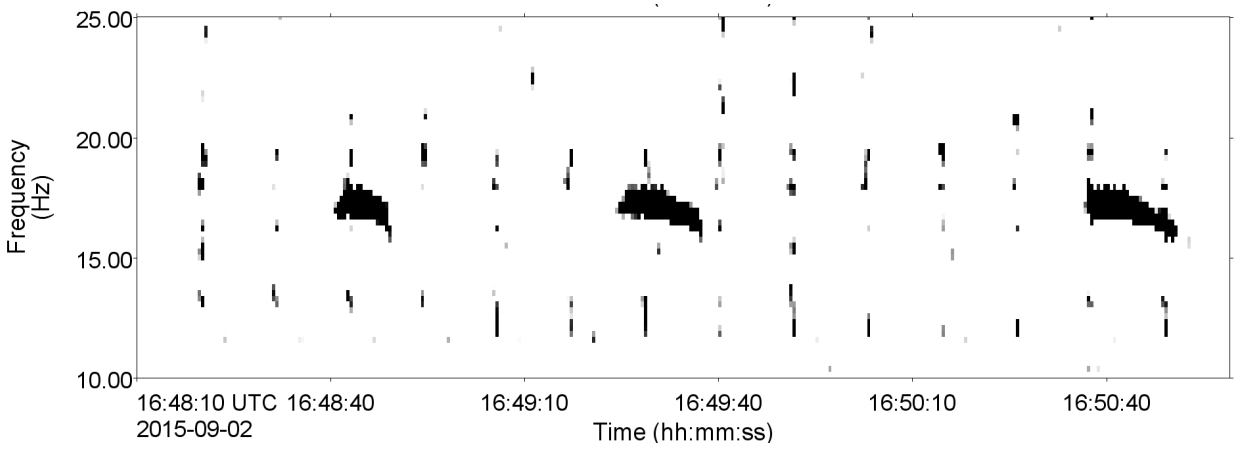

Figure 44. Spectrogram of blue whale infrasonic moans recorded on 2 Sep 2015 (0.4 Hz frequency resolution, 2 s time window, 0.5 s time step, Hamming window).

Table 14. Blue whales: Summary of manually validated acoustic detections.

Year	Deployment	First detection	Last detection	Record end	Number of days with manual detections
2014	2 Jun	7 Aug	2 Oct	9 Oct	2
2015	9 May	2 Sep	10 Sep	11 Sep	3

3.4.3.2. *Fin Whales*

A low number of fin whale calls were manually detected, as the detector was falsely triggered by seismic noise during the study period and some calls were likely masked by these same noises. Fin whale calls were detected on 3 Jun 2014 and occurred sporadically in Aug (22) and Sep (5–8) 2015 (Table 15). The 20-Hz notes detected in late summer to early fall coincided with the beginning of the period associated with song production (Figure 45) (Watkins et al. 1987).

Table 15. Fin whales: Summary of manually validated acoustic detections.

Year	Deployment	First detection	Last detection	Record end	Number of days with manual detections
2014	2 Jun	3 Jun	3 Jun	9 Oct	1
2015	9 May	22 Aug	8 Sep	11 Sep	5

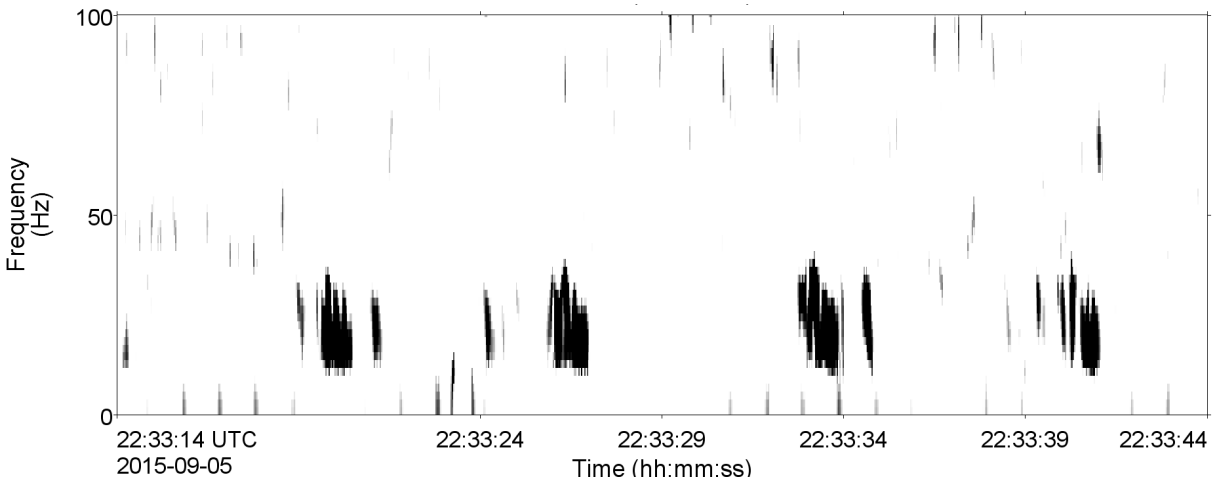

Figure 45. Spectrogram of fin whale 20 Hz notes recorded on 5 Sep 2015 (2 Hz frequency resolution, 0.128 s frame size, 0.032 s time step, and Hamming window).

4. Discussion and Conclusion

4.1. Identifying the Effects of Drilling Operations and Seismic Surveys on the Measured Sound Levels

The data collected at CM2 provide an opportunity to analyze the sounds generated by a semi-submersible drilling operation and seismic surveys. In Figure 46 the mean power spectral density for ESRF STN 19 from 15 Nov 15 – 1 Jun 16 is provided as a baseline for deep water sound levels in the general area of the Flemish Pass. The seismic signature from CM2 in 2014 is 30-35 dB above this baseline up to 100 Hz, and remains 10 dB above the baseline even at 4 kHz. This result is typical for an area within 10-100 km from a seismic survey. A single day's mean power spectral density from 7 Oct 2014 during which there was no seismic surveys or close passes of vessels is also provided. This curve closely follows the baseline, which indicates that ESRF STN 19 is a good proxy for the conditions in the Statoil 2014-2016 drilling area and that differences in recording depth did not affect our ability to compare the measurements.

The period of 25 May – 17 June 2015 was selected as representative of the sounds from the semi-submersible drilling operation in the absence of seismic surveys (see Figure 16). The mean power spectral density for this period exceeds the baseline in the frequency range of 30 – 2000 Hz, with two notable tones at 200 Hz and 290 Hz that were also barely detectable in the baseline (see Figure 16, Figure 18 and Figure 46). A third tone at 120 Hz may be associated with the power generation systems on the semi-submersible drill rig. To further compare the sound levels, a box-and-whisker plot of the decade band SPL from 100-1000 Hz is provided (Figure 47). The mean sound levels from the semi-submersible drill rig were 13 dB above the baseline, while the seismic was 25 dB above baseline in this band.

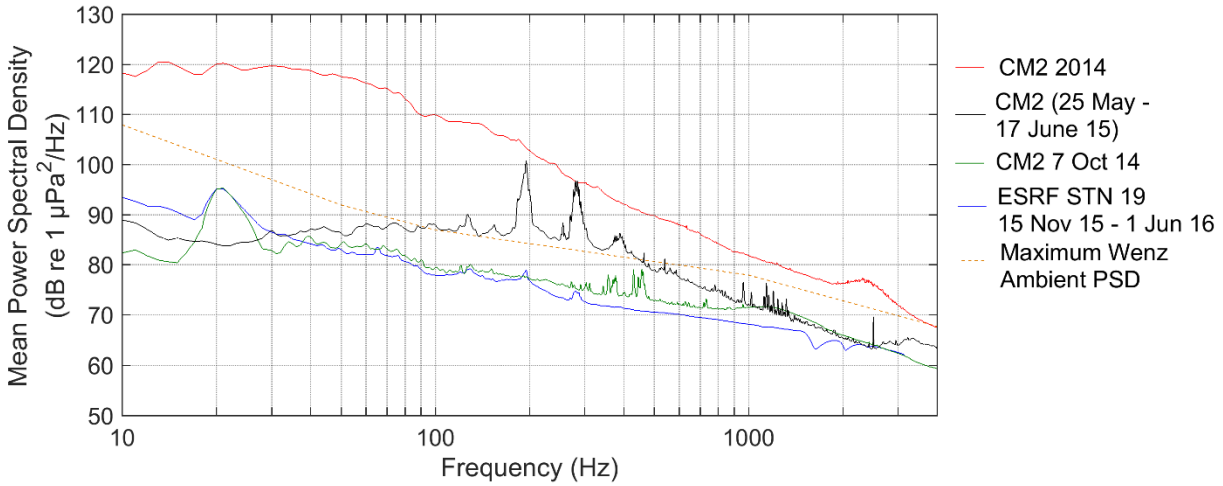

Figure 46. Mean power spectral densities for the complete CM2 2014 data set and three data sets without seismic: CM2 on 7 Oct 14, CM2 2015 for the period of 25 May – 17 Jun 15 and ESRF STN 19 for 15 Nov 15 – 1 Jun 16.

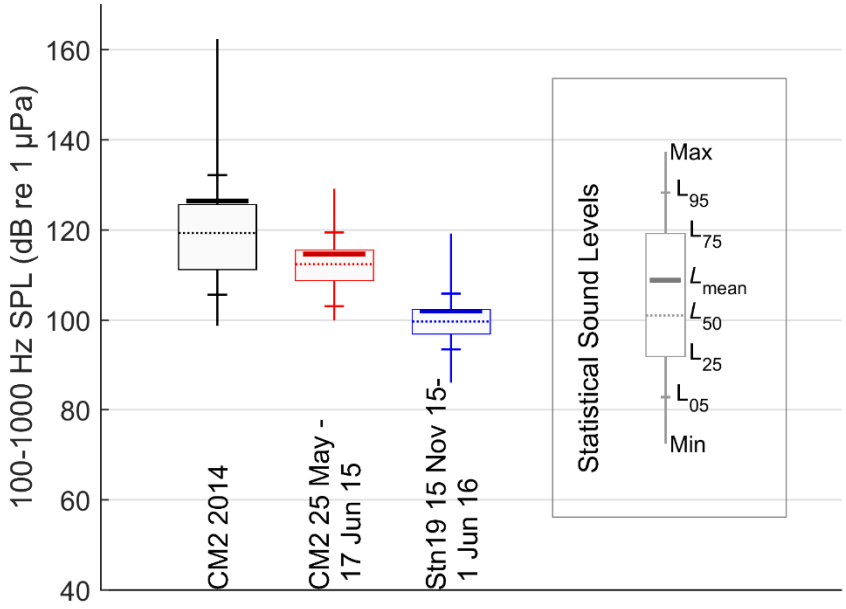

Figure 47. Comparison of the 100-1000 Hz SPLs for all of the CM2 2014 data, CM2 2015 for three weeks without seismic, and ESRF STN 19 without seismic.

JASCO previously measured the sound levels from the Stena IceMax drill ship during Shell Canada's drilling at the Monterey Jack well site (MacDonnell and Martin, 2017). This rig had six Rolls-Royce UUC-505 5,500 kW dynamic positioning thrusters. This rig has a similar shape to it's power spectral density signature, but without the distinct tones at 200 and 290 Hz (Figure 48). The broadband source level of the Stena IceMAX was computed to be 187.7 dB re 1 µPa. Based on the current results and a conservative estimate of the propagation loss differences between the Stena IceMAX measurement and the CM2 location, the *West Hercules* likely has a similar source level. Detailed acoustic modeling could be performed in the future to estimate a more accurate source level if required.

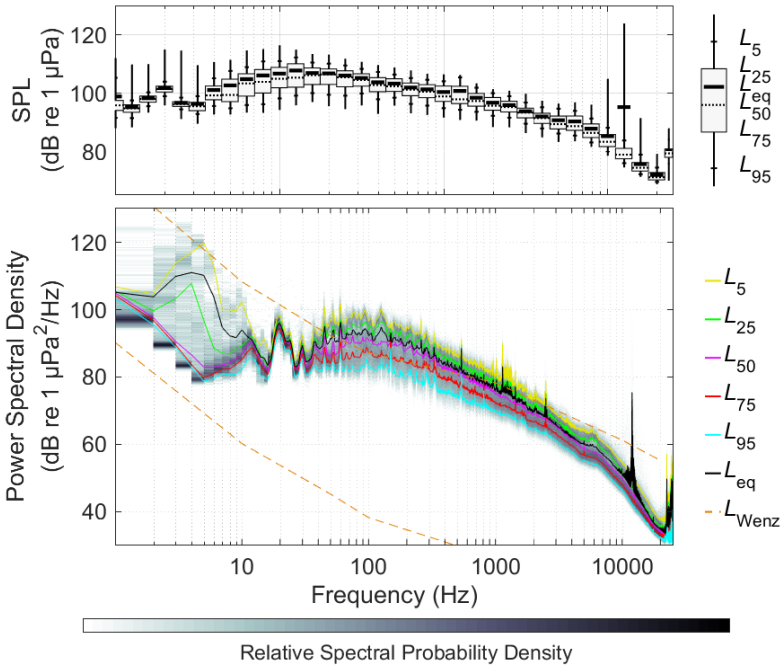

Figure 48 . Power Spectral density plot from 1 day of data collected 2800 m slant range from the Stena IceMAX (MacDonnell and Martin, 2017).

4.2. Marine Mammals

The acoustic detections of marine mammals presented in this report provide an index of acoustic occurrence for each species. They do not represent the number of individuals present at the time of detections. An absence of detections could be the result of an absence of animals, individuals near the acoustic recorders not vocalizing, masking of calls by environmental or anthropogenic noise sources, or a combination of these factors. We compare the acoustic occurrence of each species in the context of noise conditions and their effect on the detectability or masking of calls. Seasonal variations in marine mammal calling behaviour, which may falsely suggest changes in occurrence, are also discussed.

4.2.1. Odontocetes

4.2.1.1. Northern Bottlenose Whales

Two northern bottlenose whale populations occur off eastern Canada (Dalebout et al. 2001): an endangered, well-studied population in the Gully and adjacent canyons (Whitehead et al. 1997, Gowans et al. 2000, Wimmer and Whitehead 2004) and a larger, predominantly unstudied population off the northeast Grand Banks, Labrador, and in the Davis Strait. The boundary between these two populations is unclear (Dalebout et al. 2001). A recent study (ESRF unpublished data) confirmed that northern bottlenose whales are present year-round along the shelf break, particularly north of the Flemish Cape and off the southern Labrador coast.

Detections were infrequent, but they do confirm that northern bottlenose whales are in the Flemish Pass throughout the summer and early fall. Northern bottlenose whale detections occurred simultaneously with seismic surveys. Similarly, the concurrent detections of the northern bottlenose whales and active seismic exploration has been previously noted in the study area (ESRF unpublished data).

4.2.1.2. *Dolphins*

Dolphin whistles were the most prevalent tonal acoustic signals in the data. We could not determine the species due to the limited manual validation performed and the lack of detailed whistle descriptions for the species potentially involved. Based on the results from previous aerial surveys (Lawson and Gosselin 2011), the species likely responsible for most of the detections are white-beaked, white-sided, and short-beaked common dolphins.

The white-beaked dolphin is the northernmost species included in this group (Mercer 1973). Their habitat is characterized by shallow depth and low water temperatures (MacLeod et al. 2007). In eastern Canadian waters they have been observed in winter and spring off Newfoundland and in summer off Labrador (Mercer 1973, Reeves et al. 1998). They are regularly observed in summer in the Strait of Belle Isle (Kingsley and Reeves 1998). White-beaked dolphins were the most abundant dolphin species recorded in the Newfoundland-Labrador strata during the 2007 TNASS aerial surveys (Lawson and Gosselin 2011).

Atlantic white-sided dolphins are known to occur in the study region (Mercer 1973). The northern limit of these species is presumably linked to that of white-beaked dolphins. As white-beaked dolphins retract to the more northern part of the east coast waters, tracking the movement of colder waters, white-sided dolphin likely expand their range to the north in summer. Their abundance was second to that of white-beaked dolphins and common dolphins in the Newfoundland-Labrador and Scotian shelf-Gulf of St. Lawrence strata of the 2007 TNASS surveys, respectively (Lawson and Gosselin 2011).

Short-beaked common dolphins prefer warmer, more saline waters than Atlantic white-sided dolphins, and they tend to inhabit the edge of the continental shelf (Selzer and Payne 1988, Gowans and Whitehead 1995). However, these species often inhabit the same area when an abundance of prey is present. Off eastern Canada, they occur mostly in summer and fall in slope waters of the Scotian Shelf and southern Newfoundland, as well as near prominent bathymetric features such as the Flemish Cape (Jefferson et al. 2009). Common dolphins were by far the most common dolphins sighted in the Scotian Shelf-Gulf of St. Lawrence strata during the 2007 TNASS surveys (Lawson and Gosselin 2011).

It is unlikely, but possible that Risso's, striped, and bottlenose dolphins are present the study area. Their relative contribution to the dolphin acoustic detections is unlikely or very limited.

Click detections followed a strong diel pattern. Detections occurred almost exclusively at night, which reflects the night-time foraging of dolphins that takes advantage of the diel vertical migration of their prey species (Au et al. 2013). Species-specific identification using clicks remains challenging due to the overlap in click characteristics and lack of published description, especially for dolphins.

4.2.1.3. *Pilot Whales*

The range of pilot whales extends in the western North Atlantic from the United States to Greenland (Abend and Smith 1999). Gowans and Whitehead (1995) reported them on the Scotian Slope, and (Sergeant 1962) reported them in Newfoundland waters. The 2007 TNASS surveys estimated the population size for the Scotian Shelf-Gulf of St. Lawrence strata at ~16,000 individuals (Lawson and Gosselin 2011). In a previous study (ESRF unpublished data), acoustic detections were more focused at stations along the continental slope, a known preferred habitat where pilot whales (Payne and Heinemann 1993) forage on long-finned squid (*Lollgo pealei*), among other species (Gannon et al. 1997, Aguilar Soto et al. 2009). In the current study, pilot whales were detected infrequently, suggesting that the animals may be less abundant in this specific region during the summer and early fall, or less vocally active. Because pilot whale calls have tonal components (pulsed calls and whistles) that can be reliably distinguished from dolphin whistles on the basis of frequency, the results presented here are believed to accurately describe the occurrence of this species.

4.2.1.4. *Sperm Whales*

Sperm whales are widely distributed in the Atlantic Ocean, including the present study region. In eastern Canada, they prefer areas near the continental slope although they have been occasionally encountered in shallow areas of the Scotian Shelf (Whitehead et al. 1992). Sperm whales in eastern Canadian waters appear to be exclusively males, with the possible exceptions of areas near the US-Canada border (Reeves and Whitehead 1997). Females remain at lower latitudes year-round, while males migrate between higher latitudes feeding grounds in the summer and lower latitude to breed in winter (Whitehead 2002). In the current study, sperm whales were acoustically detected throughout summer and early fall, in both 2014 and 2015. The almost continuous detections presented here confirm the importance of the Flemish Pass and continental slope area for this species.

4.2.2. Mysticetes

4.2.2.1. *Blue Whales*

Blue whale calls were infrequent, occurring only on two days in the late summer to early fall of 2014 and three days during the beginning of September in 2015. Besides localized, well-studied, summer concentrations, such as the Gulf of St. Lawrence (Sears and Calambokidis 2002), the distribution and movements of endangered blue whales off Atlantic Canada and in the north Atlantic in general remain poorly understood (Reeves et al. 2004). Some of these detections may be from individuals foraging in the Davis Strait in summer and migrating south in fall (Sears and Calambokidis 2002). In most areas of the North Atlantic, peak song detections occur in December and January, with a sharp decline in February and March (Charif and Clark 2000, Clark and Gagnon 2002, Nieukirk et al. 2004). The idnetificaion of blue whale calls is reliable; therefore, some blue whale calls in this area may have been masked by seismic and vessel noise and the detections presented here offer a mininum estimate of acoutic occurence.

4.2.2.2. *Fin Whales*

Previous results (ESRF unpublished data) indicate that the Grand Banks is an important area for fin whales, particularly in fall and winter. Our sparse detections in the early fall are consistent with these results, and with the fin whales' known preference for shelf break and deep water habitats. An ongoing analysis of songs suggest that at least three acoustic populations, characterized by different song structure (Hatch and Clark 2004, Delarue et al. 2009), occur in Canadian waters. One occurs in the Gulf of St. Lawrence, eastern Scotian Shelf and southern Newfoundland; a second is found in the Bay of Fundy, western Scotian Shelf and farther south; the third one prefers areas on the Grand Banks and off Labrador (Delarue et al. 2009; Delarue, unpublished data). Fin whale produce loud sequences of low-frequency notes (~20 Hz) repeated every 9–15 s for hours at a time (Watkins et al. 1987). This calling behaviour translates into a high detection probability. The lack of detections during the study period may not represent the number of individuals in the area, rather some calls may have been masked by seismic noise and various other low-frequency noises.

Literature Cited

[CNLOPB] Canada-Newfoundland Offshore Petroleum Board. 2016. *2015-16 Annual report*. 18 pp. http://www.cnlopb.ca/pdfs/ar2016e.pdf?lbisphpreq=1.

[NMFS] National Marine Fisheries Service. 2016. *Technical Guidance for Assessing the Effects of Anthropogenic Sound on Marine Mammal Hearing: Underwater Acoustic Thresholds for Onset of Permanent and Temporary Threshold Shifts*. U.S. Department of Commerce, NOAA. NOAA Technical Memorandum NMFS-OPR-55. 178 pp. http://www.nmfs.noaa.gov/pr/acoustics/Acoustic%20Guidance%20Files/opr-55_acoustic_guidance_tech_memo.pdf.

[NRC] National Research Council. 2003. *Ocean Noise and Marine Mammals*. National Research Council (U.S.), Ocean Studies Board, Committee on Potential Impacts of Ambient Noise in the Ocean on Marine Mammals. The National Academies Press, Washington, DC. 192 pp. http://www.nap.edu/openbook.php?record_id=10564.

Abend, A., G. and T. Smith, D. 1999. *Review of the distribution of the long-finned pilot whale (Globicephala melas) in the North Atlantic and Mediterranean*. *In*: U.S. Department of Commerce, National Oceanic and Atmospheric Administration, National Marine Fisheries Service, and Northeast Fisheries Science Center. Volume 117. NOAA Technical Memorandum NMFS-NE-117. 1-22 pp. www.nefsc.noaa.gov/nefsc/publications/tm/tm117/tm117.pdf.

Aguilar Soto, N., M.P. Johnson, P.T. Madsen, F. Diaz, I. Dominguez, A. Brito, and P. Tyack. 2009. Cheetahs of the deep sea: deep foraging sprints in short-finned pilot whales off Tenerife (Canary Islands). *Journal of Animal Ecology* 77: 936-947.

Amorim, M.C.P. 2006. Diversity of sound production in fish. *Communication in fishes* 1: 71-104.

Arveson, P.T. and D.J. Vendittis. 2000. Radiated noise characteristics of a modern cargo ship. *Journal of the Acoustical Society of America* 107(1): 118-129.

Au, W.W., R.A. Kastelein, T. Rippe, and N.M. Schooneman. 1999. Transmission beam pattern and echolocation signals of a harbor porpoise (Phocoena phocoena). *The Journal of the Acoustical Society of America* 106(6): 3699-3705.

Au, W.W., G. Giorli, J. Chen, A. Copeland, M. Lammers, M. Richlen, S. Jarvis, R. Morrissey, D. Moretti, et al. 2013. Nighttime foraging by deep diving echolocating odontocetes off the Hawaiian islands of Kauai and Ni'ihau as determined by passive acoustic monitors. *The Journal of the Acoustical Society of America* 133(5): 3119-3127.

Au, W.W.L. and K. Banks. 1998. The acoustics of the snapping shrimp Synalpheus parneomeris in Kaneohe Bay. *Journal of the Acoustical Society of America* 103(1): 41-47.

Berchok, C.L., D.L. Bradley, and T.B. Gabrielson. 2006. St. Lawrence blue whale vocalizations revisited: Characterization of calls detected from 1998 to 2001. *Journal of the Acoustical Society of America* 120(4): 2340-2354. <Go to ISI>://000241258400059.

Charif, R.A. and C.W. Clark. 2000. Acoustic Monitoring of Large Whales off North and West Britain and Ireland: a two-year study, October 1996 - September 1998. *Joint Nature Conservation Committee (JNCC)* (313): 1-33

Clark, C.W. 1990. Acoustic behaviour of mysticete whales. *In* Thomas, J. and R.A. Kastelein (eds.). *Sensory Abilities of Cetaceans*. Plenum Press, New York. 571-583.

Clark, C.W. and G.J. Gagnon. 2002. Low-frequency vocal behaviors of baleen whales in the North Atlantic: Insights from integrated undersea surveillance system detections, locations, and tracking from 1992 to 1996. *U.S. Navy J. Underwater Acoust.* 52: 609–640.

Dalebout, M., S. Hooker, and I. Christensen. 2001. Genetic diversity and population structure among northern bottlenose whales, *Hyperoodon ampullatus*, in the western North Atlantic Ocean. *Canadian Journal of Zoology* 79(3): 478-484.

Deane, G.B. 2000. Long time-base observations of surf noise. *Journal of the Acoustical Society of America* 107(2): 758-770.

Delarue, J., S.K. Todd, S.M. Van Parijs, and L. Di Iorio. 2009. Geographic variation in Northwest Atlantic fin whale (*Balaenoptera physalus*) song: Implications for stock structure assessment. *Journal of the Acoustical Society of America* 125(3): 1774-82. http://www.ncbi.nlm.nih.gov/pubmed/19275334.

Delarue, J., L. Bailey, J. MacDonnell, and K. Kowarski. 2016. *Acoustic Characterization of the Bay of Fundy Shipping Lanes: Marine Mammal Occurrence, Vessel Source Levels, and Soundscape Description, September 2015 to April 2016*. Document Number Document 01227, Version 4.0. JASCO Applied Sciences, Stantec.

DFO. 2016. *Fisheries and Oceans Canada. 2016. Management Plan for the Sowerby's Beaked Whale (Mesoplodon bidens) in Canada [Proposed]. Species at Risk Act Management Plan Series. Fisheries and Oceans Canada, Ottawa. iv + 48 pp.*

Edds-Walton, P.L. 1997. Acoustic communication signals of mysticetes whales. *Bioacoustics* 8: 47-60.

Erbe, C., A. Verma, R. McCauley, A. Gavrilov, and I. Parnum. 2015. The marine soundscape of the Perth Canyon. *Progress in Oceanography* 137: 38-51. http://www.sciencedirect.com/science/article/pii/S0079661115001123.

Gannon, D., A. Read, J. Craddock, K. Fristrup, and J. Nicolas. 1997. Feeding ecology of long-finned pilot whales Globicephala melas in the western North Atlantic. *Marine Ecology Progress Series* 148: 1-10.

Gowans, S. and H. Whitehead. 1995. Distribution and habitat partitioning by small odontocetes in the Gully, a submarine canyon on the Scotian Shelf. *Canadian Journal of Zoology* 73(9): 1599-1608. http://www.nrcresearchpress.com/doi/pdf/10.1139/z95-190.

Gowans, S., H. Whitehead, J.K. Arch, and S.K. Hooker. 2000. Population size and residency patterns of northern bottlenose whales (Hyperoodon ampullatus) using the Gully, Nova Scotia. *Journal of Cetacean Research and Management* 2(3): 201-210.

Hatch, L. and C. Clark. 2004. Acoustic differentiation between fin whales in both the North Atlantic and North Pacific Oceans, and integration with genetic estimates of divergence. *Unpublished paper to the IWC Scientific Committee*.

Hawkins, A.D., L. Casaretto, M. Picciulin, and K. Olsen. 2002. Locating spawning haddock by means of sound. *Bioacoustics* 12(2-3): 284-286.

Hildebrand, J.A. 2009. Anthropogenic and natural sources of ambient noise in the ocean. *Marine Ecology Progress Series* 395: 5-20.

Hooker, S.K. and H. Whitehead. 2002. Click characteristics of northern bottlenose whales (*Hyperoodon ampullatus*). *Marine Mammal Science* 18(1): 69-80.

Jefferson, T.A., D. Fertl, J. Bolaños-Jiménez, and A.N. Zerbini. 2009. Distribution of common dolphins (Delphinus spp.) in the western Atlantic Ocean: a critical re-examination. *MARINE BIOLOGY* 156(6): 1109-1124.

Kingsley, M.C.S. and R.R. Reeves. 1998. Aerial surveys of cetaceans in the Gulf of St. Lawrence in 1995 and 1996. *Canadian Journal of Zoology* 76(8): 1529-1550. <Go to ISI>://000080497900016.

Larsen, S.B. and W. Ashby. 2015. *Successful completion of 2015 seismic acquisition season in offshore Newfoundland Labrador*. Houston. http://www.tgs.com/News/2015/Successful_completion_of_2015_seismic_acquisition_season_in_Offshore_Newfoundland_Labrador/.

Lawson, J. and J. Gosselin. 2011. *Fully-corrected cetacean abundance estimates from the Canadian TNASS survey. Department of Fisheries and Oceans, Ottawa*. ON. Working Paper 10.

MacLeod, C.D., C.R. Weir, C. Pierpoint, and E.J. Harland. 2007. The habitat preferences of marine mammals west of Scotland (UK). *Journal of the Marine Biological Association of the United Kingdom* 87(01): 157-164.

Mead, J.G. 1989. Beaked whales of the genus Mesoplodon. *In* Ridgway, S.H. and R. Harrison (eds.). *Handbook of marine mammals, Vol. 4: River Dolphins and toothed whales.* Academic press, San Diego.

Measures, L., B. Roberge, and R. Sears. 2004. Stranding of a pygmy sperm whale, Kogia breviceps, in the northern Gulf of St. Lawrence, Canada. *The Canadian Field-Naturalist* 118(4): 495-498.

Mellinger, D.K. and C.W. Clark. 2003. Blue whale (*Balaenoptera musculus*) sounds from the North Atlantic. *Journal of the Acoustical Society of America* 114(2): 1108-1119.

Mercer, M. 1973. Observations on distribution and intraspecific variation in pigmentation patterns of odontocete Cetacea in the western North Atlantic. *Journal of the Fisheries Board of Canada* 30(8): 1111-1130.

Mohl, B., M. Wahlberg, P.T. Madsen, L.A. Miller, and A. Surlykke. 2000. Sperm whale clicks: Directionality and source level revisited. *Journal of the Acoustical Society of America* 107(1): 638-648.

Nieukirk, S.L., K.M. Stafford, D.K. Mellinger, R.P. Dziak, and C.G. Fox. 2004. Low-frequency whale and seismic airgun sounds recorded in the mid-Atlantic Ocean. *Journal of the Acoustical Society of America* 115(4): 1832-1843.

Nordeide, J.T. and E. Kjellsby. 1999. Sound from spawning cod at their spawning grounds. *ICES Journal of Marine Science* 56(3): 326-332. http://icesjms.oxfordjournals.org/content/56/3/326.abstract.

Payne, P.M. and D.W. Heinemann. 1993. The distribution of pilot whales (*Globicephala* spp.) in shelf/shelf edge and slope waters of the north-eastern United States, 1978-1988. *Report of the International Whaling Commission* Special Issue 14: 51-68.

Reeves, R.R. and H. Whitehead. 1997. Status of the sperm whale, Physeter macrocephalus, in Canada. *Canadian field-naturalist. Ottawa ON* 111(2): 293-307.

Reeves, R.R., C. Smeenk, C.C. Kinze, R. Brownell, and J. Lien. 1998. White-beaked dolphin Lagenorhynchus albirostris Gray, 1846. *Handbook of Marine Mammals: the Second Book of Dolphins and the Porpoises* 6: 1-30.

Reeves, R.R., T.D. Smith, E.A. Josephson, P.J. Clapham, and G. Woolmer. 2004. Historical Observations of Humpback and Blue Whales in the North Atlantic Ocean: Clues to Migratory Routes and Possibly Additional Feeding Grounds. *Marine Mammal Science* 20(4): 774-786.

Rendell, L.E., J.N. Matthews, A. Gill, J.C.D. Gordon, and D.W. Macdonald. 1999. Quantitative analysis of tonal calls from five odontocete species, examining interspecific and intraspecific variation. *Journal of Zoology* 249: 403-410.

Risch, D., C.W. Clark, P.J. Corkeron, A. Elepfandt, K.M. Kovacs, C. Lydersen, I. Stirling, and S.M. Van Parijs. 2007. Vocalizations of male bearded seals, Erignathus barbatus: classification and geographical variation. *Animal Behaviour* 73: 747-762. <Go to ISI>://000246908300002.

Ross, D. 1976. *Mechanics of Underwater Noise*. Pergamon Press, New York. 375 pp.

Sears, R. and J. Calambokidis. 2002. Update COSEWIC status report on the Blue Whale Balaenoptera musculus in Canada. *COSEWIC assessment and update status report on the Blue Whale Balaenoptera musculus in Canada. Committee on the Status of Endangered Wildlife in Canada. Ottawa*: 1-32.

Selzer, L.A. and P.M. Payne. 1988. The distribution of white-sided (Lagenorhynchus acutus) and common dolphins (Delphinus delphis) vs. environmental features of the continental shelf of the northeastern United States. *Marine Mammal Science* 4(2): 141-153.

Sergeant, D.E. 1962. The biology of the pilot or pothead whale *Globicephala melaena* in Newfoundland waters. *Bulletin of the Fisheries Research Board of Canada* 132: 84.

Steiner, W.W. 1981a. Species-specific differences in pure tonal whistle vocalizations of five western North Atlantic dolphin species. *Behavioral Ecology and Sociobiology* 9(4): 241-246.

Steiner, W.W. 1981b. Species-specific differences in pure tonal whistle vocalizations of five western North Atlantic dolphin species. *Behavioral Ecology and Sociobiology* 9: 241-246.

Tyack, P.L. and C.W. Clark. 2000. Communication and acoustic behavior of dolphins and whales. *In* Au, W.W.L., A.N. Popper, and R.R. Fay (eds.). *Hearing by Whales and Dolphins*. Springer-Verlag, New York. 156-224.

Wahlberg, M., K. Beedholm, A. Heerfordt, and B. Møhl. 2012. Characteristics of biosonar signals from the northern bottlenose whale, *Hyperoodon ampullatus*. *Journal of the Acoustical Society of America* 130(5): 3077-3084.

Watkins, W.A., P. Tyack, K.E. Moore, and J.E. Bird. 1987. The 20-Hz signals of finback whales (*Balaenoptera physalus*). *Journal of the Acoustical Society of America* 82(6): 1901–1912.

Wenz, G.M. 1962. Acoustic ambient noise in the ocean: Spectra and sources. *Journal of the Acoustical Society of America* 34(12): 1936-1956.

Whitehead, H., S. Brennan, and D. Grover. 1992. Distribution and behaviour of male sperm whales on the Scotian Shelf, Canada. *Canadian Journal of Zoology* 70(5): 912-918.

Whitehead, H., S. Gowans, A. Faucher, and S.W. Mccarrey. 1997. Population analysis of northern bottlenose whales in the Gully, Nova Scotia. *Marine Mammal Science* 13(2): 173-185.

Whitehead, H. 2002. Sperm whale *Physeter macrocephalus*. *In Encyclopedia of Marine Mammals*. Academic Press. 1165-1172.

Wimmer, T. and H. Whitehead. 2004. Movements and distribution of northern bottlenose whales, Hyperoodon ampullatus, on the Scotian Slope and in adjacent waters. *Canadian Journal of Zoology* 82(11): 1782-1794. <Go to ISI>://000227497100012